بسم الله الرحمن الرحيم

Graduation Project

Terrestrial Laser Scanner Data Processing and Evaluation

TX5

WORKING TEAM:

Anwar Sbitan Nour Qassas

Manar Wahdeen

Supervisor:

Dr.Ghadi Zkarneh

College of Engineering

Department of Civil and Architectural Engineering

Palestine _ Hebron

2018

جامعة بوليتكنك فلسطين

كلية الهندسة

دائرة الهندسة المدنية والمعمارية

اسم المشروع :-

Terrestrial Laser Scanner Data Processing and Evaluation

أسماء الطلبة :-

أنوار عماد سبيتان نور يوسف قصاص منار سمير وهادين

بناء على نظام كلية الهندسة والتكنولوجيا وإشراف ومتابعة المشرف المباشر على المشروع وموافقة أعضاء اللجنة الممتحنة تم تقديم هذا المشروع إلى دائرة الهندسة المدنية و المعمارية وذلك للوفاء بمتطلبات درجة البكالوريوس في الهندسة تخصص هندسة المساحة والجيوماتكس.

توقيع المشرف

.....

توقيع اللجنة الممتحنة

....

توقيع رئيس الدائرة

.....

2017-2018

الاهداء

قال تعالى : (وَلَقَدْ آتَيْنا لُقْمانَ الْحِكْمَةَ أَنِ اشْكُرْ لِلَّهِ وَمَنْ يَشْكُرْ فَإِنَّما يَشْكُرُ لِنَفْسِهِ) (لقمان١٢)

الى منارة العلم والامام المصطفى الى سيد الخلق الى رسولنا الكريم محمد صلى الله عليهم وسلم

الى الينبوع الذي لا يمل العطاء الى من حاكت سعادتي بخيوط منسوجة من قلبها الى والدتي العزيزة

الى القلوب الطاهرة الرقيقة والنفوس البريئة اخوتي واخواتي

الى من علمونا حروفا من ذهب وكلمات من درر الى من صاغو لنا علمهم حروفا ومن فكرهم منارة تنير لنا سير العلم الى اساتذتنا الكرام

الى من وقف بجانبنا خطوة بخطوة لانجاز هذا العمل الى مشرف المشروع د.غادي زكارنة

فريق العمل

الى من سعى وشقى لانعم بالراحة الذي لم يبخل بشيء من اجل دفعي في طريق النجاح الى والدي العزيز

الى من ساندني لشق طريق النجاح الى رفيق دربي وزوجي الغالي محمود

الى ابنتي الحبيبة لجين

نور يوسف قصاص

يا من احمل اسمك بكل فخر يا من افتقدك منذ الصغر يا من يرتعش قلبي لذكرك يا من أودعتني لله الى ابي الغالي رحمه الله

انوارعمادسبيتان

الى من سعى وشقى لانعم بالراحة الذي لم يبخل بشيء من اجل دفعي في طريق النجاح الى والدي العزيز

الى من ساندني لشق طريق النجاح الى رفيق دربي وزوجي الغالي

أمجد

الى ابني الحبيب محمد

منار سمير وهادين

Acknowledgement

We thanks Allah, the most Merciful who granted us the ability and willing to start this project

We thank our University and Department of civil and architectural engineering .We express our thanks to Dr Ghadi Zakarneh who gave us Knowledge,valuable help ,encouragement supervision and guidance in solving the problems that we faced from time during this project

Finally, sincere thanks to our lab suprvisors: Eng Ahmad Herbawi ,Eng Sawsan Aljaaberi, Eng Alia'Alzeer.

Who helps us during our work .

Working Team

WORKING TEAM:

Anwar Sbitan **Nour Qassas**

Manar Wahdeen

Supervisor:

ENG. Ghadi Zkarneh

Project Abstract :

This project aims to the evaluate TX5 Laser Scanner at Palestine Polytechnic University for the data processing possibilities and evaluation of accuracy and limitation.

Different objects are scanned from interior and exterior, the object are scanned from different station, the different scans are gathered to form the surface of the objects, 3D models are constructed and finished, an evaluation of the processes, limitation and accuracies are done.

Finally, a report that contains best procedures to apply scans of small and large objects from interior and exterior by means of many stations are prepared, this are include the expected accuracy and limitations of the scanner.

جامعة بوليتكنك فلسطين

فريق العمل:

انوار سبيتان نور قصاص

منار وهادين

إشراف:

د.غادي زكارنة

الملخص:

يهدف هذا المشروع الى تقييم اداء جهاز الليزر سكنر في جامعة بوليتكنك فلسطين من حيث امكانية معالجة البيانات وتقدير الدقة.

تم تطبيق عملية مسح الكائنات المختلفة من الداخل والخارج ، وتم مسح الكائن من اكثر من محطة مختلفة ،وتم تجميعها من خلال اشعة الليزر لتشكيل سطح الكائنات، وتم انشاء نموذج ثلاثي الابعاد.

وأخيرًا ، تم إعداد تقرير يحتوي على أفضل الإجراءات لتطبيق فحوصات الكائنات الصغيرة والكبيرة من الداخل والخارج بواسطة العديد من المحطات ، وهذا يشمل الدقة والقيود المتوقعة للماسحة الضوئية.

Table Of Content:

Index Of Figure

Index of Tables

Chapter One

Introduction

1-1 Background

1-2 Objectives

1-3 Literature Review

1-4 Problem Statement

1-5 Methodology

1-6 Scope of Work

1-7 Time Table

Chapter One

Introduction

1-1 Background

Laser scanning is an emerging data acquisition technology that has remarkably broadened its application field and has been a serious competitor to other surveying techniques. Due to rapid technological development, the increased accuracy of global positioning systems and improving demands to even more accurate digital surface models, airborne laser scanning showed significant development in the 1990s. Somewhat later terrestrial laser scanning became a reasonable alternative method in many kinds of applications that previously by ground based surveying or close-range photogrammetry. [1]

Along with the penetration of laser scanning, significant paradigm change can be observed in geodesy, e.g. direct orientation instead of indirect orientation, surface detection instead of point measurements, complex 3D model product instead of simple coordinates etc. Laser scanning nicely demonstrates how these new paradigms work in practice. In the last years, due to the sensor fusion techniques, navigation solutions including inertial measurements and the improving demand for urban modeling, mobile laser scanning is gaining more and more momentum, as it can be seen even in the sensor manufacturers' product lists. [1]

All the technologies above based on the same principle: the scanner emits a laser beam through the ground/object, and computes the distance by measuring the traveling time or the phase difference of the laser beam. The emission rate of the cutting edge sensors is in the 100-200 kHz range. The direction of the beam is determined by different types of rotating or oscillating mirrors that enable the scanning of the area of interest. In case of airborne and mobile laser scanning, the position of the sensor is given by high accuracy GNSS and INS. [1]

As in many sources, laser scanning here is often referred as LiDAR (Light Detection And Ranging). ALM (Airborne Laser Mapping) or ALS (Airborne Laser Scanning) abbreviations are also widely used for airborne laser scanning, whilst term "terrestrial laser scanning" is used for ground-based laser scanning. [1]

1-2ProblemStatement

In 2017 ,Palestine Polytechnic University had laser scanner TX5 with characteristic :High accuracy, High resolution, High speed, Intuitive control via the built in touchscreen display, High mobility due to its small size, light weight, and the integrated quick charge battery, Photorealistic 3D color scans due to the integrated color camera, Integrated dual axis compensator to automatically level the captured scan data and Integrated compass and altimeter to give the scans an orientation and a height information. This project is aimed as training for use in the most proper and practical application.

1-3 Objectives

The project aims to:

1- The evaluate TX5 Laser Scanner at Palestine Polytechnic University for the data processing possibilities and evaluation of accuracy and limitation.

2- Apply scans of small and large objects from interior and exterior.

3- The different scans will be gathered to form the surface of the objects, 3D models will construct and finished.

4- Will include the expected accuracy and limitations of the scanner.

1-4 Literature Review

Y.M. Mogahed and M. Selim (2016) have done a study named Ability of Terrestrial Laser Scanner Trimble TX5 in Cracks Monitoring at Different Ambient Conditions: These approaches are indoor and outdoor system calibration, with the intention to specifically identify the accuracy of the Trimble TX5 scanner with different resolutions in detecting the various widths of small cracks from 1 mm to 9 mm. This calibration has been processed using the 3D Laser Scanning Trimble TX5,The calibration of data has been useful in order to identify and analyze over time, accuracy and it also gives us some elements about the validity of the technique for this kind of applications.[2]

Mr Brenton Light (2014) has done a study named Terrestrial Laser scanning for Building Information Model (BIM) Development and Application: This project aims to analyze the advantages and disadvantages of a TLS over conventional surveying techniques, it will aim to assess the accuracies of each method and then develop workflows to extract geometric and structural information from laser scanning point cloud data, and test these applications in building information modeling.[2]

Yelda Turkan, Simon Laflamme and Liangyu Tan (2016) have done a study named Terrestrial Laser Scanning-Based Bridge Structural Condition Assessment: This research project proposed to measure the performance of TLS for the automatic detection of cracks for bridge structural condition assessment. Laser scanning is an advanced imaging technology that is used to rapidly measure the three-dimensional (3D) coordinates of densely scanned points within a scene.[2]

1-5 Methodology

The project is to be achieved using the following steps:

1-Working on the device in different conditions.
2-Different objects are scanned from interior and exterior.

3-The object are scanned from different station.

4-The different scans are gathered to form the surface of the objects, 3D models are constructed and finished.

5-An evaluation of the processes, limitation and accuracies are done.

1-6 Scope of Work

The projects do will consist of the following chapters:

Chapter one (Introduction):This chapter gives an introduction about the project,its aims , goals and the working methodology used it

Chapter two: Introduces the principles of terrestrial laser scanners

Chapter three: The Application of Laser Scanner in different fields

Chapter four :Shows result and their Test Analysis of data collected by the laser the laser scanner and compared to the real measurement

Chapter five: Shows the Conclusions and recommendations of the project

Chapter Two

Laser Scanner

Chapter Two

Laser scanner

2-1 Introduction

Within a time frame of only two decades airborne and terrestrial laser scanning have become well established surveying techniques for the acquisition of geospatial information. A wide variety of instruments is commercially available, and a large number of companies operationally use airborne and terrestrial scanners, accompanied by many dedicated data acquisition, processing and visualisation software packages. The high quality 3D point clouds produced by laser scanners are nowadays routinely used for a diverse array of purposes including the production of digital terrain models and 3D city models, forest management and monitoring, corridor mapping, revamping of industrial installations and documentation of cultural heritage.[3]

Airborne and terrestrial laser scanning clearly differ in terms of data capture modes, typical project sizes, scanning mechanisms, and obtainable accuracy and resolution. Yet, they also share many features, especially those resulting from the laser ranging technology. In particular, when it comes to the processing of point clouds, often the same algorithms are applied to airborne as well as terrestrial laser scanning data. In this book we therefore present, as far as possible, an integral treatment of airborne and terrestrial laser scanning technology and processing. [3]

2-2 Laser Scanning Technology

In the last 50 years, many advances in the fields of solid-state electronics, photonics, and computer vision and graphics have made it possible to construct reliable, high resolution and accurate terrestrial and airborne laser scanners. Furthermore, the possibility of processing dense point clouds in an efficient and cost-effective way has opened up a multitude of applications in fields such as topographic, environmental, industrial and cultural heritage 3D data acquisition. [3]

Airborne and terrestrial laser scanners capture and record the geometry and sometimes textural information of visible surfaces of objects and sites. These systems are by their nature non-contact measurement instruments and produce a quantitative 3D digital representation (e.g. point cloud or range map) of a surface in a given field of view with a certain measurement uncertainty. Full-field optical 3D measurement systems in general can be divided into several categories (Figure 2.1). Airborne and terrestrial laser scanners are usually part of what are classified as time-of-flight based optical 3D measurement systems. These systems use a laser source to scan a surface in order to acquire dense range data. Triangulation systems using light sheet or strip projection techniques and passive systems exploiting surface texture (stereo image processing) will be covered only briefly here. [3]

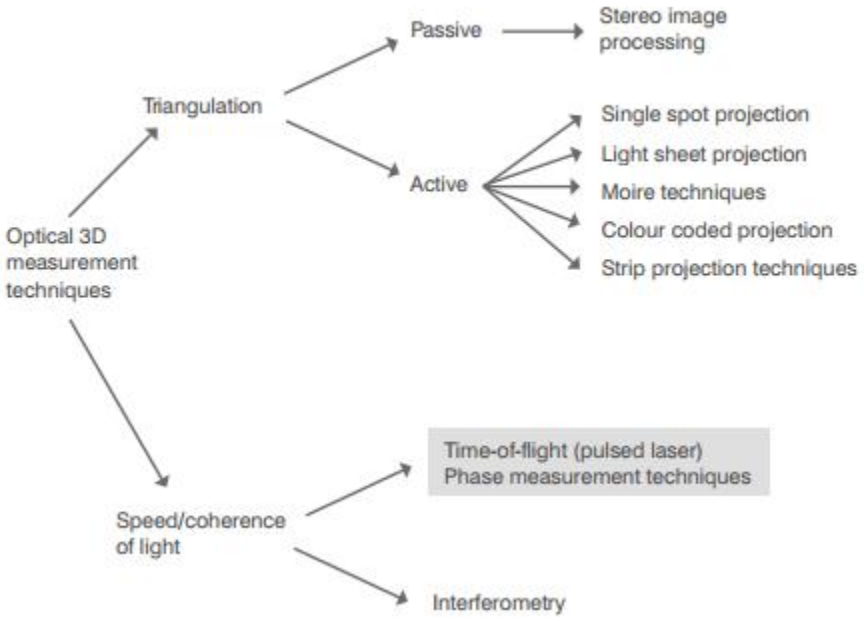

Figure (2-1): Classification of optical 3D measurement systems [2]

2-2-1 Basic measurement principles of laser scanners

There are two basic active methods for optically measuring a 3D surface: light transit time estimation and triangulation. As illustrated in Figure 2.2(a), light waves travel with a known velocity in a given medium. Thus, the measurement of the time delay created by light travelling from a source to a reflective target surface and back to a light detector offers a very convenient method of evaluating distance. Such systems are also known as time-of-flight or lidar (light detection and ranging) systems. Time-of- flight measurement may also be realised indirectly via phase measurement in continuous wave (CW) lasers. Triangulation exploits the cosine law by constructing a triangle using an illumination direction (angle) aimed at a reflective surface and an observation direction (angle) at a known distance (base distance or baseline) from the illumination source . Interferometry (which is not covered here) can be classified separately as a third method or included with time-of-flight methods depending on how the metric used to measure shape is seen. [14]

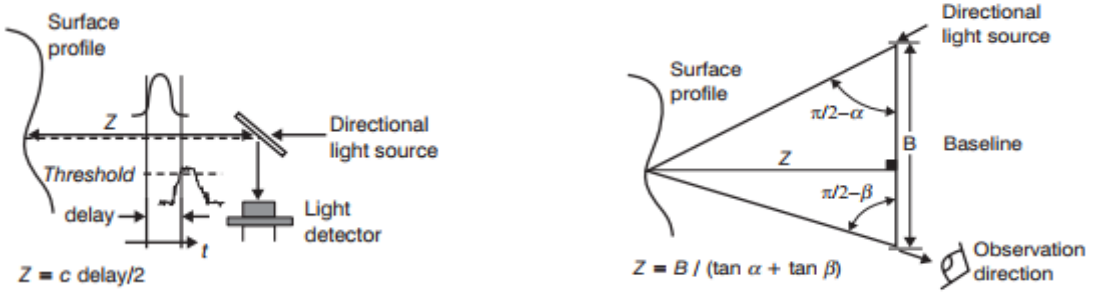

a) light transit time

b) triangulation

Figure (2-2): Active methods for optically measuring a 3D [14]

2-2-2 Time-of-flight measurement

Early work on time-of-flight ranging systems used radio waves in what became known as radar (radio detection and ranging). The fundamental work can be traced back to experiments conducted by Hertz in the late 1880s. With the advent of lasers in the late 1950s it became possible to image a surface with angular and range resolutions much higher than that obtained with radio waves. The theoretical principles are the same for all systems that use radiated electromagnetic energy for ranging except for their implementations, the differences in their performance and obviously their use. [14]

A fundamental property of a light wave is its propagation velocity. In a given medium, light waves travel with a finite and constant velocity. Thus, the measurement of time delays (also known as time-of-flight) created by light travelling in a medium from a source to a reflective target surface and back to the source (round trip, τ) offers a very convenient way to evaluate the range [14]

$$\rho = \frac{c}{n}\frac{\tau}{2} \qquad (2.1)$$

The current accepted value for the speed of light in a vacuum is c = 299 792 458 m/s. If the light waves travel in air then a correction factor equal to the refractive index, which depends on the air temperature, pressure and humidity, must be applied to c, n ≈ 1.00025. Let us assume c = 3 × 10^8 m/s and n = 1 in the rest of the discussion. More than one pulse echo can be measured due to multiple returns that are caused by the site characteristics, especially when vegetation (the canopy) is scanned. [7]

Airborne systems capture at least the first returned pulse or echo and also the last echo for each emitted pulse. Most airborne systems are capable of capturing four to five separate echoes. Multiple echo measurements are also becoming available for terrestrial time-of-flight scanners.It is important to have a more detailed look at pulse shape and pulse repetition time. The characteristics of a transmitted pulse are the pulse width t_p and the pulse rise time tr (Figure 1.3). A typical pulse width of tp 5 ns corresponds to a length of about 1.5 m at the speed of light, while a pulse rise time tr 1 ns corresponds to a length of 0.3 m. [14]

According to Equation (2.1), the relationship between S (the distance between the laser scanner and the illuminated spot) and time-of-flight τ is given by [7]

$$\tau = n\frac{2\rho}{c}$$

With n= 1, the time-of-flight is 6.7 μs at a distance (the survey height in an airborne system) of 1000 m. When assuming that from a distance S two or more echoes are generated from only one pulse P1 , different ranges can only be discriminated if the echoes E11 and E12 are separated, i.e. do not have an overlap. [7]

$$\tau^{12} \geq \tau^{11} + l_p$$

With the above relation between time-of-flight and distance and the pulse length lp , which is given by $t_p = \frac{n}{c} l_p$, this leads to

$$2\frac{n}{c}\rho^{12} - 2\frac{n}{c}\rho^{11} \geq \frac{n}{c}l_p$$

$$\rho^{12} - \frac{n}{c} \geq \frac{1}{2}l_p \qquad (2.2)$$

Two echoes (for example related to objects heights) can only be discriminated if their distance is larger than half of the pulse length lp . This means that for a pulse width of 5 ns objects can be detected as separate objects if their distance is at least larger than 0.75 m. [14]

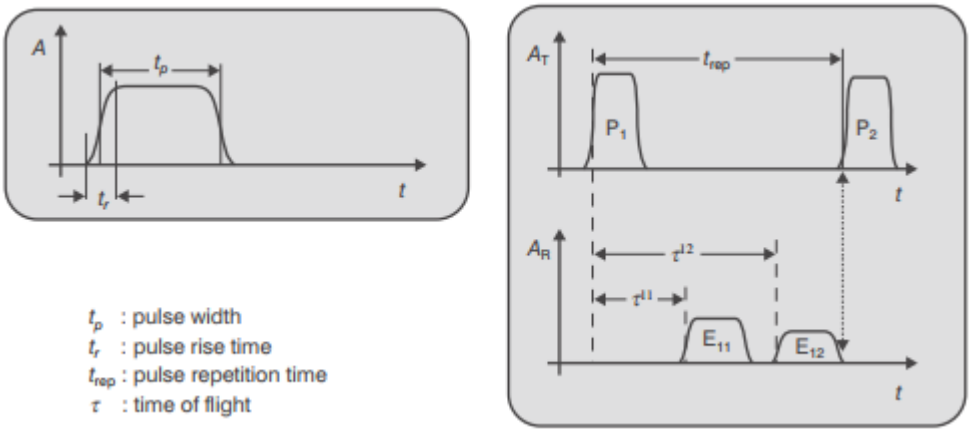

Figure (2-3): Pulse characteristics and measurement principle. [14]

An essential part of the time-of-flight measurement is the detection method for determining the time-of-flight (and thus the range). The detector will generate a time tagged trigger pulse depending on the implemented criterion. Some detection methods take characteristic points of the path of the pulse as the decisive factor. Due to the rapidity of data capture and the ability to obtain point clouds instantaneously, laser scanning has become an essential tool along with image-based documentation methods. Total station surveys, on the other hand, require more time on site and usually do not deliver the same level of surface detail. [14]

Peak detection: The detector generates a trigger pulse at the maximum (amplitude) of the echo. Time-of-flight is the time delay given by the time span from the maximum of the emitted pulse to the maximum of the echo. Correct detection can become problematic if the echo provides more than one peak. [14]

Threshold or leading edge detection: Here the trigger pulse is actuated when the rising edge of the echo exceeds a predefined threshold. The disadvantage of this method is that the time-of-flight strongly depends on the echo's amplitude. [14]

Constant fraction detection: This method produces a trigger pulse at the time an echo reaches a preset fraction (typically 50%) of its maximum amplitude. The advantage of this method is that it is relatively independent of an echo's amplitude. [14]

Each detector has its pros and cons, however constant fraction has proven to be a good compromise. [14]

The range uncertainty for a single pulse buried in additive white noise is approximately given by equation (2.3): [14]

$$\delta_{r-p} = \frac{c}{2}\frac{t_r}{\sqrt{SNR}} \quad (2.3)$$

where tr is the rise time of the laser pulse leading edge and the SNR (signal-to-noise ratio) is the power ratio of signal over noise. Assuming SNR =100, tr=1 ns, and a time interval counter with adequate resolution then the range uncertainty will be about 15 mm. Most commercial time-of-flight based laser scanner systems provide a range uncertainty in the order of 5–10 mm (with a few at 50 mm) as long as a high signal-to-noise ratio is maintained. In the case of uncorrelated 3D samples, averaging N independent pulse measurements will reduce Er-p by a factor proportional to the square root of N. Obviously this technique reduces the data rate by N and is of limited applicability in scanning modes. [14]

2-3 Airborne laser scanning

In the early 1970s, it was shown that airborne lidar systems were able to measure distances between aircraft and ground targets to a precision of less than 1 m. However, laser altimeter systems did not come into widespread use for precise topographic mapping mainly for two reasons. First, for precise mapping, the vertical position of the aircraft had to be known to a level of accuracy comparable to the measurement capability of the lidar system. Second, the horizontal position of the illuminated spot on the ground (laser footprint) had also to be known. Although the second requirement is less stringent, the means to determine both aspects for larger areas with sufficient quality were not available at that time. Trials were done to determine aircraft altitude by recording pressure data with precise aircraft aneroid barometric altimeters and vertical accelerometers. Horizontal control was a tedious process as it was done post-flight by means of time-tagged photographs and rarely by IMU. [14]

At the end of the 1980s with the availability of GPS, a method was developed allowing precise registration of position and orientation over larger areas. With the introduction of differential GPS (DGPS) the scanner position became known in horizontal and vertical coordinates in the sub-decimetre range. Enhancements in DGPS technology along with Kalman filtering and use of IMUs provided sufficient accuracy from the beginning of the 1990s. The standard accuracy of elevation data became $\mp$10 cm in height, and $\mp$50 cm in position. [14]

Until the end of the 1980s range measurements were done by laser profilers providing laser pulses but no scanning mechanism. In the early 1990s profilers were replaced by scanning devices which generated 5000 to 10 000 laser pulses per second at that time. Nowadays, laser

pulse rates reach 300 kHz, however, depending on the kind of scanning mechanism 100% of the instrument's pulse rate may not really be available on the ground. [14]

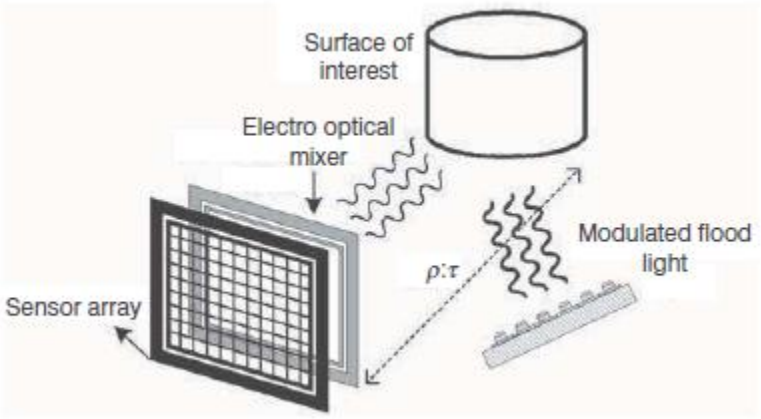

a) detection using an external mixer and correlator

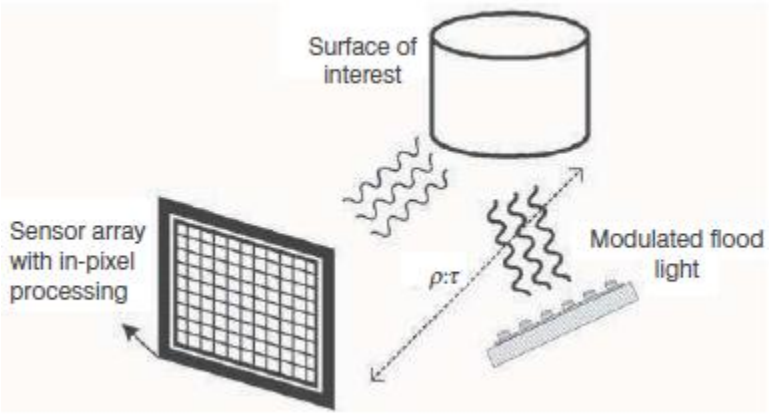

b) detection on a specially designed sensor or focal plane array.

Figure (2-4): Flash 3D system with floodlight [14]

Airborne laser scanning is now a common technique for generating high quality 3D presentations (digital elevation models) of the landscape .The following will outline the principle and system components of airborne laser scanning. Characteristics of this measurement technique as well as accuracies and limitations will be discussed. The specifics of calibration, processing of gathered data and product generation will not be discussed as these are covered in other chapters. Several airborne laser scanners are commercially available and in operational service.

2-3-1 Principle of airborne laser scanning

Airborne laser scanning is done either from a fixed wing aircraft or a helicopter. The technique is based on two main components: a laser scanner system which measures the distance to a spot on the ground illuminated by the laser and a GPS/IMU combination to measure exactly the position and orientation of the system. Active systems based on laser scanning are relatively independent of sunlight. They may be operated during the day or at night. This characteristic is a considerable advantage of airborne laser scanning compared to other methods of surveying landscapes. [14]

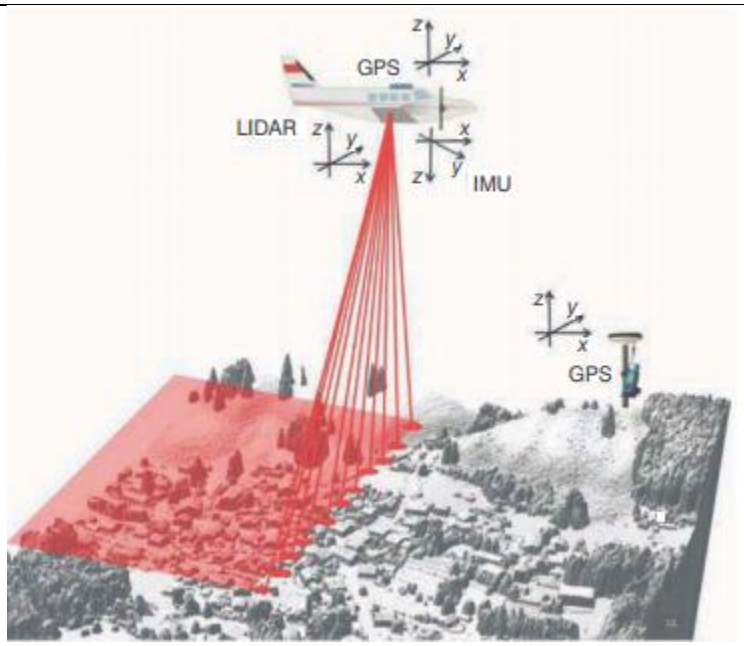

Figure (2-5): Airborne laser scanning principle [14]

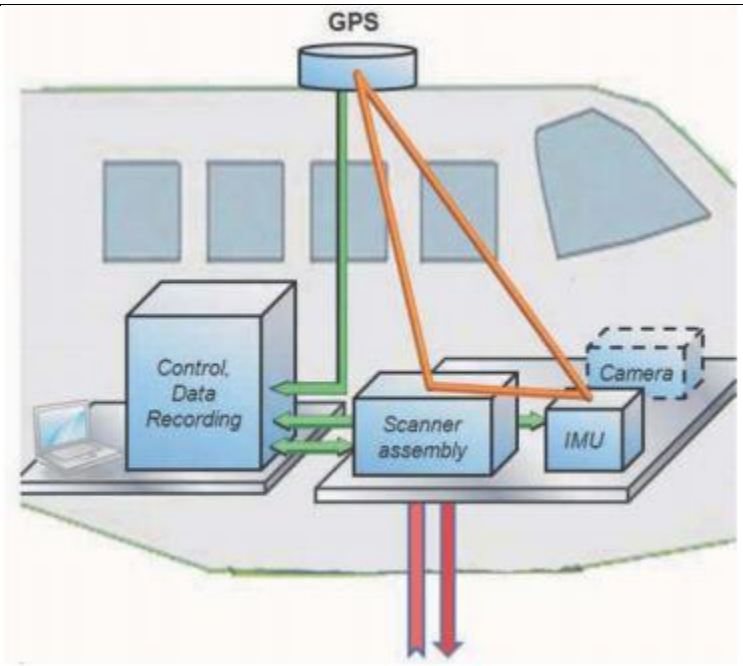

Figure (2-6): On-board components of an airborne laser scanner [14]

the distance to a spot on the ground illuminated by the laser and a GPS/IMU combination to measure exactly the position and orientation of the system. Active systems based on laser scanning are relatively independent of sunlight. They may be operated during the day or at night. This characteristic is a considerable advantage of airborne laser scanning compared to other methods of surveying landscapes The basic components of an airborne laser scanner [4]

Scanner assembly comprising laser, scanning mechanics and optics. The laser system (mostly a pulsed time-of-flight measurement system), mounted over a hole in the aircraft's fuselage, continuously sends laser pulses towards the terrain as the aircraft flies. Depending on aircraft velocity and survey height, current technology allows measurement densities between 0.2 and about 50 points/m2 . Modern scanner assemblies provide a roll compensation to compensate for the roll of the aircraft. This feature helps to avoid gaps in coverage which might occur between adjacent swaths due to roll. Roll compensation allows the overlap between flight lines to be planned to be smaller and therefore gives an economic advantage. [4]

Airborne GPS antenna: the standard is a dual frequency antenna recording GPS signals at a sampling rate of 2 Hz. The antenna is mounted at an exposed position on top of the aircraft, providing an undisturbed view to GPS satellites. [4]

Inertial measurement unit (IMU): the IMU is either fixed directly to the laser scanner or close to it on a stable survey platform. Typically it records acceleration data and rotation rates at a sampling rate of 200 Hz. Acceleration data can be used to support the interpolation of the platform position on the GPS trajectory, while rotation rates are used to determine platform

orientation. The combination of GPS and IMU data allows one to reconstruct the flight path (air trajectory) to an accuracy of better than 10 cm. [4]

Control and data recording unit: this device is responsible for time synchronisation and control of the whole system. It stores ranging and positioning data gathered by the scanner, IMU and GPS. Modern laser scanners, which generate up to 300 000 laser pulses per second, produce about 20 Gbyte of ranging data per hour, while GPS and IMU data only sum up to about 0.1 Gbyte per hour. [4]

Operator laptop: this serves as a means of communications with the control and data recording unit, to set up mission parameters, and to monitor the system's performance during the survey. [4]

Flight management system: this is a means for the pilot to display the preplanned flight lines, which provides support for him in completing the mission. [4]

An airborne laser scanner is completed by a GPS ground station. The ground station serves as a reference station for off-line differential GPS (DGPS) calculation. Differential GPS is crucial for compensating atmospheric effects disturbing precise position determination and for achieving decimetre accuracy. In order to cope with varying atmospheric conditions, the distance between the aircraft and the GPS ground station should not exceed 30 km (although sometimes adequate accuracy is reached for longer distances). Nowadays, several countries operate a network of permanent GPS stations, so there is often no need to set up one's own station. [6]

Airborne laser scanners are often complemented by a medium-sized digital camera system. Image data taken simultaneously with range data may support data interpretation significantly in cases where it is difficult to recognize objects only from range data. Image data will usually offer a better spatial resolution and form a basis for integrated 3D point cloud and image data processing. The camera head and the recording unit are separate. The optimum location for the camera is on the scanner assembly's ground plate, because then the existing IMU registrations can be shared for georeferencing. A separate IMU will be needed if the dimensions of the scanner assembly do not allow accommodation of a camera and a scanner assembly on the same survey platform. [2]

2-3-2 Laser scanner properties

Commercial airborne laser systems for land applications operate at wavelengths between 800 nm and 1550 nm. The spectral width is typically between 0.1 and 0.5 nm. As the reflectivity of an object depends on the wavelength, different laser systems show different pros and cons when scanning the Earth's surface: at wavelengths close to the visible part of the spectrum, the absorption of water is high. Therefore, water surfaces will rarely be seen by laser scanners operating in that part of the spectrum. At about 1550 nm the reflectivity of ice and snow is low, therefore scanners operating at 1550 nm will not be the optimum choice when surveying snow fields. Attention must also be paid to eye safety which means that the human eye must not be damaged when looking into a laser beam. [4]

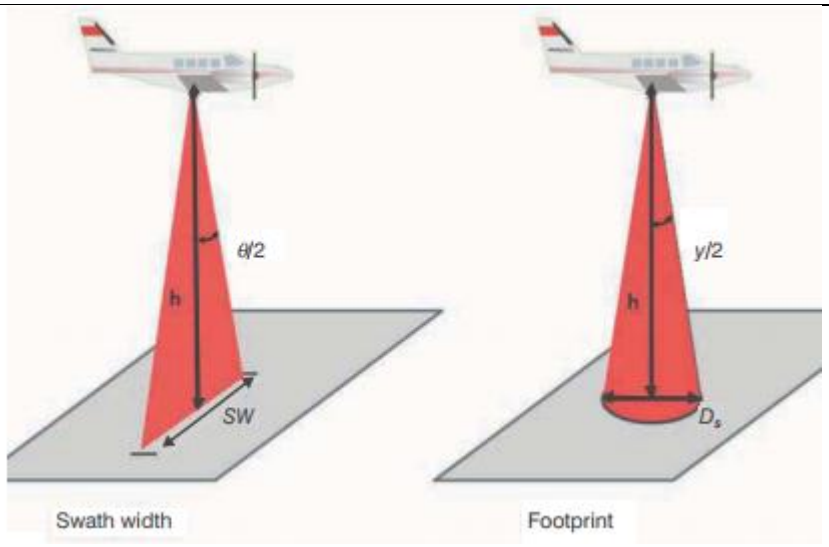

Figure (2-7): Swath and laser footprint (footprint is much smaller in reality) [4]

The swath width sw of a scanner is given by equation (2.4):

$$sw = 2h \tan\frac{\theta}{2} \qquad (2.4)$$

where θ is the full scan angle and h is the height above ground (Figure 1.14). Airborne scanners allow scan angles between about 5° and 75°. For example, the swath width will be 574 m at a height of 1000 m and a scan angle of 32°. [16]

The laser beam widens with the distance from the laser scanner. A relationship, similar to the previous one, describes the diameter Ds of the illuminated footprint on the ground.[16]

$$D_{s=2h \tan\frac{\gamma}{2}} \qquad (2.5)$$

where γ (full angle) is the beam divergence and h the height above the ground assuming the spot shape to be a circle (Figure 2.7). Typically, beam divergences are between 0.1 rad and 1 rad. So, the footprint will be 0.2 m from a survey height of 1000 m and a divergence of 0.2 rad. The laser beam profile does not have sharp edges, but the irradiance falls off gradually away from the centre of the beam. Usually, the diameter Ds is determined at a position at which the irradiance drops to $1/e^2$ times the total irradiance. [2]

2-3-3 Advantages and limitations of airborne laser scanning

As an active system operating with light, a laser scanner needs a clear view to the ground. It cannot penetrate clouds, fog and dense vegetation. The laser beam will easily go through the canopy of deciduous trees, especially in winter time when the leaves are off. However, it will not see the ground below dense conifers and in multistorey rainforest. Total reflection might be the reason if a water surface is seen only close to the nadir direction, and a wet street or a wet roof may also lead to drop-outs. [2]

Despite its limitations, airborne laser scanning has turned out to be a very effective means for producing high quality digital elevation models. Laser scanning technology has some advantages compared to other methods of generating elevation data. Some of its pros are: [6]

High measurement density and high data accuracy: The highest measurement densities (about 30 measurements/m^2) are reached from a helicopter. The standard accuracy of elevation data in the local coordinate system is 0.05– 0.20 m for height and 0.2–1.0 m for position. [2]

Fast data acquisition: For point densities of 1 point/m^2 and higher airborne laser scanning is accepted to be a very fast means of generating accurate elevation models.Fast acquisition is supported by the fact that scanning can be done at any time, day and night. [4]

Canopy penetration: If the canopy is not too dense, part of the laser light beam may penetrate to the ground enabling production of an elevation model of the forest floor. High penetration rates are reached in the case of deciduous trees in winter time, when the leaves are off.

Minimum amount of ground truth data: Terrestrial work is minimized because even for large flight blocks only few ground references are needed. [2]

2-4 Laser Ranging

All laser ranging, profiling, and scanning operations are based on the use of some type of laser-based ranging instrument—usually described as a laser ranger or laser ran gefi nder—that can measure distance to a high degree of accuracy. As will be discussed in more detail later in this chapter, this measurement of distance or range, which is always based on the precise measurement of time, can be carried out using one of the two main methods. [2]

1. The first of these involves the accurate measurement of the TOF of a very short but intense pulse of laser radiation to travel from the laser ranger to the object being measured and to return to the instrument after having been reflected from the object—hence the use of the term "pulse echo" mentioned above. Thus, the laser ranging instrument measures the precise time interval that has elapsed between the pulse being emitted by the laser ranger located at point A and its return after reflection from a ground object located at point B. [2]

$$R = \frac{v.t}{c} \qquad (2.5)$$

where R is the slant distance or range v is the speed of electromagnetic radiation, which is a known value t is the measured time interval From this, the following simple relationship can be derived: [2]

$$\Delta R = \Delta v.\frac{t}{2} + v.\frac{\Delta t}{2} \qquad (2.6)$$

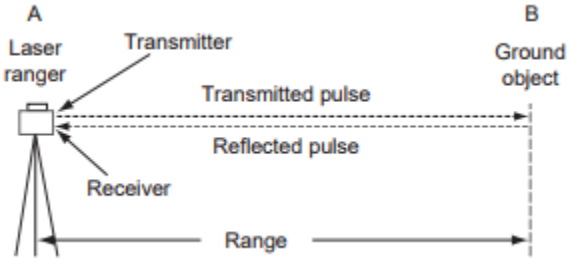

Figure (2-8): Basic operation of a laser rangefinder that is using the timed pulse or TOF method [2]

Where:

ΔR is the range precision

Δv is the velocity precision

Δt is the corresponding precision value of the time measurement

Since the speed of light is very accurately known, in practice, the range precision or resolution is determined by the precision of the time measurement. [2]

2. In the second (alternative) method, the laser transmits a continuous beam of laser radiation instead of a pulse. In this case, the range value is derived by comparing the transmitted and received versions of the sinusoidal wave pattern of this emitted beam and measuring the phase difference between them. Since the wavelength (λ) of the carrier signal of the emitted beam of laser radiation is quite short—typically around 1 μm, and there is no need for such a measuring accuracy in topographic mapping applications, a modulation signal in the form of a measuring wave pattern is superimposed on the carrier signal and its phase difference can be measured more precisely. Thus, the amplitude (or intensity) of the laser radiation will be modulated by a sinusoidal signal, which has a period Tm and wavelength λ m. The measurement of the slant distance R is then carried out through the accurate measurement of the phase difference (or the phase angle, j) between the emitted signal at point A and the signal received at the instrument after its refl ection either from the ground itself or from an object that is present on the ground at point B. This phase measurement is usually carried out using a digital pulse counting technique. This gives the fractional part of the total distance $\Delta\lambda$ (Figure 2.9). By changing the modulation pattern, the integer number. [2]

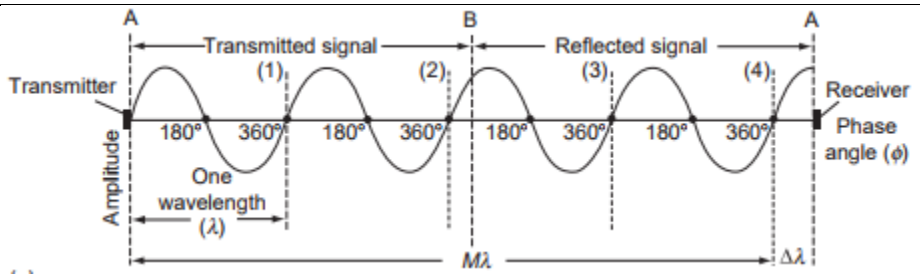

Figure (2-9): Phase comparison is carried out between the transmitted and reflected signals from a CW laser [4]

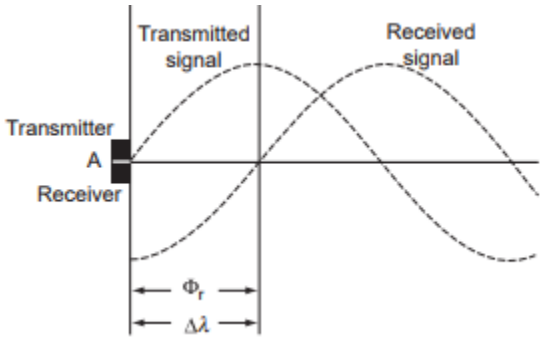

Figure (2-10): phase comparison between the two signals takes place at the laser rangefinder located at A. [2]

of wavelengths (M) can be determined and added to the fractional values to give the final slant range (R).

$$R = (M\lambda + \Delta\lambda)/2 \quad (2.5)$$

of wavelengths (M) can be determined and added to the fractional values to give the final slant range (R).

where

M is the integer number of wavelengths

λ is the known value of the wavelength

$\Delta\lambda$ is the fractional part of the wavelength = $(\phi/2\pi) \cdot \lambda$, where ϕ is the phase angle [2]

2-5 Laser scanner TX5

The Trimble TX5 3D laser scanner is a high-speed three-dimensional laser scanner for detailed measurement and documentation. The laser scanner uses laser technology to produce exceedingly detailed three-dimensional images of complex environments and geometries in only a few minutes. The resulting images are an assembly of millions of 3D measurement points. [11]

The main features are:

- High accuracy
- High resolution
- High speed.
- Intuitive control via the built in touchscreen display.
- High mobility due to its small size, light weight, and the integrated quick charge battery
- Photorealistic 3D color scans due to the integrated color camera.
- Integrated dual axis compensator to automatically level the captured scan data
- Integrated compass and altimeter to give the scans an orientation and a height information
- WLAN to remotely control the scanner. [11]

Figure (2-11): Terrestrial Laser Scanner TX5 [11]

2-5-1 How laser scanner works

In principle, the TX5 3D laser scanner works by sending an infrared laser beam into the center of its rotating mirror. The mirror deflects the laser beam on a vertical rotation around the environment being scanned; scattered light from surrounding objects is then reflected back into the scanner. [11]

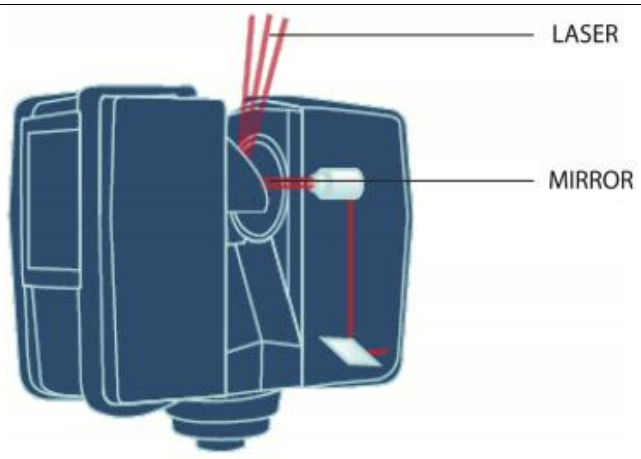

Figure (2-12): Principle of Terrestrial Laser scanner TX5 [11]

To measure the distance, the laser scanner uses phase shift technology, where constant waves of infrared light of varying length are projected outward from the scanner. Upon contact with an object, they are reflected back to the scanner. The distance from the scanner to the object is accurately determined by measuring the phase shifts in the waves of the infrared light. HYPERMODULATION greatly enhances the signal-to-noise ratio of the modulated signal with the help of a special modulation technology. The x, y, z coordinates of each point are then calculated by using angle encoders to measure the mirror rotation and the horizontal rotation of the laser scanner. These angles are encoded simultaneously with the distance measurement. Distance, vertical angle and horizontal angle make up a polar coordinate (δ, α, β), which is then transformed to a Cartesian coordinate (x, y, z). The scanner covers a 360° x 300° field of view**.** [11]

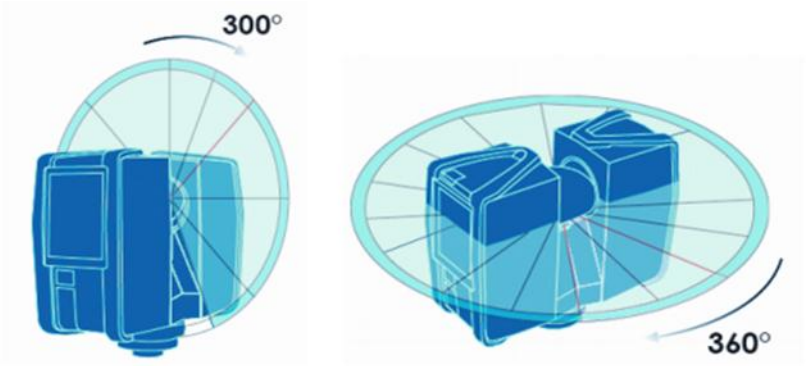

Figure (2-13): The scanner covers a 360X 300 field view [11]

Additionally, the laser scanner determines the reflectivity of the captured surfaces by measuring the intensity of the received laser beam. In general, bright surfaces reflect a greater portion of the emitted light than do dark surfaces. This reflectivity value is used to assign a corresponding grey value to each single point. The single point measurements are repeated up to 976,000 times per second. The result is a point cloud, a three-dimensional dataset of the scanner's environment (hereinafter referred to as the "laser scan" or "scan"). Depending on the selected resolution (points acquired per rotation) each point cloud consists of millions ofscan points. The laser scans are recorded to the removable SD memory card, enabling easy and secure transfer to Trimble TX5 SCENE software.[11]

2-6 3D Modeling

Building footprint, height, volume, and three-dimensional (3D) shape information can be used to estimate energy demand, quality of life, urban populations, property tax, and surface roughness .Three-dimensional building models are essential for 3D city or urban landscape models, urban flooding prediction, and assessment of urban heat island effects. Building models can be divided into two categories: simple and sophisticated. Geometric attributes for a simple building model consist of a footprint polygon and a height value. [5]

The geometric attributes for a sophisticated building model include not only a footprint polygon but also planes or other types of surfaces for various parts of the roof as well as their projections (polygons) on the ground plane. Only one fixed building height exists for a simple model, while building heights of the sophisticated model are variable. The advantage of the simple model is that it requires fewer geometric attributes to delineate a building. The buildings are represented by various types of 3D boxes; therefore, the 3D rendering is fast. Many commercial GIS software packages such as ArcGIS (www.esri.com) can display simple building models effectively. The simple building model is sufficient for applications such as numerical modeling of urban flooding and heat island effect, estimating urban population and energy demand, and large-scale 3D visualization, all of which do not require the details of buildings. The key to extracting a simple building model from LiDAR measurements is to derive footprints. The building height value can be represented using statistical height values such as mean and median of LiDAR measurements within a footprint. [16]

The disadvantage of the simple building model is the lack of detail and accuracy of building shapes. The sophisticated models overcome this limitation by offering more geometric information for 3D buildings. The sophisticated models are required by applications such as hurricane wind damage models for individual properties, property tax estimation, and detailed urban landscape modeling. The disadvantage of sophisticated models is that the 3D rendering is slow. Most existing commercial GIS software cannot display sophisticated models efficiently due to compound geometric structures. [3]

High-resolution data needed for extracting 3D building models can be derived through airborne light and detection (LiDAR) mapping systems. However, airborne LiDAR systems generate voluminous and irregularly spaced 3D point measurements of objects, including ground, building, trees, and cars scanned by the laser beneath the aircraft. The sheer volumes of point data require dedicated algorithms for automated building reconstruction. This paper focuses on presenting a framework for the construction of simple and sophisticated building models from LiDAR measurements. [15]

2-6-1 Separation of Ground and Non ground Points

The critical step in building model construction is to identify building measurements from LiDAR data. Two ways are often utilized to identify building measurements from LiDAR data. One is to separate ground, buildings, trees, and other measurements from LiDAR data simultaneously using segmentation. Examples of this method can be found in Maas and Filin and Pfeifer.[5]

The other way is to separate the ground from non-ground LiDAR measurements first and then identify the building points from nonground measurements. Numerous algorithms have been developed to identify ground measurements from LiDAR data. For example, Vosselman proposed a slope-based filter to remove non ground measurements by comparing slopes between a LiDAR point and its neighbors.[15]

Shan and Sampath applied a slope-based 1D bidirectional filter to LiDAR measurements along the cross track direction to label non ground points [5]. Zhang et al. used mathematical morphology to identify ground measurements. The non-ground measurements can be simply derived by removing identified ground data from a raw data set. To facilitate the data processing, digital surface models (DSMs) interpolated from raw LiDAR measurements and digital terrain model (DTM) interpolated from ground measurements are often produced. The image for non-ground objects is derived by subtracting DTM from DSM. Examples using this method to derive non ground objects can be found in Refs.[1]

2-6-2 Building Measurement Identification

The next step is to extract building point measurements or pixels in the data set for non-ground objects, which are dominated by trees and buildings. The distinct difference between buildings and trees is that the roof surfaces are approximately planar, while canopy surfaces are irregular. Several parameters based on this difference have been proposed for segmenting buildings and trees. For example, the first derivatives of heights are either a zero (fl at roof) or constant (sloped roof) for a planar surface, and the second derivatives of a sloped planar surface are zero. The first and second derivatives of an irregular surface should be variable. Morgan and Tempfl i applied Laplacian and Sobel operators to height surfaces to separate building and tree measurements [8]. The problem with this method is that the derivatives from LiDAR measurements for roofs are not constant because of measurement errors. Small features such as chimneys, water tanks, and pipes on a roof surface can also produce abnormal derivative values. In addition, the derivatives at the edge of a building have a large variation, making itdiffi cult to separate buildings from adjacent trees.

Another technique to separate building and tree measurements involves using a least squares method to estimate the parameters for a plane that fits a LiDAR point and its neighbors within a local window. It is expected that the deviations of roof points from their fitted planes

will be small and the plane parameters will be similar and consistent, while deviations and plane parameters for tree points will be large and variable. Compared to derivatives, the plane parameters are less sensitive to individual outliers caused by chimneys and water tanks. The drawback of this method is that plane parameters are not robust at the boundary of the buildings because fewer points are available for parameter estimation.[15]

Many airborne LiDAR systems are capable of deriving the first and last return measurements produced by multiple reflections of a laser pulse by the objects on the earth's surface. The height difference between the first and last return measurements can be used to separate building and tree measurements [14]. The height difference is usually large for tree measurements and close to zero for building measurements. A measurement is identified as a building measurement by comparing its height difference to a predefined threshold. However, this method does not work for areas covered by dense trees where laser pulses cannot penetrate. In addition, the elevation difference between the first and last returns less than 3–4 m is not reliable because of the influence of the laser pulse width, which is typically 10 ns. [1]

Hough transform has also been used to separate building points from tree measurements or to identify them directly from a raw LiDAR data set. Data in the physical space are transformed to and analyzed in the parameter space. The advantage of the Hough transform is its tolerance of gaps in the feature boundary. However, it is difficult to define the optimum cell size for voting in the parameter space, which is influenced by the error range of LiDAR measurements, the sampling density, and local height changes of a roof surface. Unfortunately, local height changes of individual surfaces are different; thus it is difficult to quantify these changes using a single value. Usually, the cell size is set empirically, and if the cell size is too large, several real-world planes could be merged into one during building identification. In contrast, if the cell size is too small, one real-world plane could be split into several smaller planes. In addition, the adjacency of point measurements is not considered by the Hough transform. Therefore, LiDAR measurements for separated but closely adjacent buildings with the same height could be mixed into the same category.[1]

The LiDAR measurements for buildings and trees can be segmented based on one or more of the above-mentioned parameters. There are two ways to perform the segmentation task. One is the point- or pixel-level classifi cation. Maas employed raw elevation , Laplace filtered height, and maximum slope from LiDAR measurements to perform a supervised maximum likelihood classification. Filin separated LiDAR measurements for buildings, vegetation, ground, and other features using an unsupervised classification based on the position of a point, the parameters of the tangent plane to the point, and the relative height difference between the point and its neighbors. Elberink and Maas used unsupervised k-means classification in their texture-based segmentation. The problem with a point-level classification is that the measurements for a building cannot be guaranteed to classify into the same category. Also, the selection of training data sets for a supervised classification can be very time consuming. An alternative way is to fi

nd a building area using a region-growing algorithm based on a seed point. This method considers the adjacency of LiDAR measurements and the robustness of region-growing processes.[14]

2-6-3 Building Model Creation

After measurements for a building are identifi ed, a raw footprint can be derived by connecting boundary points of LiDAR measurements for a building. The raw footprint polygon has to be generalized for building models because the raw footprint includes considerable noise due to irregularly spaced LiDAR points. Alharthy and Bethel employed the histogram of boundary points to generalize the footprint edges by assuming that the buildings have only two dominant directions that are perpendicular with each other. Based on the same assumption, Sampath and Shan used the least squares model to regularize the footprint edges. Recently, Zhang et al. have published a method to refine a footprint iteratively based on estimated dominant directions. Footprints with oblique edges, which are not perpendicular to dominant directions, are allowed in this method as long as the total length of the oblique edges is less than the total length of the edges parallel or perpendicular to the dominant directions.[12]

Simple building models can be derived by adding a uniform height value once a refined building footprint is derived. However, the process to derive sophisticated building models is more complicated. Schwalbe et al. categorized the methods to derive 3D building models into two categories: model-driven and data-driven. In the model-driven method, building models are identified by fitting predefined models into the LiDAR measurements For example, Maas and Vosselman estimated parameters for primitive building models based on the invariant moment analysis. Brenner extended this method to complex buildings by splitting a building into simple primitives fi rst and then fi tting individual primitives using point clouds [15]. However, building models for a study area are not always available in advance, which limits the application of the model-driven method.

In the data-driven method, building measurements are grouped first for different roof planes. Then, the 2D topology of each building, which is represented by a set of connected planar roof surfaces projected onto a horizontal plane, is derived. Rottensteiner and Jansa approximated pixels on edges with line segments first and then intersected these line segments to derive the vertices of the 2D topology. Alharthy and Bethel derived the polygon for each roof plane by connecting the boundary points and simplifying the polygon edges using the Douglas–Peucker algorithm. Polygons for each roof plane are then snapped into the 2D topology. Since neighboring roof polygons may overlap or be separated from each other, it is not easy to snap the neighboring polygons together. [9]

Raw 3D building models can be directly created from the derived 2D topologies and identified roof planes. However, the quality of such building models is poor because a 2D topology is often noisy due to irregularly spaced LiDAR measurements. Uncertainty in estimated

roof plane parameters due to errors in LiDAR measurements and segmentation also distort raw building models. A refinement of 2D topology and roof plane parameters is often needed to derive high quality building models. Many geometric constraints have been proposed to regularize and refine the 2D topology. Gruen and Wang proposed seven constraints formulated into weighted observation equations, and they enforced these constraints by using least squares adjustment (LSA). Before LSA is applied, points, lines, or planes related to each constraint should be grouped together manually, a step that limits the application of this method. Other methods realized the difficulty in enforcing many constraints simultaneously and only enforced important constraints, especially parallelism. The parallelism constraint assumes that a building has two dominant directions perpendicular to each other, and the building edges on the 2D topology should be parallel to either of the dominant directions. However, this assumption is too strict and cannot be applied to buildings with edges oblique to both dominant directions.[5]

Chapter Three

Application of Laser scanner

Chapter Three

Application of Laser scanner

3-1 Introduction

Turning next to laser ranging, profiling, and scanning, which are the main subjects of the present volume, lasers started to be used by surveyors for distance or range measurements in the mid- to late-1960s. These measurements were made using instruments that were based either on phase comparison methods or on pulse echo techniques. The latter included the powerful solid-state laser rangers that were used for military ranging applications such as gunnery and tracking. On the field surveying side, from the 1970s onwards, lasers started to replace the tungsten or mercury vapor lamps that had been used in early types of EDM (electronic distance measuring) instruments. Initially these laser-based EDM instruments were mainly used as stand-alone devices measuring the distances required for control surveys or geodetic networks using trilateration or traversing methods. The angles required for these operations were measured separately using theodolites. [10]

Later, these two types of instruments were merged with the laser-based ranging technology being incorporated into total stations, which were also capable of making precise angular measurements using opto-electronic encoders. These total stations allowed topographic surveys to be undertaken by surveyors with field survey assistants setting up pole-mounted reflectors at the successive positions required for the construction of the topographic map or terrain model. This type of operation is often referred to aselectronic tacheometry. With the development of very small and powerful (yet eye-safe) lasers, reflectorless distance measurements then became possible. These allowed manually operated ground-based profiling devices based on laser rangers to be developed, initially for use in quarries and open-cast pits and in tunnels (Petrie, 1990). [2]

Given all this prior development of lasers for numerous different field surveying applications, it was a natural and logical development for scanning mechanisms to be added to these laser rangers and profilers. This has culminated in the development of the present series of terrestrial laser scanners that are now being used widely for topographic mapping applications, either from stationary positions when mounted on tripods or in a mobile mode when mounted on vehicular platforms. [10]

3-2 Terrestrial Laser Scanning in Bridge Inspection

Heavy traffic and aggressive environmental conditions can cause unexpected bridge deterioration. Traditional condition evaluation is expensive. An alternative is Terrestrial laser scanning (TLS) which is a non-contact approach that safe, fast, and applicable to a range of weather conditions. This paper reviews applications of TLS on bridge measurement involving geometric documentation, surface defect determination, and corrosion evaluation, and crack identification. Currently, most post-processing of TLS is manual or within third party software. [16]

3-2-1 Principal of Terrestrial laser Scanner

TLS uses either ranging or triangulation scanners. With ranging, the distance between the transmitter and reflecting surface is computed either as the time of travel between signal transmission and reception called the time of flight (ToF) of a laser pulse or the phase difference between the transmitted and received wave, which is referred to as the phase comparison method. The latter one uses a transmitting device and a charge-coupled device sensor to detect the laser spot on an object. Then the three dimensional (3D) position of the reflecting surface element can be derived from the resulting triangle. For bridges and other large structures, ToF scanners are preferred because of their longer range. [15]

The ToF scanner generates scanned points through a series of range measurements with uniform angular increments in both horizontal and vertical planes. This is controlled by rotating and nodding mirrors and rotating head mechanisms. Thus, each sampled point is defined by spherical coordinates with the range measurement, R, horizontal direction, θ, and vertical angle,. α.[15]

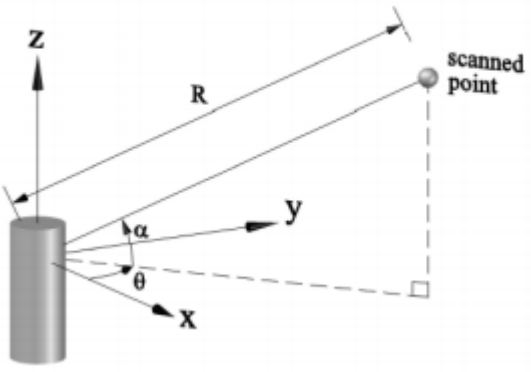

Figure (3-1): The principal of laser beam scanning [4]

A range measurement is the distance from the transmitter to a reflecting surface, R, as expressed in Equation (3.1): [14]

$$R = CT\frac{1}{2} \quad (3.1)$$

where t is the time interval between the emission and the pulse and its reception of the backscattered portion, and c is the velocity of light through air (3x10^8 m/s). A scanner's accuracy is largely based on the accuracy of the time measurement of the electronics integrated into the circuit (Equation 3.1). Furthermore, the ranging accuracy is inversely proportional to the ratio of signal to noise, which depends on various factors such as the power of the received signal, input bandwidth, background radiation, and amplifier noise. [14]

$$\Delta = \frac{1}{2}c\Delta t \quad (3.2)$$

Each raw scanned point (R, θ, α) is automatically converted into a set of three-dimensional Cartesian coordinates (x, y, z) by the scanner software, where the origin coordinate is at the scanner. Beyond the 3D coordinates of the scanned points, the scanner also acquires intensity values, which is a measure of the electronic signal strength obtained by converting and amplifying the backscattered optical power. Pfeifer et al. proposed the relationship between the emitted power, PE and the received power. PR as expressed in Equation (3.3) when the temporal variations of the pulse power are neglected. [14]

$$PR = PE\frac{\cos\alpha}{4R2}\pi\rho\,\eta_{Atm}\eta_{\mathrm{Sys}} \quad (3.3)$$

where ρ is the reflectance of material, R is the range measurement, and ηAtm and ηSys are respectively the atmospheric and system losses. Equation 3 implies that the intensity values strongly depend on the reflectance of the material, the incidence angle underlying a constant of atmosphere, and the range measurement. [14]

By integrating a camera within the scanner, photographs of the scene can be taken simultaneously. From these images red, green, and blue (RGB) values can then be mapped onto each positional data point. Thus, information with each point cloud provided by TLS involves 3D coordinates, intensity values, and RGB values. To understand the capabilities of TLS in surveying bridge structures for inspection, the next section investigates recent work on TLS data processing in that field. [14]

3-1-3 Bridge Inspection

TLS acquires 3D geometric data of a structure's surfaces as discrete data points. That information can be used to either reconstruct 3D models of the structures or to detect surface changes over time. [1]

3-1-3-1 Geometric reconstructions

Some of the earliest applications of TLS to bridges have been for the acquisition of historical arch bridges geometries. In some cases, the surfaces were then derived by mesh triangulation to generate solid models and create a permanent record. In some instances, such as the work by Riveiro et al TLS was combined with close range photogrammetry. Similarly, Lubowiecka et al. combined TLS with ground penetrating radar for a medieval bridge models to provide insight into the internal structure (fill material, arch stones and air water interface) of the bridge. Typically, these efforts rely on third party software or researcher driven algorithms such as that by Armesto et al. who proposed fitting a non-parametric regression method based on a local bivariate kernel smoothing approach from the point clouds for Spain's Segura Roma bridge. [1]

3-1-3-2 Vertical bridge displacement

The first published vertical deflection measurements for bridges was done by Lichti et al. in 2002, who measured displacements of stringers of a wood bridge in Perth, Australia. Vertical displacements were estimated by comparing fitting lines of the bottom and top of each stringer cross-section under loaded and unloaded conditions. Results showed that stringers deflections based on TLS data were larger than ones from image-based methods. [1]

Subsequently, Zogg and Ingensand monitored deformations of the Felsenau bridge subjected to a static load of 54 tons performed at several sections of the viaduct. Third party software was used to determine vertical displacements by comparing the 3D point cloud from the unloaded condition against the loaded condition. The TLS-based results were no more 3.5mm larger than ones based on precision levelling. [1]

When measuring deflections of the Pentele bridge under the static load, Lovas et al reported that vertical displacements from TLS data gave strong correlations with traditional methods, although it over predicted the high-precision levelling and under predicted the total stations. [1]

Paffenholz et al. proposed a cell-based method to estimate vertical displacements. The scanned region was divided into sub-areas of 0,25m x 0,25m, and the median of z coordinates of each sub-area was used to determine the vertical displacements. Deflections up to 3mm were reported, but the accuracy was not. Finally, Berenyi et al. noted that TLS can be used to measure the movements of the pylons and cables, whereas the traditional method cannot be done or unaffordable. [1]

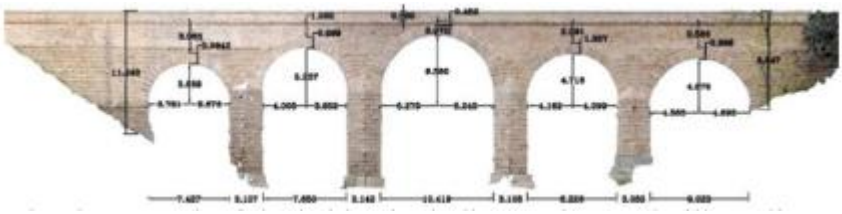

a) Orthophotograph of the bridge including arches and pillars dimensions

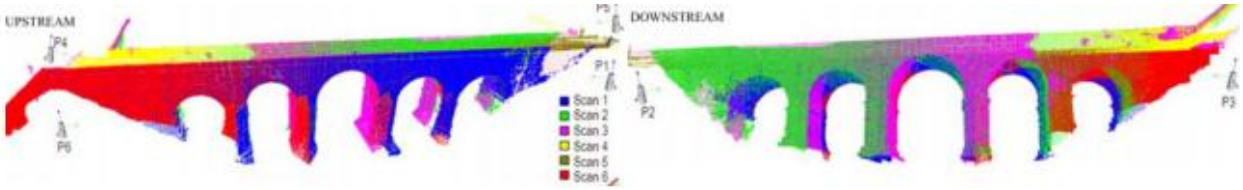

b) Scan stations and point clouds of the bridge

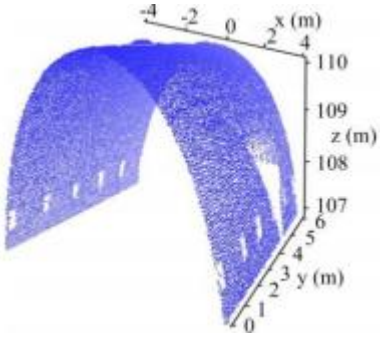

c) Point cloud of the second arch of the bridge

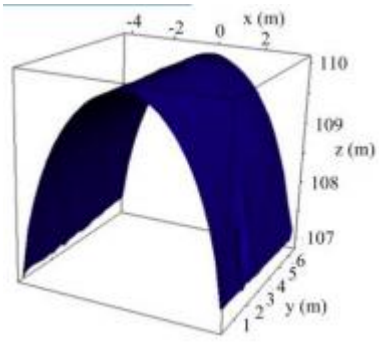

d) 3D arch model obtained for the bandwidth of 0,06 used in the kernel estimation

Figure (3-2): Reconstructing bridge models from TLS data by a non-parametric estimation algorithm [1]

3-3 Cultural Heritage Applications

Cultural heritage is a testimony of past human activity and, as such, cultural heritage objects exhibit great variety in their nature, size and complexity, from small artefacts and museum items to cultural landscapes, from historic buildings and ancient monuments to city centers and archaeological sites. Due to the rapidity of data capture and the ability to obtain point clouds instantaneously, laser scanning has become an essential tool along with image-based documentation methods. Total station surveys, on the other hand, require more time on site and usually do not deliver the same level of surface detail. [3]

Cultural heritage objects and sites are often a conglomerate of irregular surface geometries. Although photogrammetry will work for similar structures, laser scanning provides dense 3D information in almost real time with a high capacity for visualization as a first on-site preresult. Laser scanning is of interest where documentation is usually a complex task. The variety of applications includes pure visualisation as well as heritage recording and as-built documentation. [3]

3-3-1 Accurate site recording: 3D reconstruction of the treasury (Al-Kasneh) in Petra, Jordan

The ancient Nabataean city of Petra has often been called the eighth wonder of the ancient world. Petra city in south-western Jordan (Figure 8.1) prospered as the capital of the Nabataean empire from BC 400 to AD 106. [9]

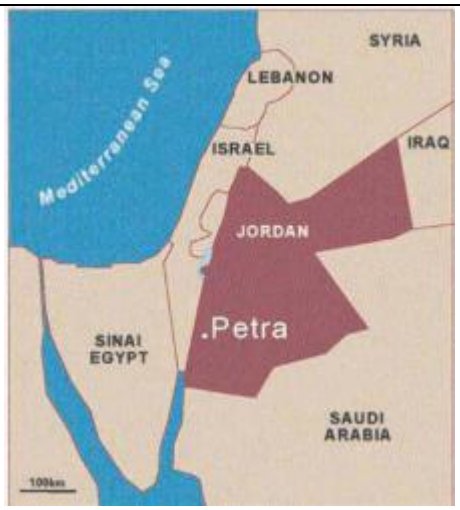

Figure (3-3): Geographical situation of Petra, Jordan [9]

Petra's temples, tombs, theatres and other buildings are scattered over 400 square miles, carved into rose-coloured sandstone cliffs. When a visitor enters Petra via Al-Siq, an impressive two-kilometre crack in the mountain, he will first see Al-Khasneh, which is probably the most famous object in Petra. The Al-Khasneh façade is 40 m high and remarkably well preserved, probably because the confined space in which it was built has protected it from the effects of erosion. The name Al-Khasneh means "treasury or tax house for passing camel caravans", but others have proposed that the Al-Khasneh monument was a tomb. Behind the impressive façade there are large square rooms that have been carved into the rock. [3]

The 3D laser scanning system Mensi GS100 was applied. The scanner features a field of view of 360o in the horizontal direction and 60o in the vertical direction, enabling the collection of full panoramic views. The distance measurement is obtained using the time-of-flight measurement principle based on a green laser at 532 nm allowing an object distance between 2 and 100 m. The system is able to measure 5000 points per second. During data collection a calibrated video snapshot of 768 s 576 pixel resolution is additionally captured, which is automatically mapped to the corresponding point measurements. Because of the complex structured sites, multiple scanner stations had to be chosen to avoid most of the occlusions. [9]

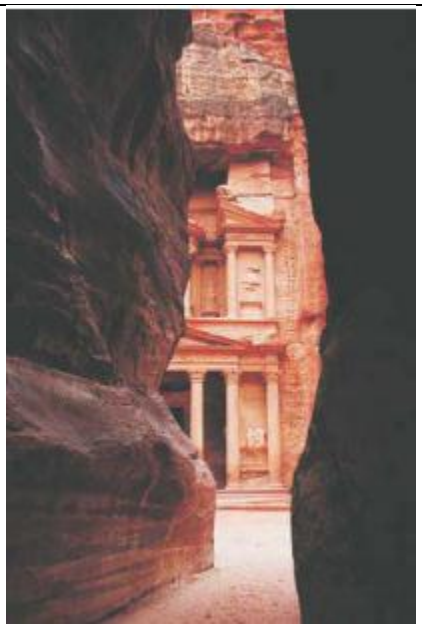

Figure(3-4): The Outer Siq at the Khasneh al-Faroun [6]

For texturing of the 3D model, additional images were collected by a Fuji S1 Pro camera, with a focal length of 20 mm and a sensor format of 1536 s 2034 pixels. [6]

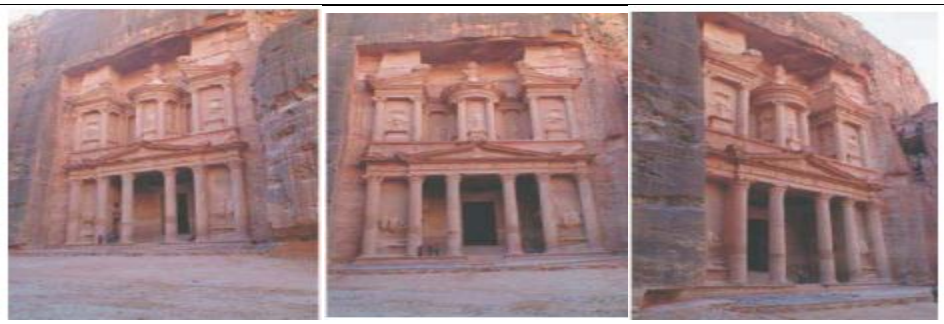

Figure (3-5): Images collected using a Fuji [9]

The acquired 3D point clouds have been processed using Innovmetric's PolyWorks™ Software. Registration of the scans for both models was done using corresponding points. The models produced have an average point spacing of 5 cm with more than 2 000 000 triangles for the entire model. [6]

Figure (3-6): 3D model of Al-Khasneh [6]

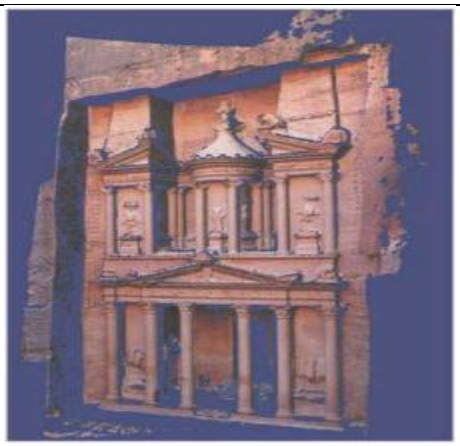

Figure (3-7): Final textured model using four images [6]

The work was carried out by Yahya Alshawabkeh and Norbert Haala, Institute for Photogrammetry (IFP), University of Stuttgart, Germany, with support from Hashemite University of Jordan, Petra, Regional Authority and Jerash Municipality ,Jordan. [11]

Performing projective texture mapping to generate photo-realistic models of the complex shaped objects with minimal effort, it was necessary to compute visibility information to map the image only onto the portions of the scene that are visible from its camera viewpoint. For this purpose an efficient algorithm addressing image fusion and visibility has been developed . [9]

The result was a textured 3D model of the site (Figure 8.5) demonstrating the possibilities of the integration of laser scanning and photogrammetry for data capture of historic scenes. [6]

3-3-2 Archaeological site: scanning the pyramids at Giza, Egypt

In 2004 was to apply Scanning of the Pyramids and test the latest state-of-the-art terrestrial laser scanners combined with a calibrated digital Final textured model using four images camera for high-accuracy, high-resolution and long-distance topographic scanning in archaeology. [7]

A long-range laser scanner Riegl LMS Z420i combined with a calibrated Nikon D100 digital camera was used for this project. The combined sensor of a high-performance long-range laser scanner and a calibrated and orientated high resolution digital camera provides scan and image data.. [6]

The three main objectives of the Scanning of the Pyramids project are:

1- The collection of high-resolution and high-accuracy topographic data for the creation of a digital elevation model of the Giza plateau.
2- 2-A 3D documentation of the Cheops Pyramid and surroundings.
3- 3-A 3D documentation of the Sphinx.
4- The Riegl Z420i scanner was taken to the top of the Great Pyramid of Cheops for a full ten hours of data collection. [14]

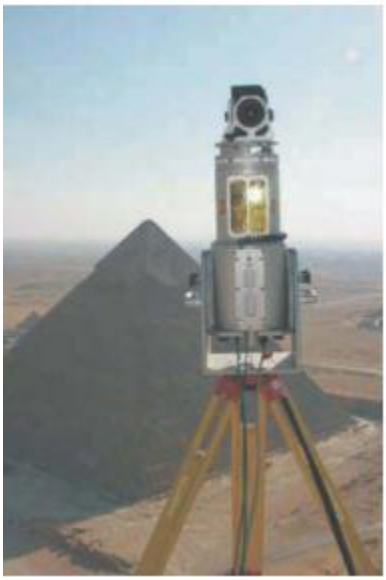

Figure (3-8): LMS-Z420i with calibrated high-resolution digital camera Nikon D100 at the top of the Cheops Pyramid, Egypt [14]

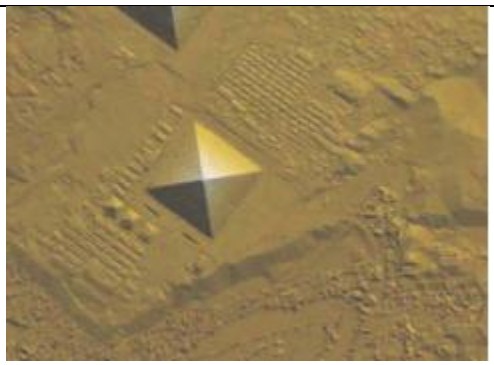

Figure (3-9): Overview and detail of the digital elevation model of the Giza Plateau created using four single scans from the top of the Cheops Pyramid visualized in ARC GIS 8.2.[14]

Figure (3-10): Single scan from the north and east faces of the Chephren Pyramid visualised as a coloured point cloud.[14]

Figure (3-11): Triangulated point cloud of the Sphinx textured in Rican Pro, combined from seven scanner positions: six from the ground and one from the Cheops Pyramid.[14]

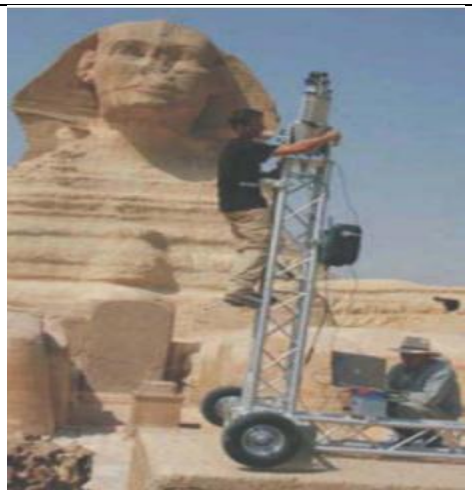

Figure (3-12): Mobile scanner in front of the Sphinx[14]

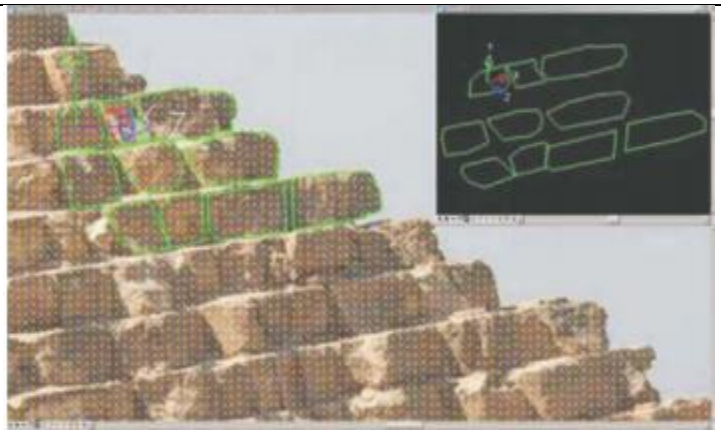

Figure (3-13): Single stones can be directly drawn in global 3D coordinates and made visible in the point cloud, superimposed with a photograph using the Micro station application PHIDIAS.[14]

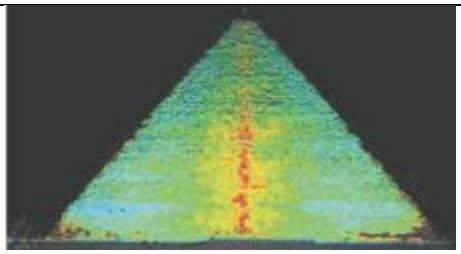

Figure (3-14): Anomalies of the Cheops Pyramid: horizontal projection of the west side with color-coded deviation from the plane.[14]

These data have been processed automatically with human interaction in some processing steps for the generation of textured triangulated surfaces (Figure 3.10) and orthophotos with depth information (Figure 3.14).

3-3-3 The archaeological project at the Abbeynof Niedermunster, France

Located at the bottom of Mount Sainte-Odile, the Abbey of Niedermunster, Alsace, France can be considered as the origin of the sanctuary. Built between AD 1150 and 1180, the Roman-style Abbey was devastated during the War of the Peasants (1525) and by two fires, in 1542 and 1572. The site was then used as a quarry until the nineteenth century. The great western massif of the basilica, still in elevation, and the relics of the crypt allow the beauty of the original buildings to be imaged. [2]

During the first stage, the archive archaeological records were georeferenced in a Geographical Information System after an accurate topographic survey. The second stage of scanning was accomplished in two steps: scanning of the abbey's area in its current state, followed by supplementary scanning site details. [2]

Data acquisition consisted of scanning the complete site using 3D terrestrial laser scanning [Koehl and Grussenmeyer, 2008]. A Trimble GX Advanced scanner was used.This allowed the acquisition of point clouds for which the density was defined by the operator according to the expected degree of detail. A grid density of 1000 points/m2 was generally used. The obtained point clouds were georeferenced; the information for every point was thus constituted by *X*-, *Y* - and *Z*-coordinates in the ground coordinate system, completed by intensity or colour. For the complete digitising of the site, about 15 scanner positions were used, which resulted in 40 different scans, giving a total of approximately 30 million points (Figure 3.15). [2]

Figure 3.16 is an illustration of the point cloud of the occidental block which is still standing up to its first level. Interior parts such as stairways and the porch have also been scanned. Eight scanning stations were used for this part of the project. Figure 3.17 illustrates the process of combination of meshed surfaces computer from the terrestrial laser scanning point clouds and a CAD model used in the case of flat surfaces. The fusion of the two models was used for the creation of the complex and ruined parts of the project. For the constitution of the 3D model, textures were mapped as shown in Figure3.18. Some parts have been textured, others were only face-coloured. The inner parts are shown by application of surface transparency. [14]

Figure (3-15): Fusion of point clouds in one project. [14]

Figure (3-16): Fusion of point clouds of the occidental block.[14]

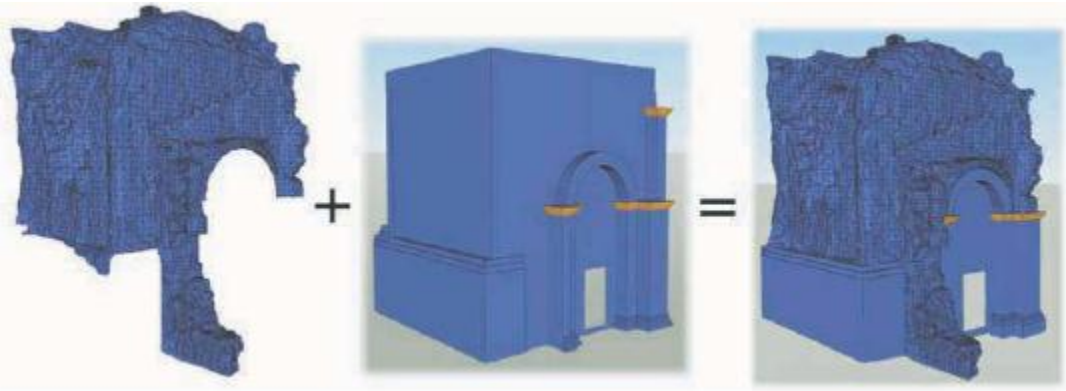

Figure (3-17): Model creation as CAD extrusions and meshed model from point clouds. [14]

Figure (3-18): Textured model of the occidental block.[14]

Figure (3-19) shows a detailed point cloud of the crypt. This part of the project is composed of two stairways, some pieces of pillar and an inner vaulted wall. As in the other parts of the abbey, the walls remained in a good state of conservation, but other parts were ruined. The resulting model (Figure 3-20) combines meshed point clouds and CAD models. The structure lines of the main parts used in the modeling process result from a manual segmentation. Figure. (3-21) is the result of the texturing process of the crypt model. [2]

Figure (3-22) illustrates the different representation modes in the case of the acquisition of a pillar base. Terrestrial laser scanning offers the possibility of viewing the different point clouds in a colour mode. This is used to show the different segmented clouds. Intensities were also acquired by the laser scanner. The intensity mode can be used to analyse the responses of the scanner according to the surface texture. The true colour rendering mode uses the colour of each point according to its position in an image acquired by the laser scanner camera. The last illustration shows the CAD. [2]

Figure (3-19): Point cloud of the crypt. [14]

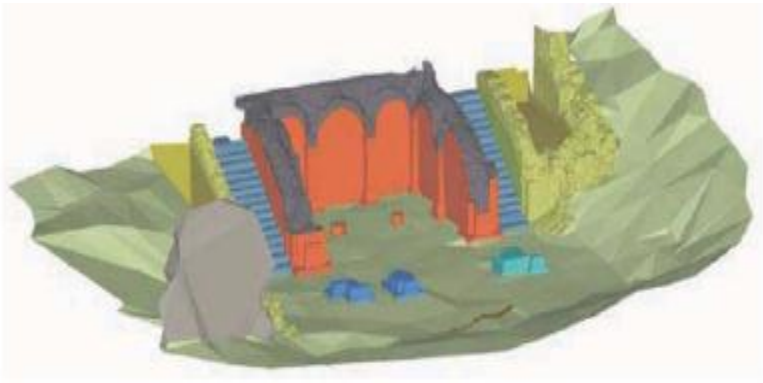

Figure (3-20): CAD model from terrestrial laser scanning data.[14]

Figure (3-21): Textured model of the crypt.[14]

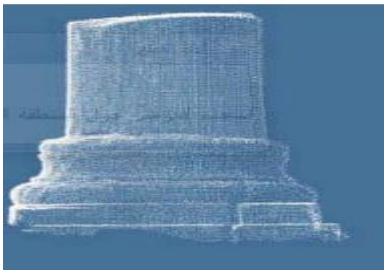

(a) white point cloud

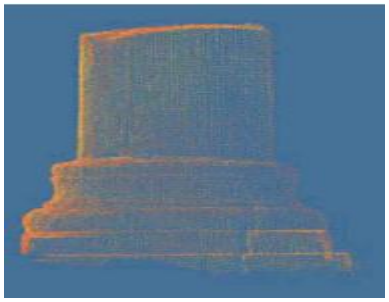

(b) intensity cloud

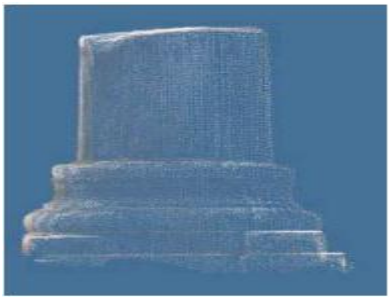

(c) true colour

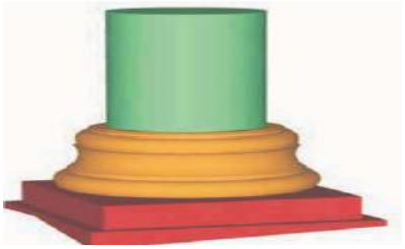

(d) CAD model.

Figure (3-22): Detail of a pillar [14]

Figure (3-23): 3D model of the Niedermunster Abbey site.[14]

model extracted from the point clouds using a segmentation of the profile. An extrusion process was then used for design of the model. [2]

Figure (3-23) shows the 3D model of the whole site, allowing animations and walkthroughs. [2]

3-4 Forest inventory applications

Forest inventory is a task which has to be fulfilled by forest authorities at regular time intervals to monitor the state of their forests. It includes the determination of a number of parameters characterizing the forest. As full area coverage is an unrealistic goal in forest inventory using conventional techniques, inventory schemes based on data acquisition in isolated plots and statistical inference methods have been developed. Some of the most important parameters to be determined in forest inventory are the number of trees in a certain plot, the determination of the diameters at breast height and the tree heights. Terrestrial laser scanning, combined with reliable automatic data-processing techniques, may provide an interesting tool to bridge the gap between conventional inventory techniques and airborne laser scanner data-processing schemes and to facilitate data acquisition for 3D individual tree geometry parameters in large plot. [6]

The data-processing chain used in the studies can be outlined as follows:
1- Digital terrain model reduction: the digital terrain model is determined by a simple height histogram analysis searching for minima in predefined XY meshes of the laser scanner data, followed by a neighborhood consistency check and bilinear interpolation in the meshes. All laser scanner points are reduced to this terrain model. [7]

2- Segmentation and counting of trees: the tree detection process is based on mathematical morphology techniques, extended from raster image analysis to irregularly distributed points in horizontal slices of the laser scanner data. [7]

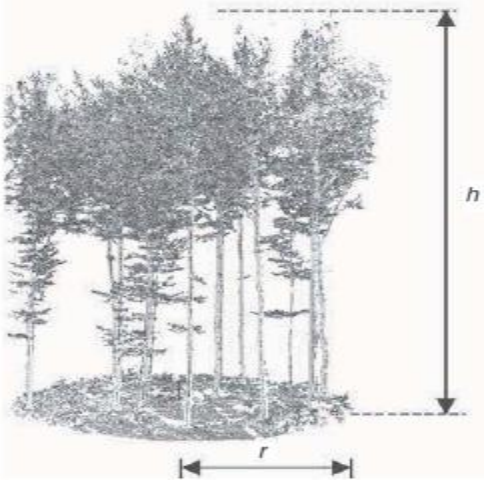

Figure (3-24): point cloud of a single panoramic scan [5]

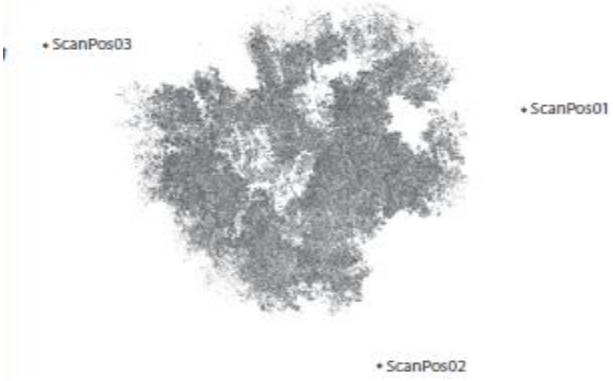

Figure (3-25): point cloud from a multiple scan mode with three instrument position [5]

3- Determination of diameter at breast height: the diameter at breast height (DBH) is defined as the diameter 1.3 m above the finished grade at the end of the trunk.It is determined by fitting a circle into the point cloud of each detected tree and analyzing the results using robust estimation techniques. [7]

4- Tree height determination: the tree height is calculated as the height difference between the highest point of the point cloud of a tree and the representative ground point using a similar procedure to that reported.Generally, tree height determination procedures remain rather vague due to under sampling, occlusions and wind effects in the crown. [7]

5- Stem profiles: repeating the technique of stem position and diameter at breast height determination in predefined height intervals at the same (X,Y)-location, stem profiles containing information on shape, uprightness and straightness can be determined. The probability of gross errors in the diameter determination is further reduced by using knowledge of the tapering of the stem in a subsequent filtering operation. [7]

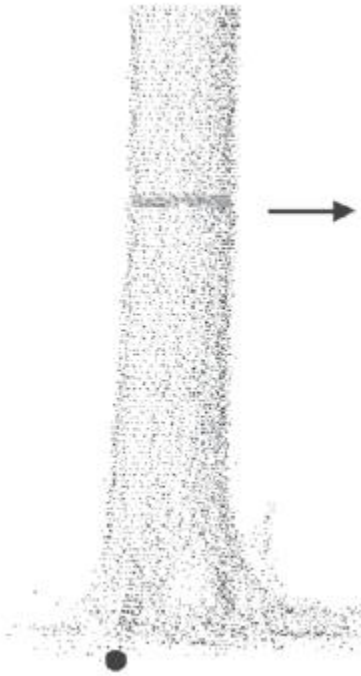

Figure (3-26): Ground point of a tree on sloping terrain [6]

Of tree detection was 97.5%. Type I errors (trees which were not detected) were mostly caused by full or partial occlusions of stems in single panoramic scan data. Type II errors (false detections) could largely be eliminated in later processing steps by checking the tree height or by an analysis of the stem profile. From a comparison with conventional calliper measurements, an RMS error of 1.8 cm could be obtained for the automatic determination of diameter at breast height. This value contains the laser scanner instrument precision as well as the precision of caliper measurement and deviations of the stem from circularity. Automatic tree height determination turned out to be much more critical: compared to hand held tachymeter height measurements, an RMS error of 2.07 m was obtained. This error has to be attributed to both occlusions in the point cloud and the limited precision of the reference measurements. Vertical stem profiles were derived by applying the circle fit procedure at multiple height steps. A comparison with harvester data yielded an RMS profile diameter difference of 4.7 cm over the whole tree, with larger deviations occurring in the lower and upper part of the stem. Over the economically most relevant branch and root free part of the stem, the RMS diameter deviation was only 1.0 cm. [6]

Chapter Four

Results and Analysis

Chapter Four

Results And Analysis

4-1 Introduction

In this chapter, photographs of the Palestine Polytechnic University mosque were taken using a drone, These images have been added to the program Agisoft Photoscsan, a three-dimensional model of the mosque was produced from all sides.

In 2017 ,Palestine Polytechnic University had laser scanner TX5 with characteristic :High accuracy, High resolution, High speed, Intuitive control via the built in touchscreen display, High mobility due to its small size, light weight, and the integrated quick charge battery, Photorealistic 3D color scans due to the integrated color camera, Integrated dual axis compensator to automatically level the captured scan data and Integrated compass and altimeter to give the scans an orientation and a height information. This project is aimed as training for use in the most proper and practical application.

Figure (4-1): First test model for Palestine Polytechnic University Mosque

4-2 Field Work Using By Agisoft Photo Scan Software

4-2-1 Agisoft PhotoScan

Agisoft PhotoScan is a stand-alone software product that performs photogrammetric processing of digital images and generates 3D spatial data to be used in GIS applications, cultural heritage documentation, and visual effects production as well as for indirect measurements of objects of various scales.

Agisoft PhotoScan is an advanced image-based 3D modeling .Based on the latest multi-view 3D reconstruction technology, it operates with arbitrary images and is efficient in both controlled and uncontrolled conditions. Photos can be taken from any position, providing that the object to be reconstructed is visible on at least two photos. Both image alignment and 3D model reconstruction are fully automated.

4-2-2 Procedure

Step 1_ Add Photos

To add photos select Add Photos... command from the Workflow menu or click Add Photo. In the Add Photos dialog browse the source folder and select files to be processed. Click Open button.

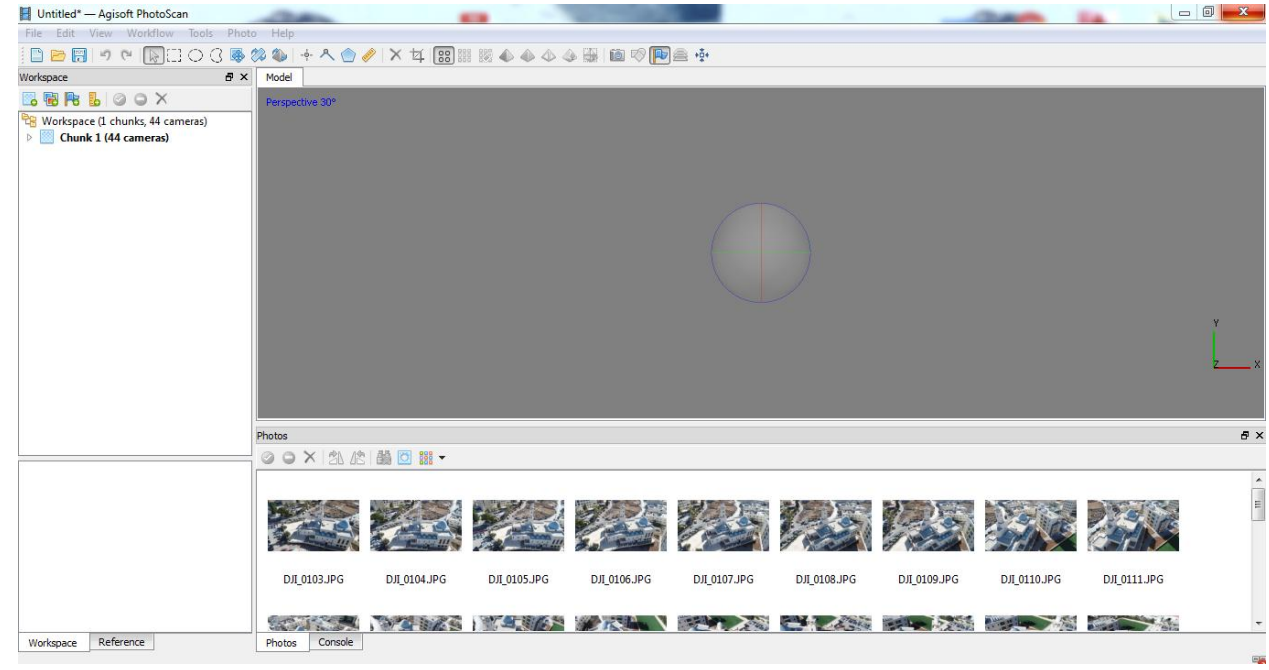

Figure (4-2): Adding photo for first test model by Agisoft photoscan

Step 2_Mask Photos

To achieve good reconstruction results it is necessary to mask all irrelevant elements on the source photos.

Step 3_Align Photos

At this stage PhotoScan refines the camera position for each photo and builds the point cloud model. Select Align Photos command from the Workflow menu.

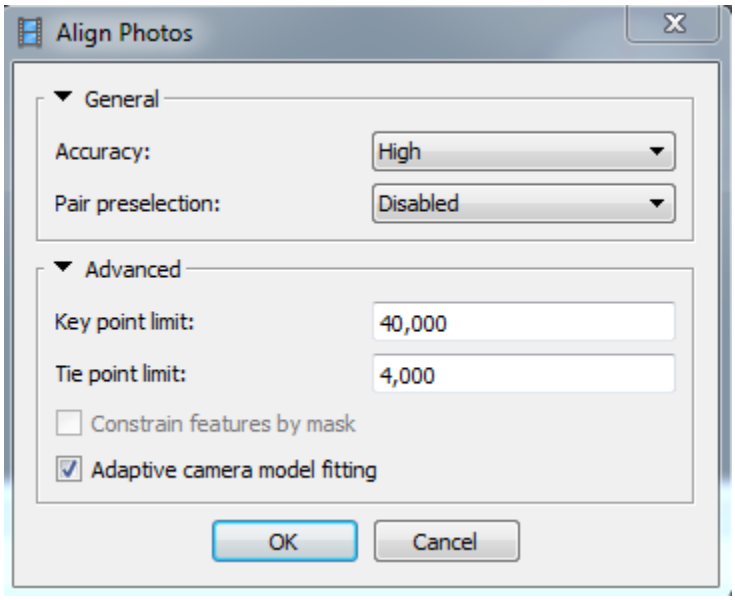

Figure (4-3): Aligning photo for first test model by Agisoft photoscan

Set the following recommended values for the parameters in the Align Photos dialog:

Accuracy: High (higher accuracy setting helps to obtain more accurate camera position estimates. Lower accuracy setting can be used to get the rough camera positions in the shorter time).

Constrain features by mask: Enabled (if the mask covers any moving objects including clouds) or Disabled (if all masked area was static during shooting).

Key point limit: 40000

Tie point limit: 4000

This step is optional since PhotoScan automatically calculates bounding box dimensions and location. But it is recommended to check if any correction is needed, because geometry reconstruction step deals only with the point cloud inside the volume.

After photo alignment is finished, refine bounding box position and orientation to fit the object:

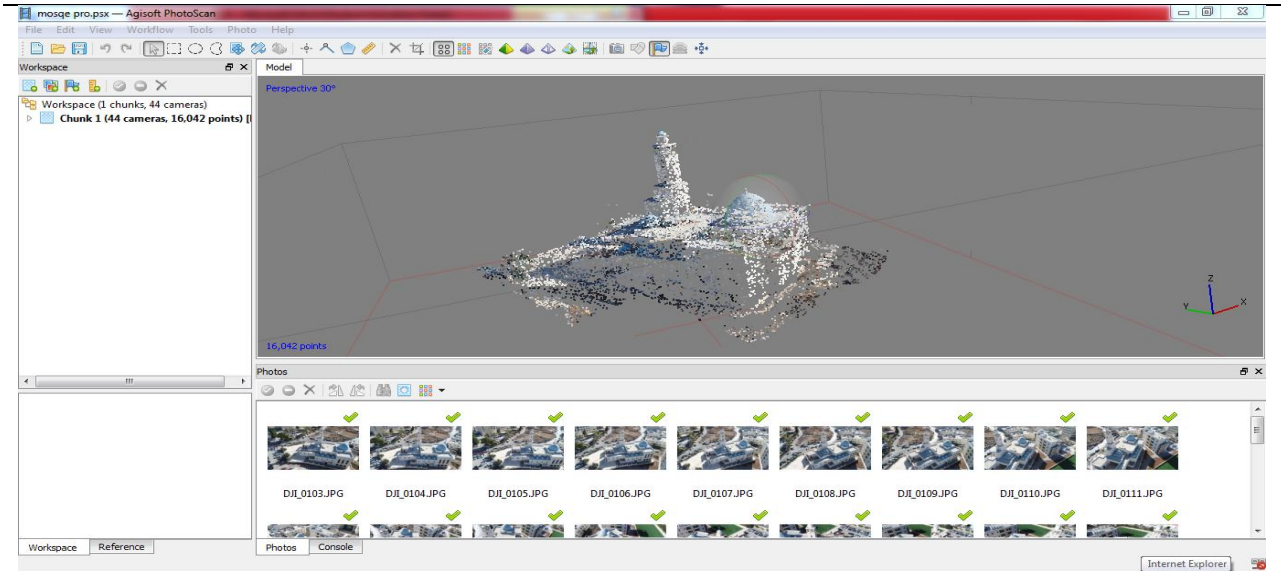

Figure (4-4): Aligning photo for first test model by Agisoft photoscan

Step 4_Build Dense Point Cloud

Dense Point Cloud Based on the estimated camera positions the program calculates depth information for each camera to be combined into a single dense point cloud. Select Build Dense Cloud command from the Workflow menu.

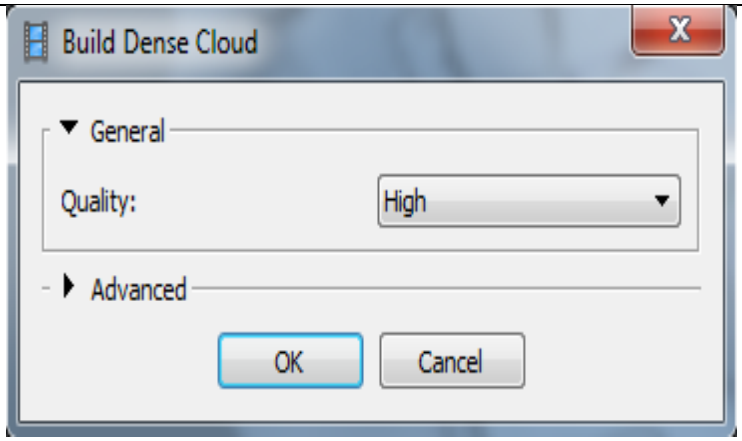

Figure (4-5): Building Dense Point Cloud for first test model by Agisoft photosca

Set the following recommended values for the parameters in the Build Dense Cloud dialog:

Quality: High

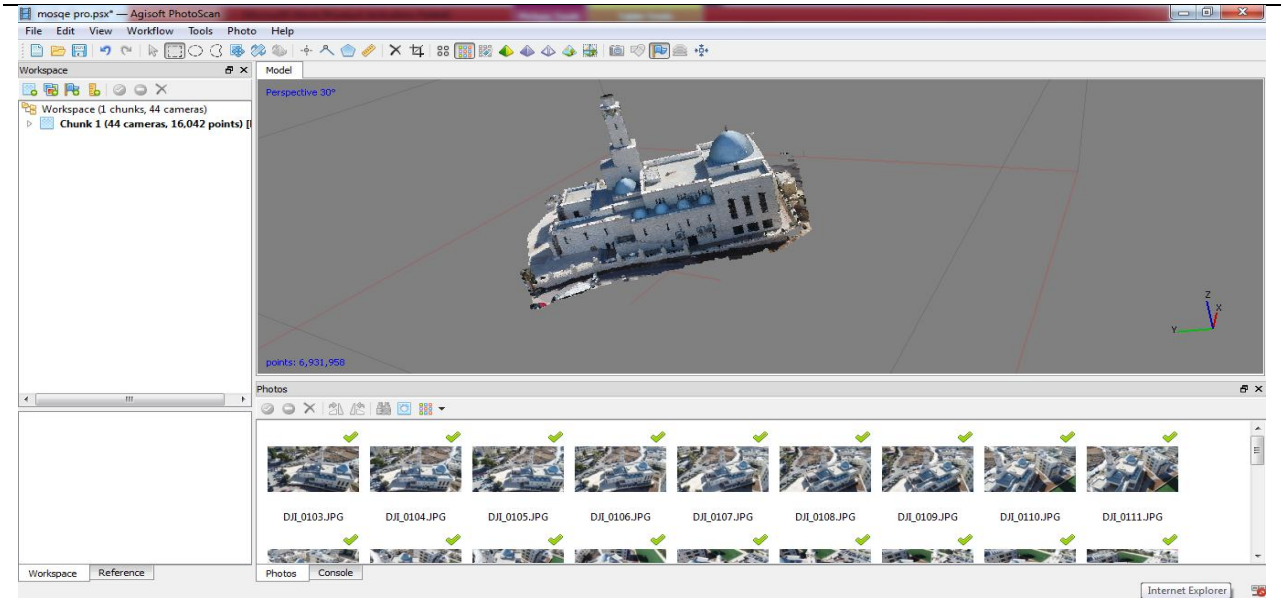

Figure (4-6): Building Dense Point Cloud for first test model by Agisoft photoscan

Points from the dense cloud can be removed with the help of selection tools and Delete/Crop instruments located on the Toolbar.

Step 5_Build Mesh

After dense point cloud has been reconstructed it is possible to generate polygonal mesh model based on the dense cloud data.

Select Build Mesh command from the Workflow menu.

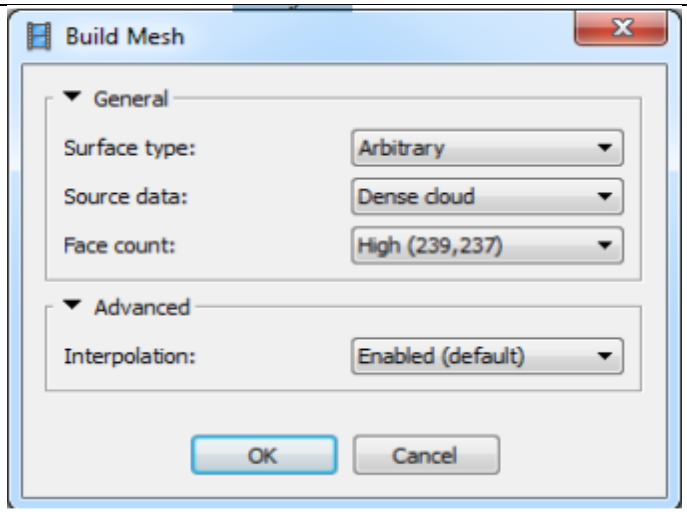

Figure (4-7): Building Mesh for first test model by Agisoft photoscan

Set the following recommended values for the parameters in the Build Mesh dialog:

Surface type: Arbitrary

Source data: Dense cloud

Polygon count: High

Interpolation: Enabled

Click OK button to start geometry reconstruction.

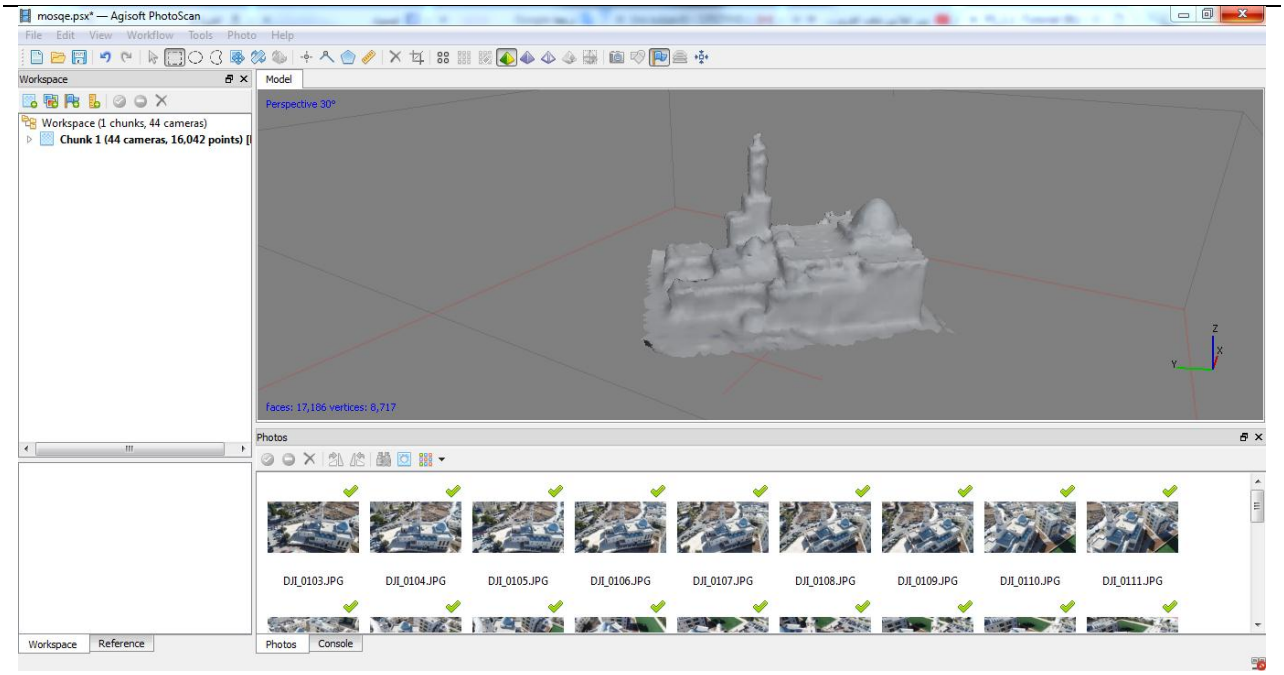

Figure (4-8): Building Mesh for first test model by Agisoft photoscan

Step 6_Build Texture

This step could be skipped if untextured model is sufficient as the final result.

Select Build Texture command from the Workflow menu.

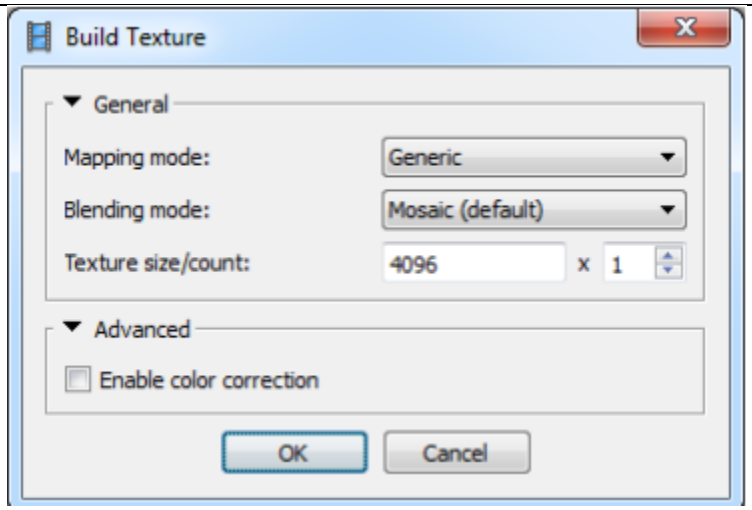

Figure (4-9): Building Texture for first test model by Agisoft photoscan

Set the following recommended values for the parameters in the Build Texture dialog:

Mapping mode: Generic

Blending mode: Mosaic

Texture size/count: 4096 x 1 (width & height of the texture atlas in pixels and determines the number of files for texture to be exported to. Exporting texture to several files allows to archive greater resolution of the final model texture, while export of high resolution texture to a single file can fail due to RAM limitations)

Enable color correction: disabled

Click OK button to start building texture.

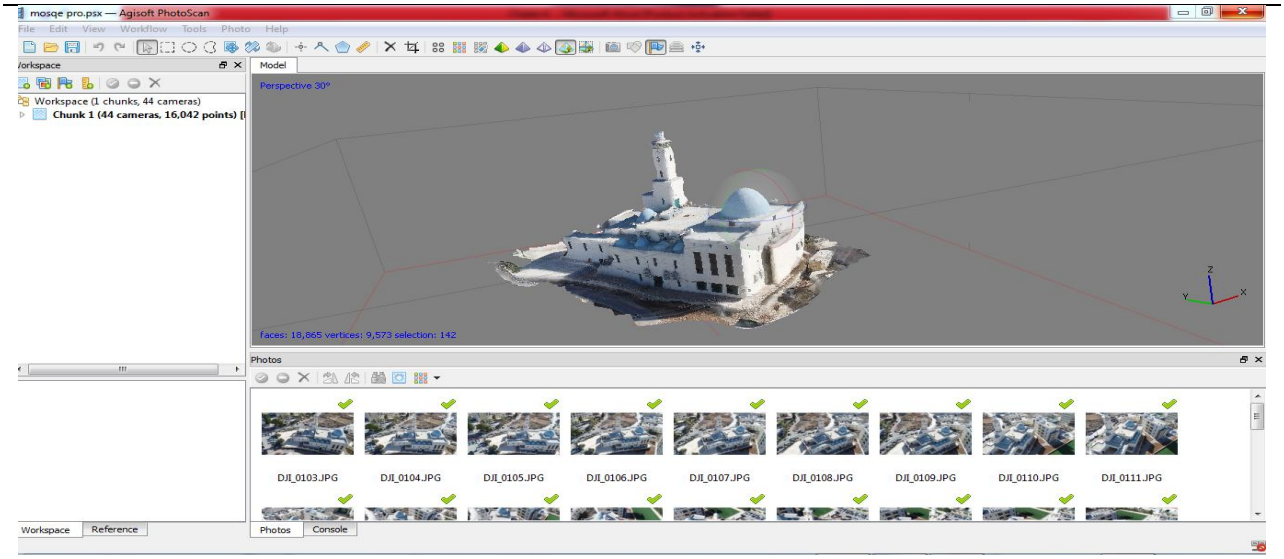

Figure (4-10): Building Texture for first test model by Agisoft photoscan

Step_5: Tilted Model

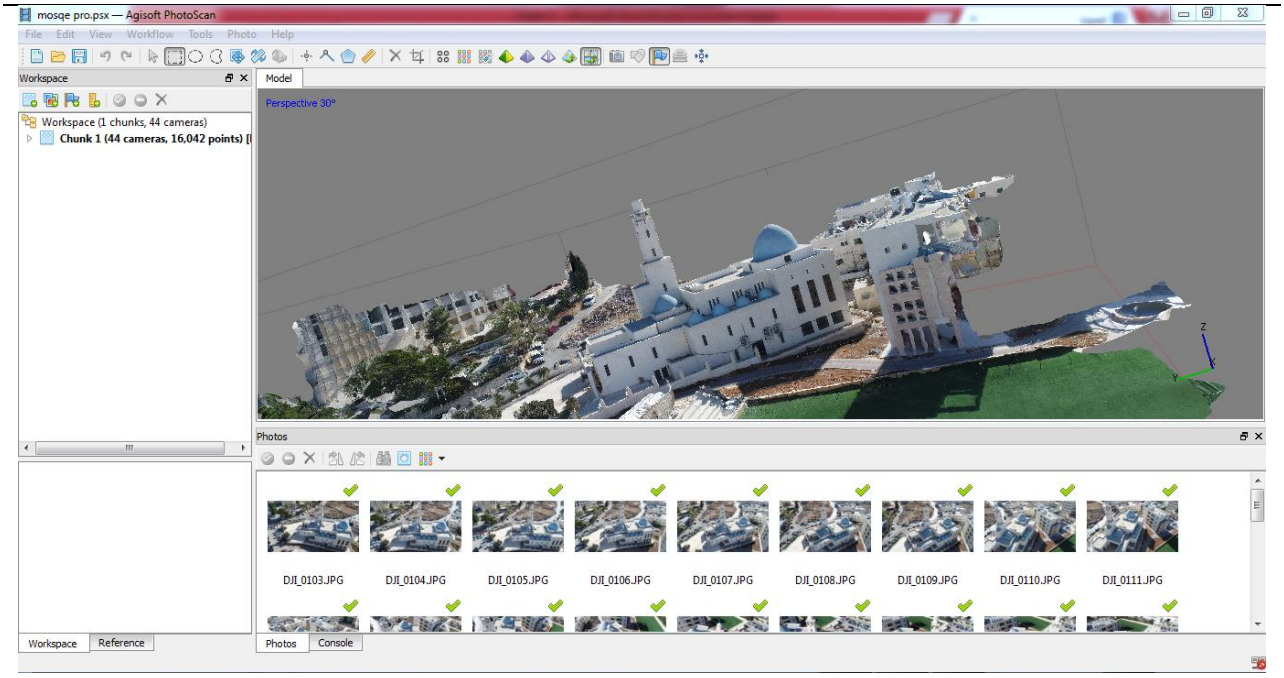

Figure (4-11): Tilted Model for first test model by Agisoft photoscan

4-3 Field Work Using By PointCap Software

4-3-1 Introduction:

Our target-based registration is a manufacturer-independent solution for rapid and exact referencing and registration of terrestrial laser scanning data.This also enables you to merge scans from different terrestrial laser scanners in one joint project.

The efficient search for target marks and spheres, and the search for assignment between the individual scanner positions, combined with optimized equalization and a detailed log make this solution an integral constituent part of the laser scanning evaluation. With the possibility to use natural point correspondences, even an inexperienced user is able to register projects for terrestrial laser scans without target marks and spheres.

With the PointCab software, the processing of high-resolution point clouds is easy as can be is the entry-level solution for the efficient processing of point clouds to create detailed 2D ground plans and façade views.

The PointCab software is compatible with all current CAD systems and is therefore used in many areas such as architecture, building industry, geodesy, civil engineering, monument protection and facility management.With the practical functions for measurement, the simple web export, and the alignment tools, getting started is child's play.

4-3-2 Applications:

Our software is used in a wide variety of industries. Here are examples of how the Point Cab software can help you with your applications.

1. Architecture: building footprints and sections, floor plans, facade plans, interior wall documentation, staircases
2. Monument protection: elevations, ceiling paintings
3. Surveying: site plans, inventory plans, site maps, roof cadastres, pit cuts, terrain profiles, tunnel sections, cross sections, road profiles
4. Factory planning: pipeline documentation, set-up and machine layout plans, cuts through production and factory halls, sections for static considerations
5. Forensics: Basis for simulations, trajectory analyzes, accident documentation.

4-3-3 Registration:

Our target-based registration is a vendor-independent solution for fast and accurate referencing and registration of terrestrial laser scanning data. This allows you to combine scans from different terrestrial laser scanners in a single project.

The efficient search of targets and bullets and the search for a match between the individual scanner positions as well as an optimized adjustment with detailed protocol make this solution an integral part of the laser scanning evaluation. With the ability to use natural point correspondence even the untrained user is able to register terrestrial laser scanning projects without targets and bullets.

4-3-4 Target based registration for surveyors

1. Required preferences:

Select File > Settings and Registration tab. Here you can set preferences for a-priori accuracy of features (checkerboard targets, spheres, points) as well as your potential geodetic points (references). The relation of accuracies is decisive. Please respect that points generally provide significantly worse accuracies than checkerboard targets and spheres. If geodetic points are set via GPS, you can assume an accuracy of 30mm, for example.

Furthermore, you can determine if checkerboard targets and/or types of spheres shall be searched. These settings are automatically applied in each new project.

In the Sketch/Panorama tab, you deactivate the settings Colorized panorama to load scan views as reflectivity image more quickly later.

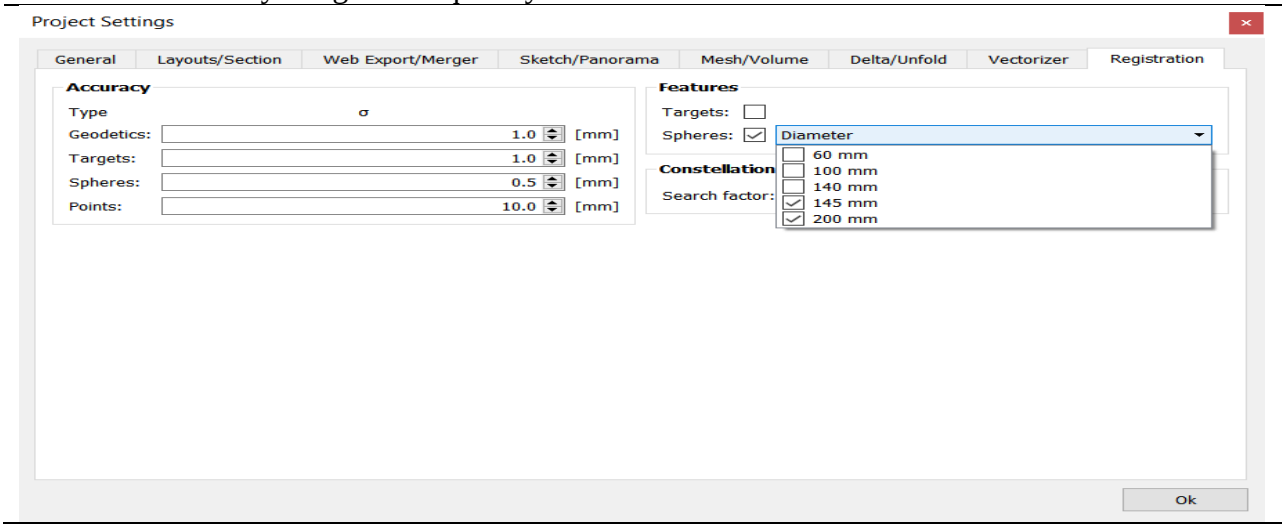

Figure (4-12): Required preferences

2. Create a project and import scans

Start a new PointCab project by selecting New > Advanced Importer. Enter a project name and save the project at a place of your choice. The Advanced Importer opens automatically.

Open your folder with FARO scans in RAW format using Windows Explorer or a comparable file browser. Select all scan folders together and drag and drop them to the free area in the Advanced Importer.

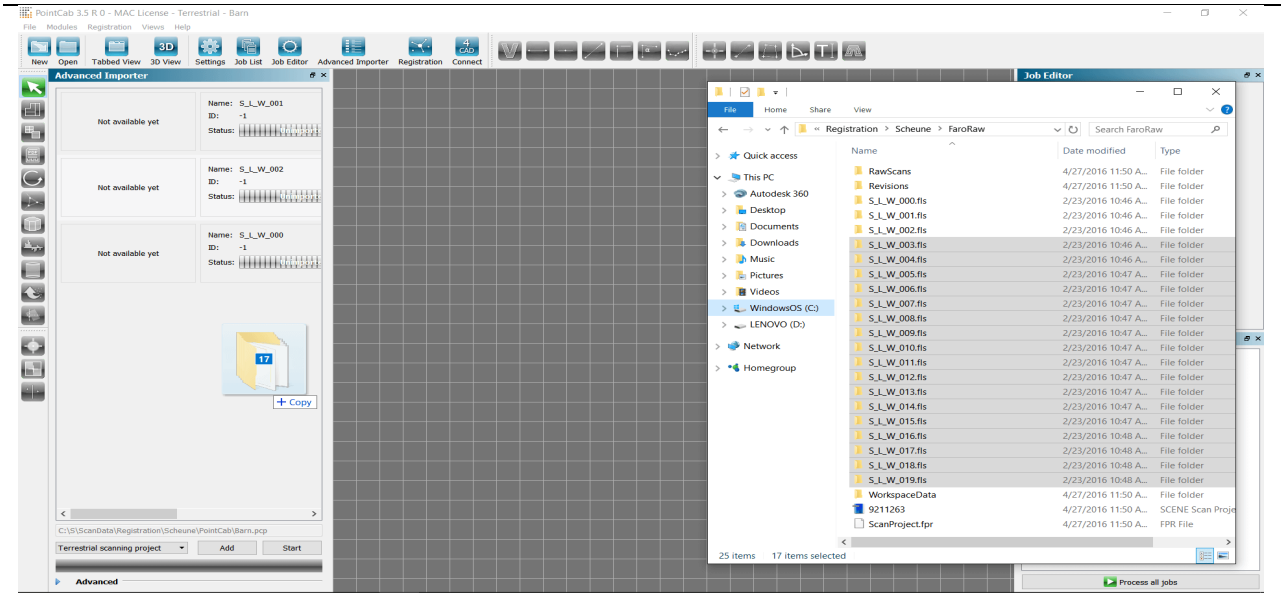

Figure (4-13): Create a project and import scans

Select “No” for the question if the scans are already registered. Now, all imported scans are listed automatically. As may be the case, add more scans in the same way. Then, start the import by selecting Start. The import may take some time depending on the number of scans, data type, scan volume as well as computer resources.

2. Registration Editor:

After import, the *Registration Editor* opens automatically; the *Advanced Importer* is closed. Make sure that *Job List* and *Job Editor* are displayed on the right (*main toolbar* or *menu Views* …)

The Registration Editor consists of 3 sections. The upper section incldes a dual view of two scans and allows to easily select corresponding points. Scans can be shifted manually for left or right side in the list box.

If you don’t need corresponding points, you can minimize or totally hide the right side by clicking and dragging into the intermediate area between both views. The dual view includes two hidden lists “Scans” and “Checkerboards & Spheres …” which can be made visible by clicking on the triangle.

The *Scan List* includes all available scans; the *Feature List* contains all available checkerboard targets, spheres etc. (currently empty).

.

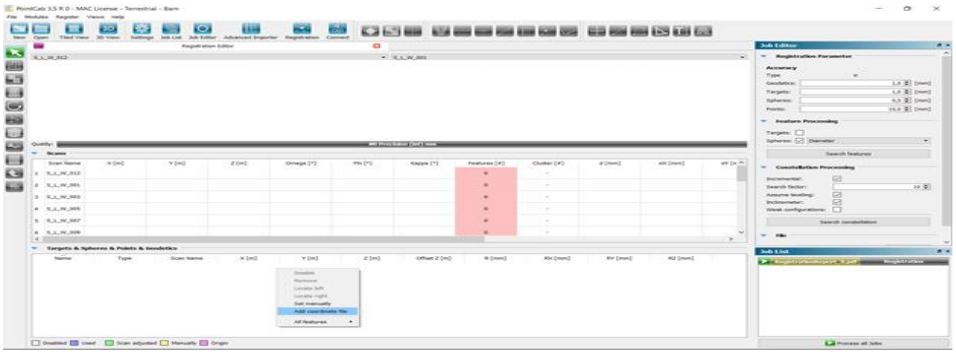

Figure (4-14): Registration Editor

The Job List shows a selected job "Registration". The Job Editor contains settings for registration. If not, simply click once on the job "Registration" in the Job List for selection. Now, you can individually adjust the settings for accuracies of features and feature search for this project.

If you have used external geodetic points in your project and if you want to import them, right-click into the Feature List and select "Load Coordinate File" in the context menu. The corresponding file formats are displayed; you can import your coordinate file that will be displayed in the list.

4. Automatic feature detection

Start the registration job in the Job List. You will receive a message that some scans don't have enough features and that they can be searched automatically. Confirm with "Yes". A job for feature search is created for each scan in the Job List and automatically started.

The Scan List contains the column "Features" that shows the number of features in each scan. If only two or less features are found, the entry is red. If three or four features are found, is yellow, otherwise green.

When the search in all scans is realized, you can open a scan in the upper view and set it using the tools "sphere" or "checkerboard". You save a lot of time since you can continue working simultaneously. For large projects, we recommend to check all scans visually and to remeasure features manually if needed.

You can open a scan in the scan list by right-clicking in the appearing context menu. In the context menu, you can activate / deactivate or set a scan as origin (as long as no geodetic points

are used).After the search process is finished, make sure that at least 3 features are found in each scan.

5. Search constellations automatically

Start the registration job in the Job List again. As the case may be, PointCab displays the same message if a scan doesn't contain at least 3 features. Otherwise, a constellation detection is performed and attributions between the scans are searched. If you have not set any geodetic points and any scan as origin, the first scan is automatically set as origin.

As a result of the search, the features are automatically renamed. If constellations can be found for all scans, a positive feedback appears and figure 0 appears in the column "group" for all scans. Otherwise, single scans or entire groups of scans could each exist in an own group. That means the groups could not be connected.

Check the scans regarding the features that should connect the groups, premeasure the missing features and restart the registration job. Perform this process as long as all scans are connected.

6. Optimize registration

Now, all scans are preregistered, highlighted in blue in the scan list and orientation data of scans exists.In the 3D view, which can be opened in the main toolbar, you can see the scan positions as well as geodetic points if available.

In the feature list, you see the initial residuals for each feature, that is the deviation of each feature from the average value of all three-dimensional coordinates of the features. The color shows how large the residuals are in relation to their a-priori accuracy. Red residuals show big deviations. Check them and delete the corresponding features if needed, and start again with step 5.

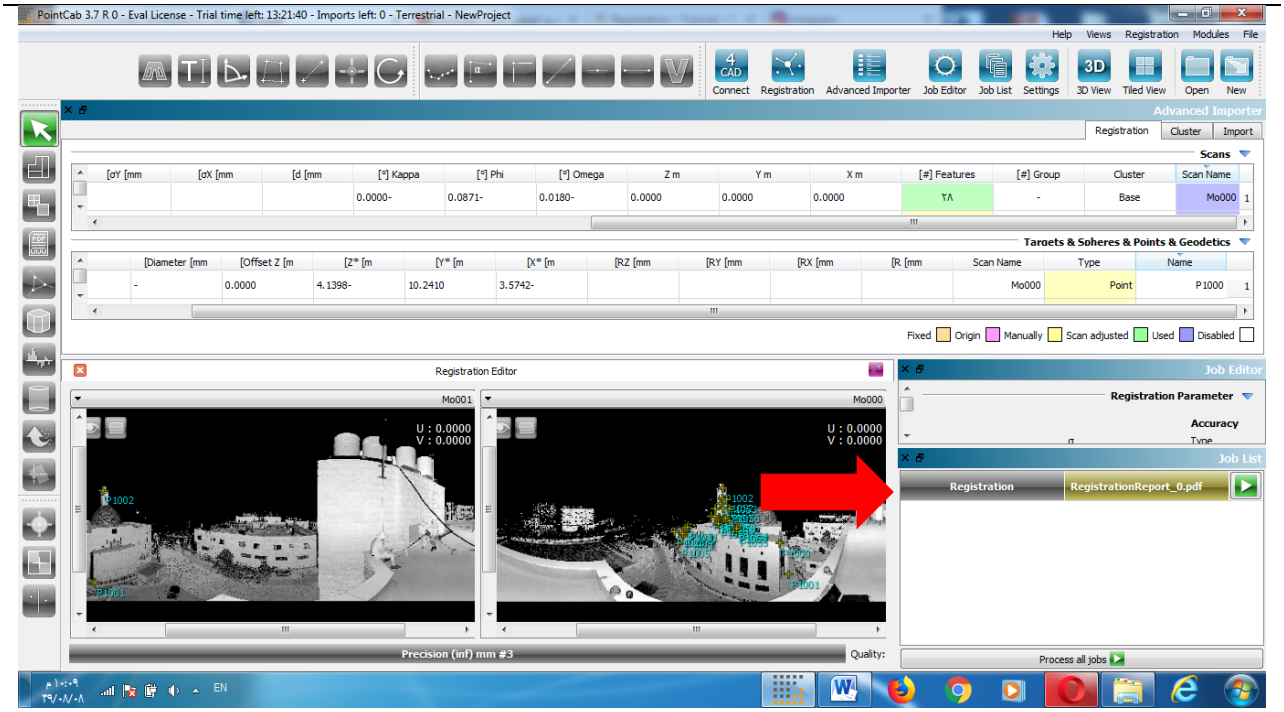

Figure (4-15): Optimize registration

Start the registration job again.

Now, PointCab performs a global optimization and tries to attribute more features. Scan positions are optimized and the residuals' square sum is minimized (Least Square Adjustment).

After adjustment is finished, all scans are green (origin scan is magenta). Check the residuals again. If required, delete the corresponding features, deactivate the option "incremental" and start again with step 5.

7. Finish registration and generate report

If desired, you can rename the log file in the File tab in the Job Editor. Restart the registration job to generate the report and to finish registration. The registration editor is closed and three default views are created automatically.

If a PDF viewer is installed, please open the report by double-clicking on the registration job. There, you find detailed information about the processed registration including accuracy specifications, a visualization of the feature graph, a detailed list of residuals as well as an accuracy analysis regarding the relative accuracy between scans (see Quality Matrix).

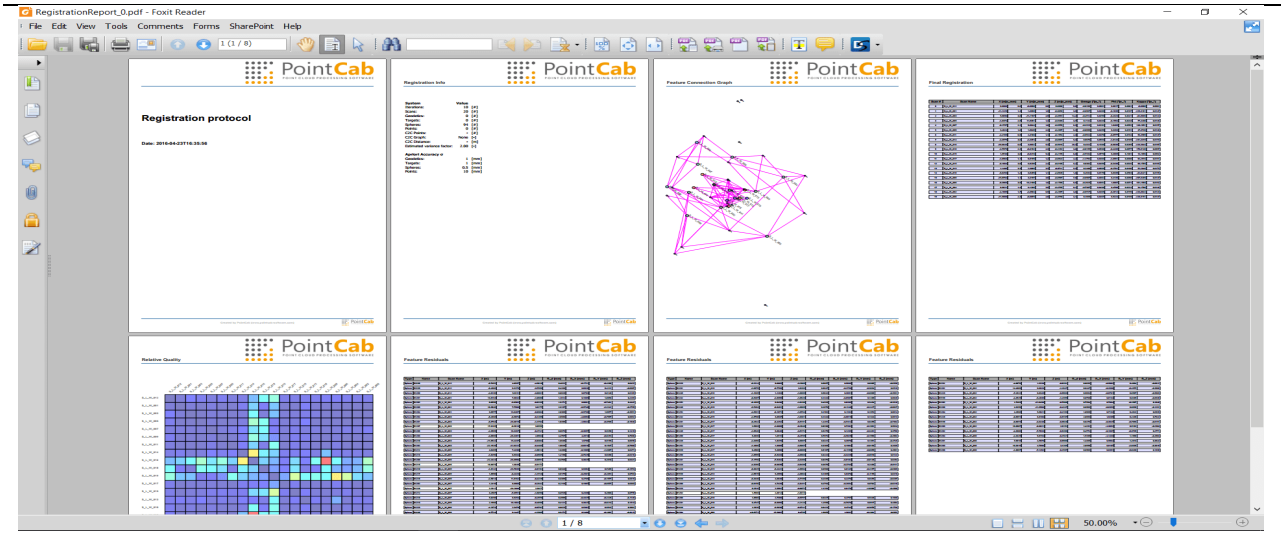

Figure (4-16): Finish registration and generate report

4-3-5 Point Cloud Export

With the Point Cloud Export module, you can export specific sections of your point cloud. Due to filters, you reduce the size of your point cloud output additionally.PointCab allows point cloud export into AutoCAD RCP format.

Select the tool “Export point cloud” and select the zone in the standard top view. Edit the selected zone by defining the upper and the lower border.

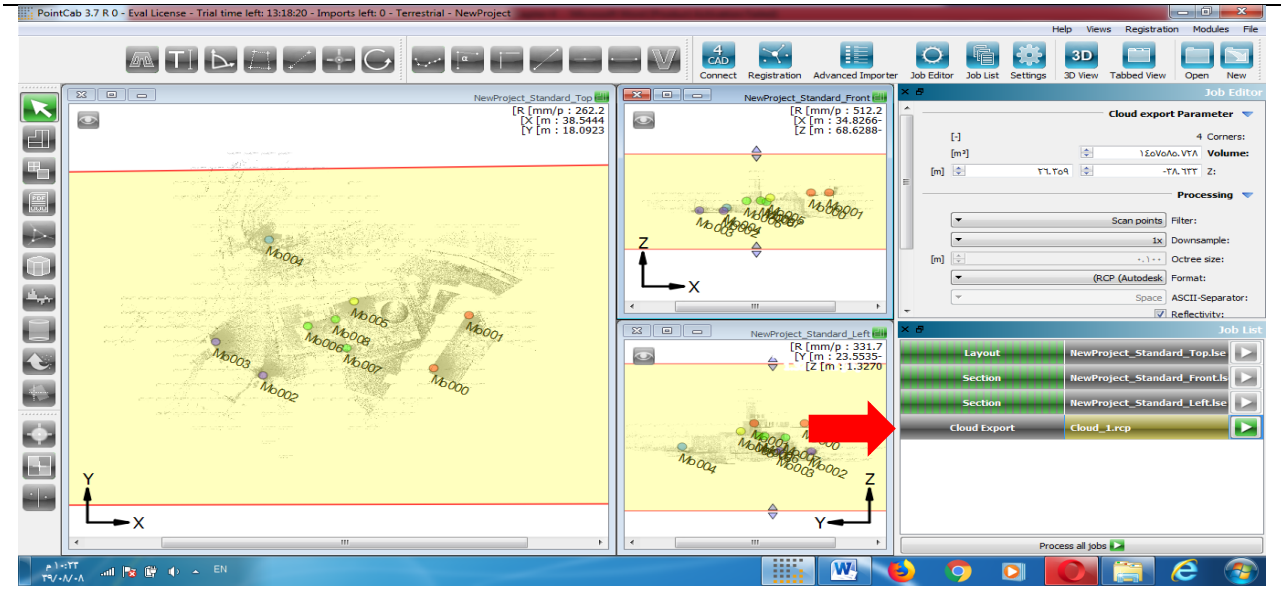

Figure (4-17): Point Cloud Export for Palestine Polytechnic University Mosque

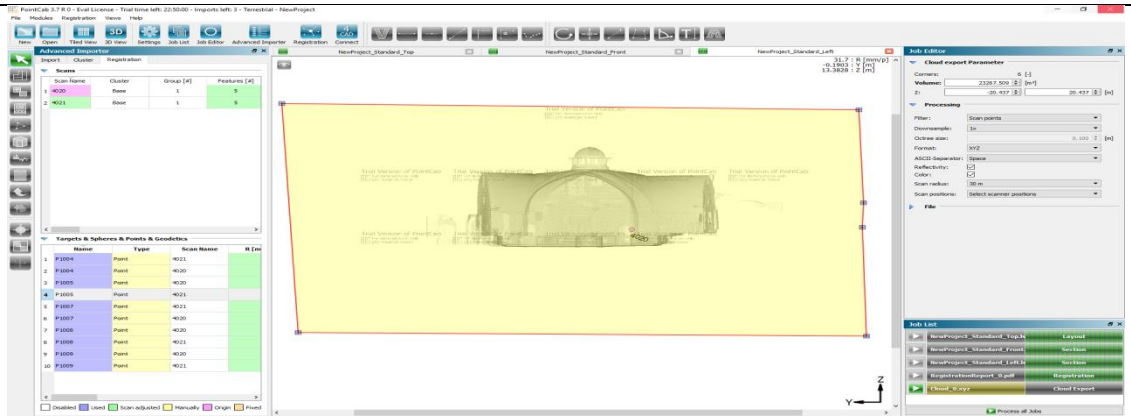

Figure (4-18): Point Cloud Export for Al-Hammam Al-Turkey

[2] Filter options:

Scan points: The number of scan points is reduced additionally by the chosen factor. If you choose the factor "2x", just each second scan point is used.

Block filter: The number of scan points is thinned spatially and thus homogenized. If you select a block size of 0.05m, just one point is exported in a cube of this edge length. That's why almost all pieces of information are maintained in areas with low point density. In areas with high point density, redundant points are excluded.

Height points ("elevationt profile"): You get the grid-shaped DTM as a point cloud for the respective layout or sectional view. The number of points depends on the image resolution selected originally for the layout or section. A predefined scan radius is ignored during point cloud export.

[3] Output formats:

XYZ, LAS, LAZ, E57

RCP: Autodesk RCP format. Import data directly in AutoCAD without the need for Autodesk ReCap.

[4] Start processing the export in the Job List.

[5] Now, the generated point cloud file (Open by right-clicking: /projectname/projectname_Results/3D/).

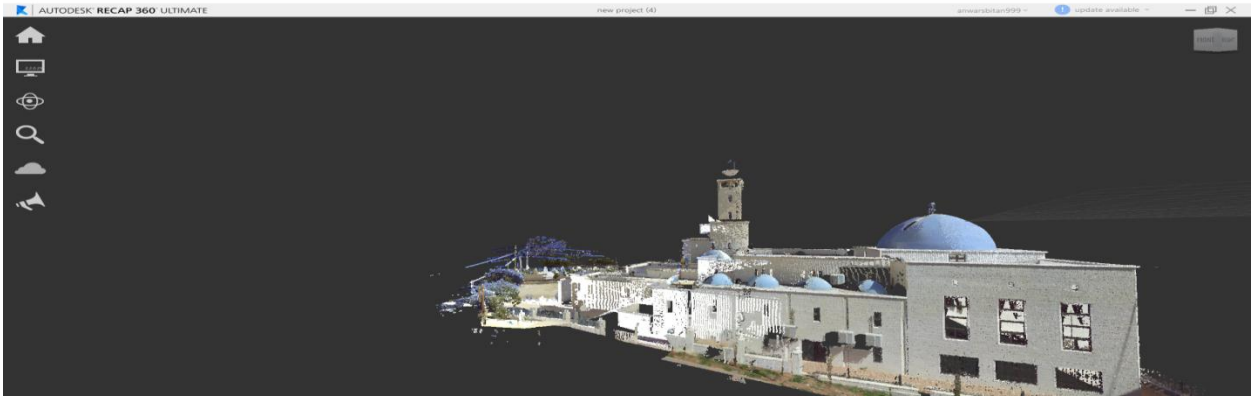

Figure (4-19): 3D Results for Palestine Polytechnic University Mosque

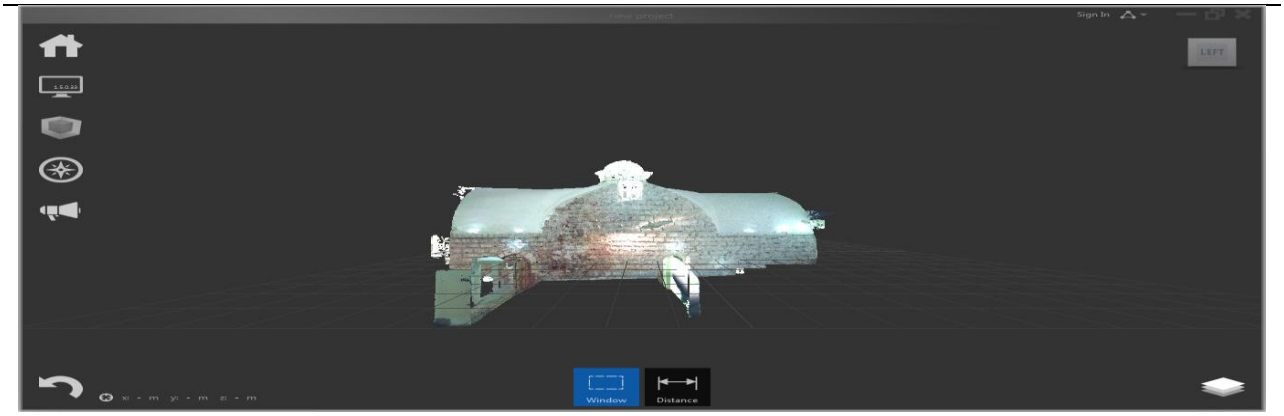

Figure (4-20): 3D Results for Al-Hammam Al-Turkey from outside

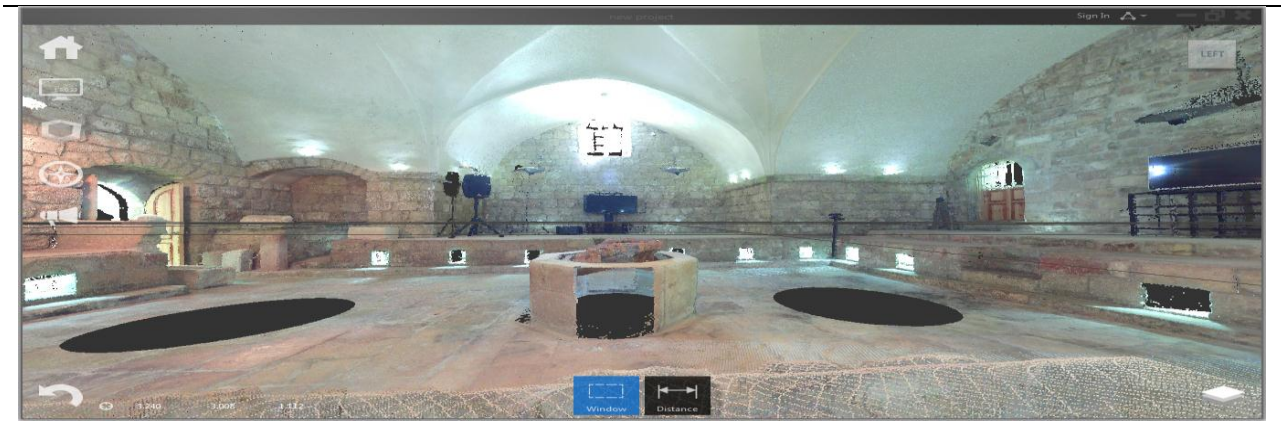

Figure (4-21): 3D Results for Al-Hammam Al-Turkey from inside

4-3-6Create a facade plan & Area model of a facade & Create Layout & 3D points

4-3-6-1 Sections: Create a facade plan

In order to do it activate Section tool ：

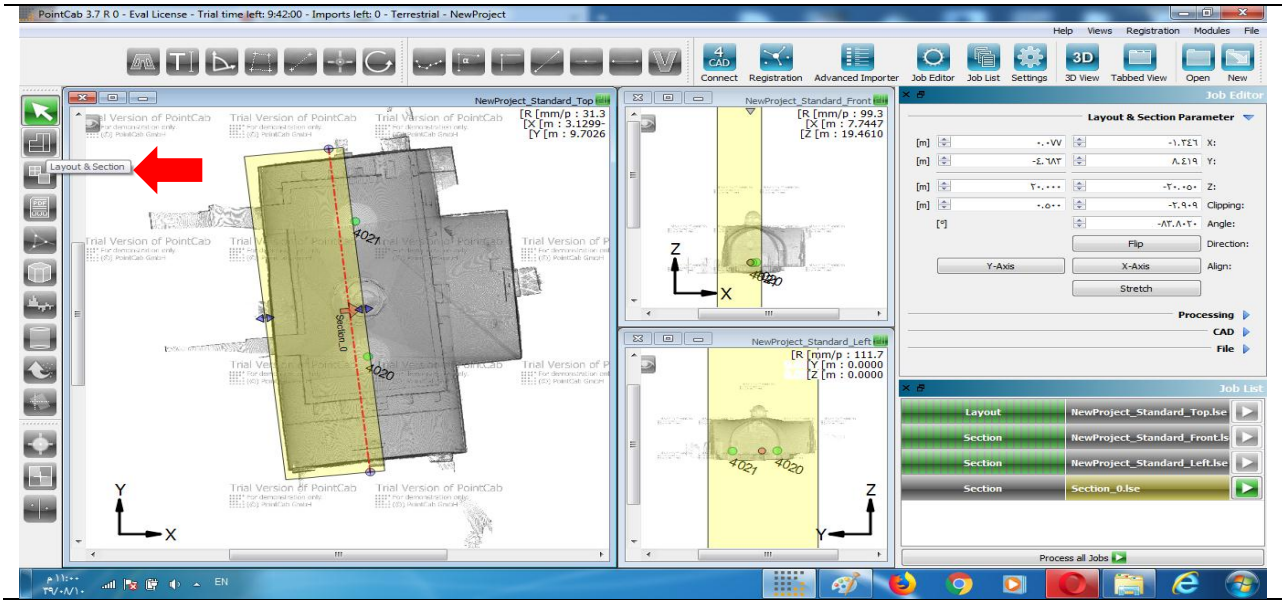

Figure (4-22): Activate Section tool

In order to define a facade you should choose for a start point we selected the left plan:

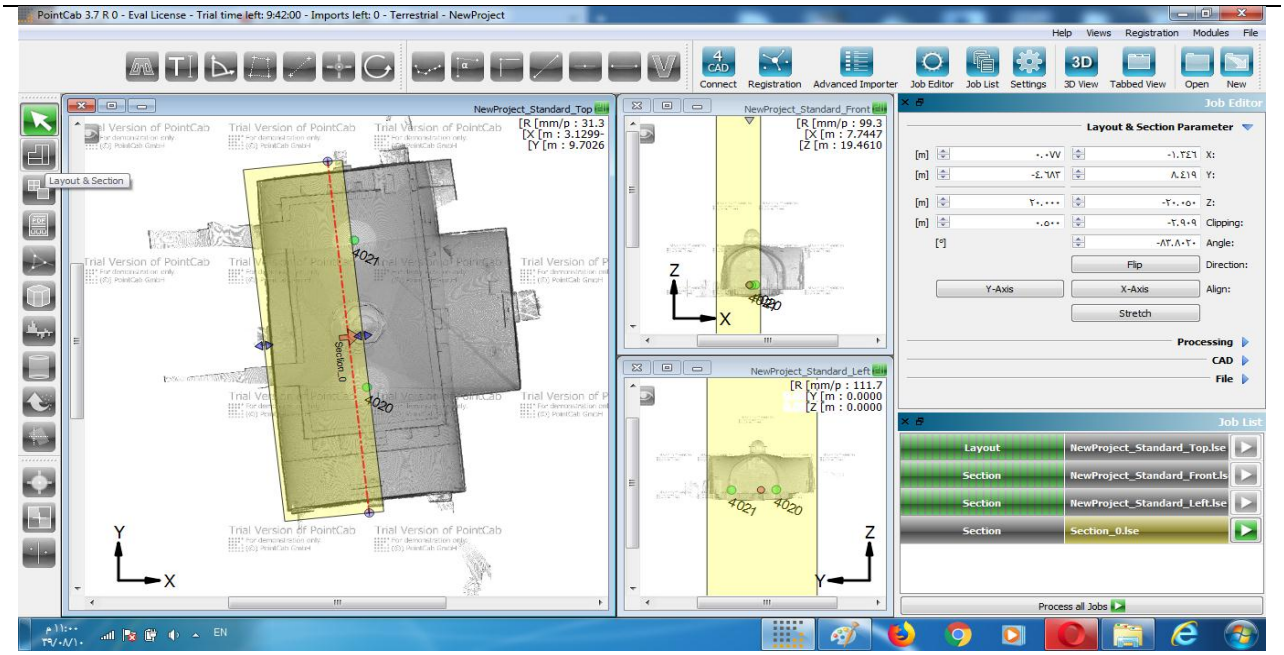

Figure (4-23): Select the left plan for Al-hmmam AL-Turkey to start

Now you can start processing :

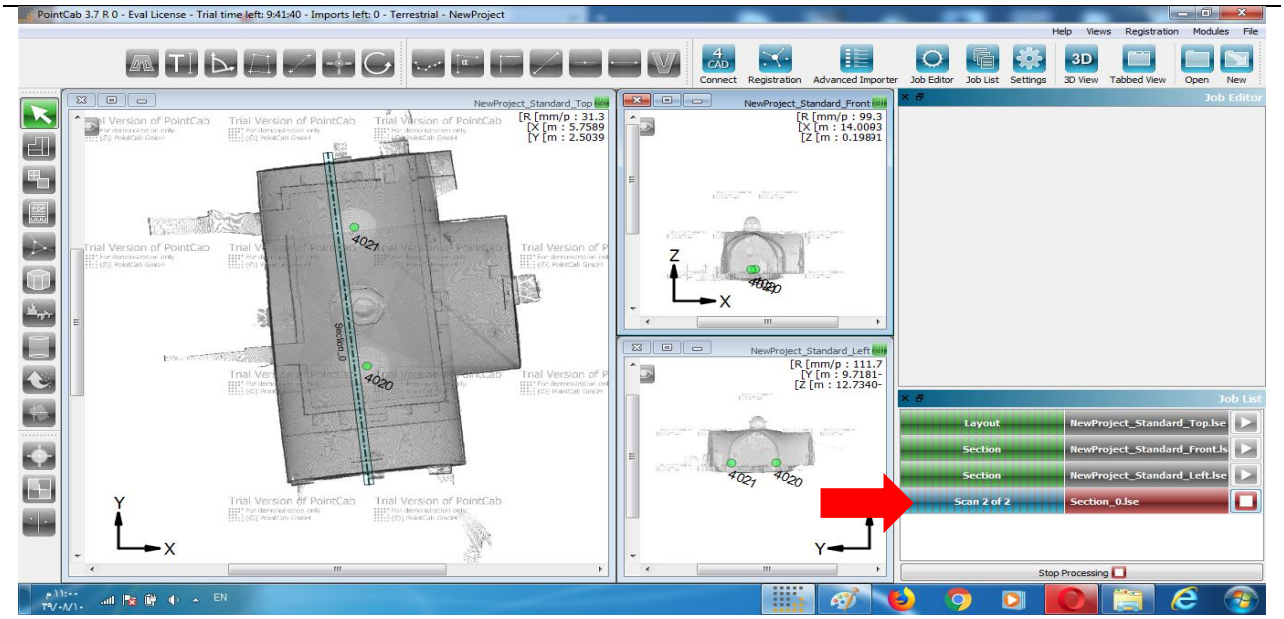

Figure (4-24): Start processing

After completion of the facade plan you can open the result by double clicking the Job in the Job List or right clicking –>Open .

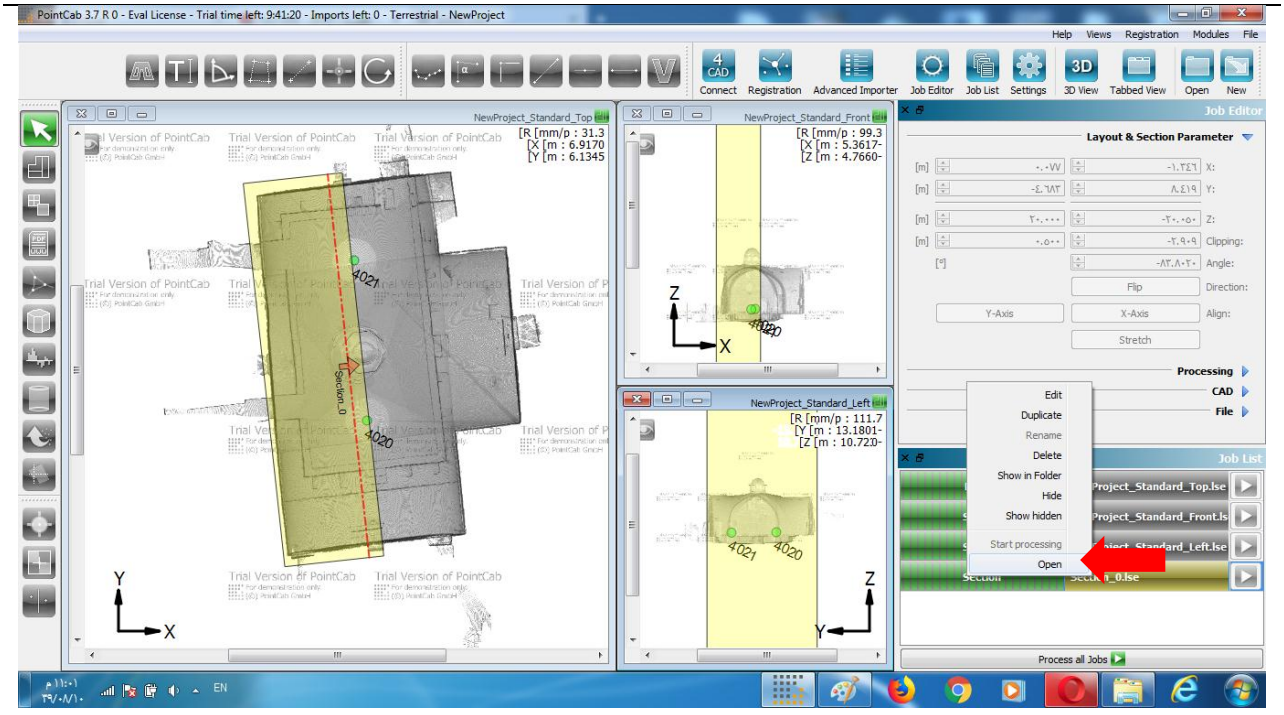

Figure (4-25): Show the result

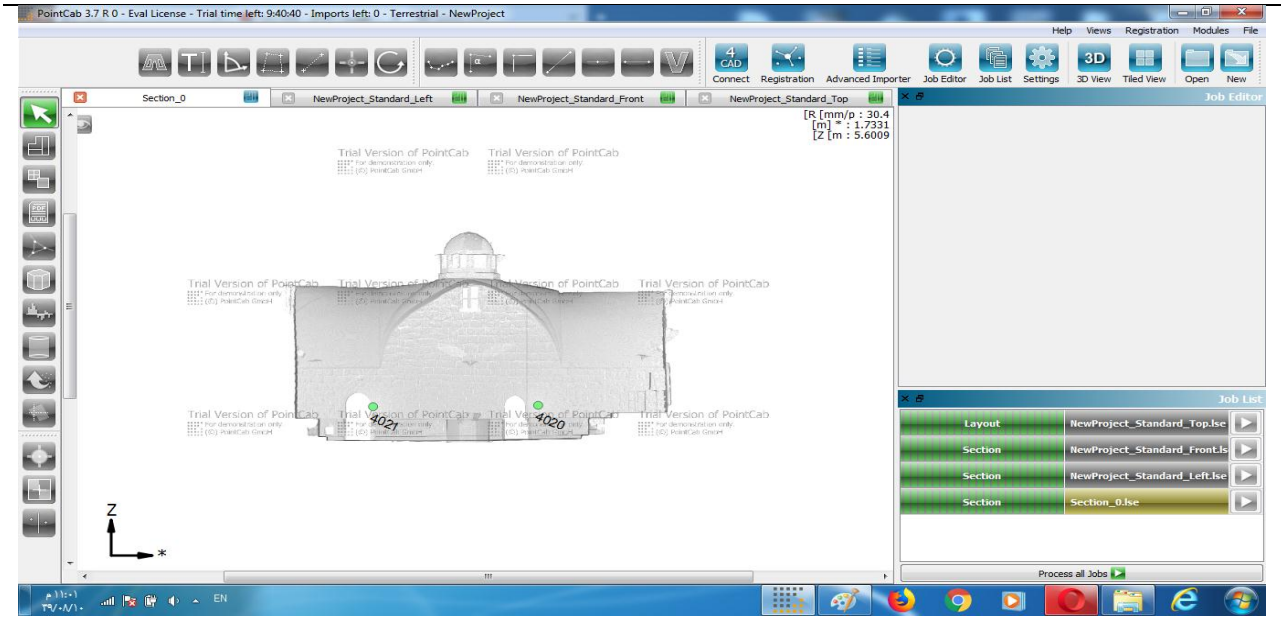

Figure (4-26): Facade plan in PointCab

4-3-6-2 Area model of a facade :

Activate the Mesh tool :

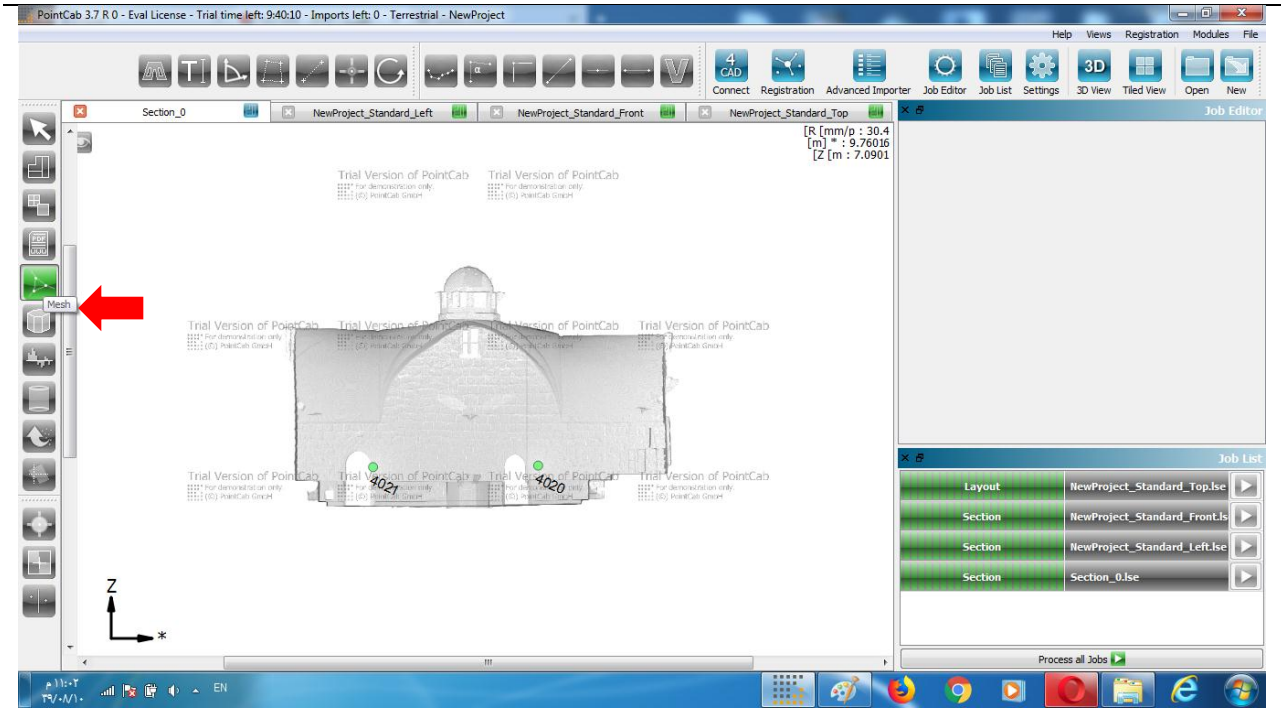

Figure (4-27): activate the Mesh tool

Select inner area of the facade :

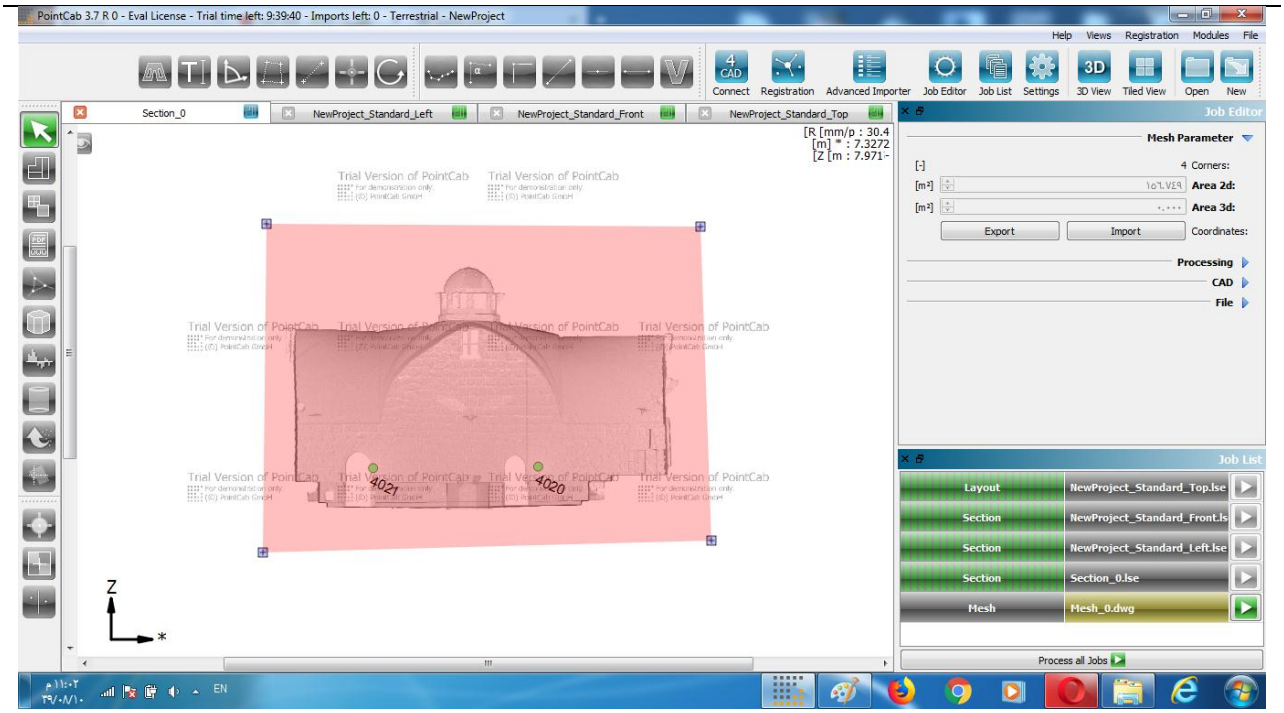

Figure (4-28): Select inner area of the façade

Now you can start processing :

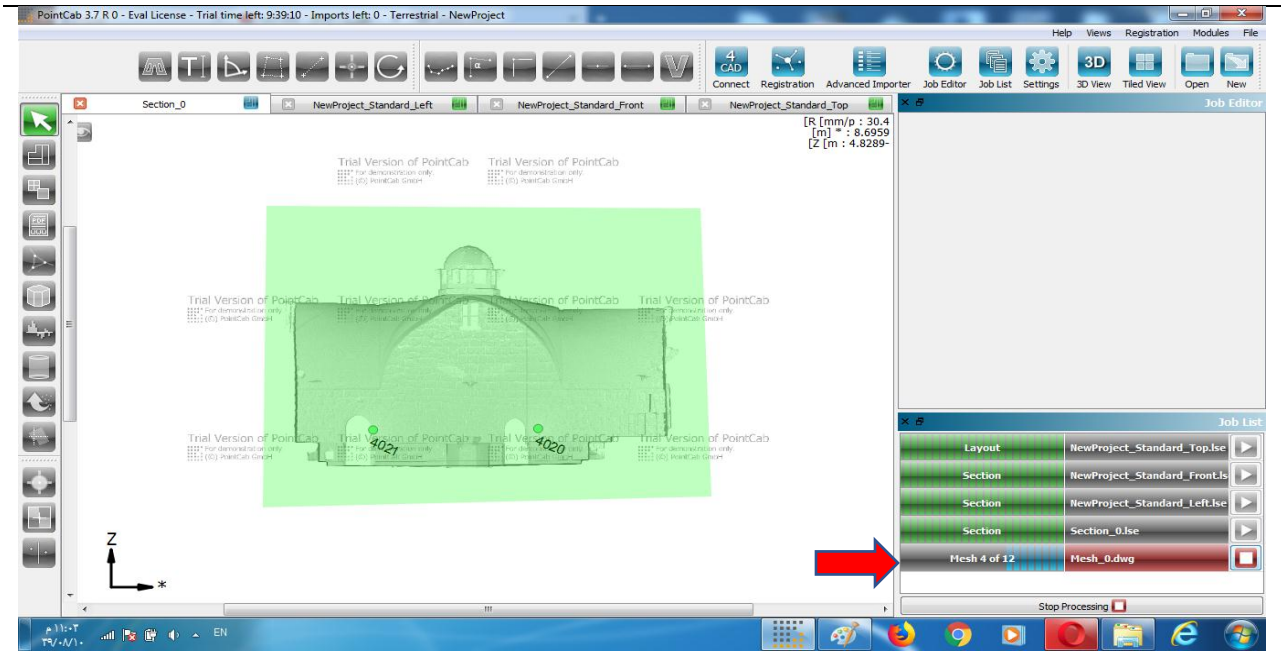

Figure (4-29): Start processing

After completing the processing, PointCab displays the mesh as an orthophoto:

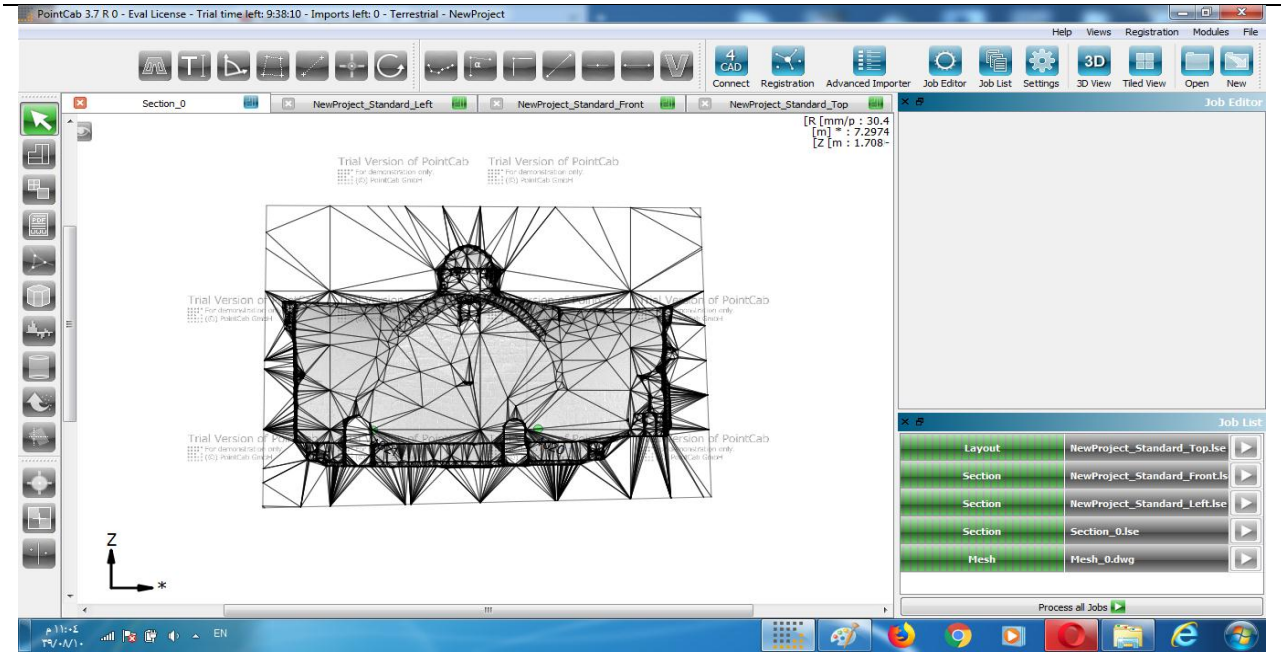

Figure (4-30): Mesh will be displayed

For further mesh analysis you can have a look on it in our 3D View. In order to start it open the Job:

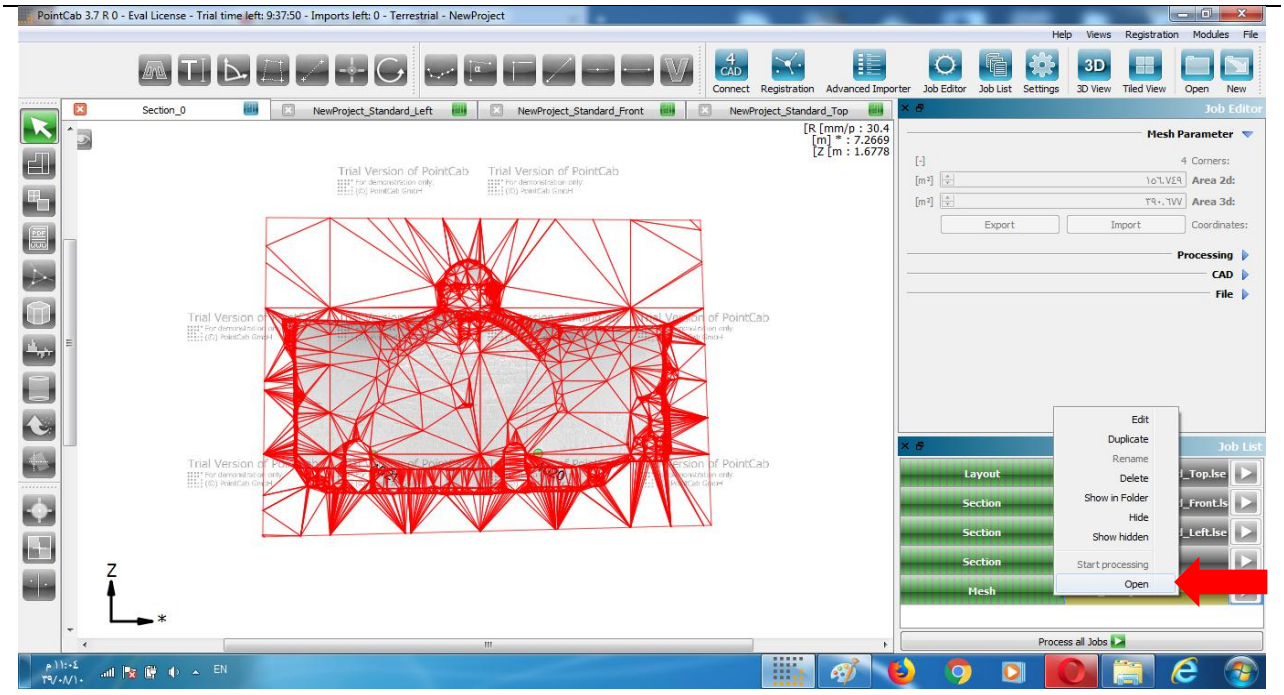

Figure (4-31): Open mesh in 3D View

3D opens in a new tab. Left click to have a look on your 3D area model :

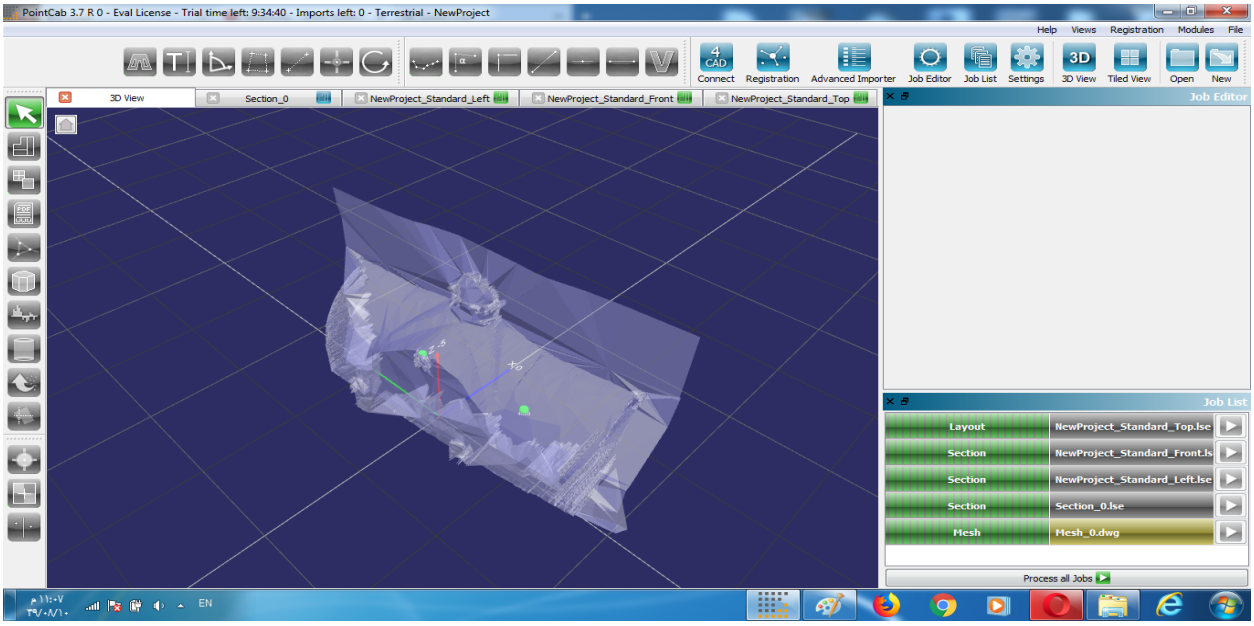

Figure (4-32): Mesh in 3D View

Finally you can open the results in your CAD Program. Right click the Job to open its storage path :

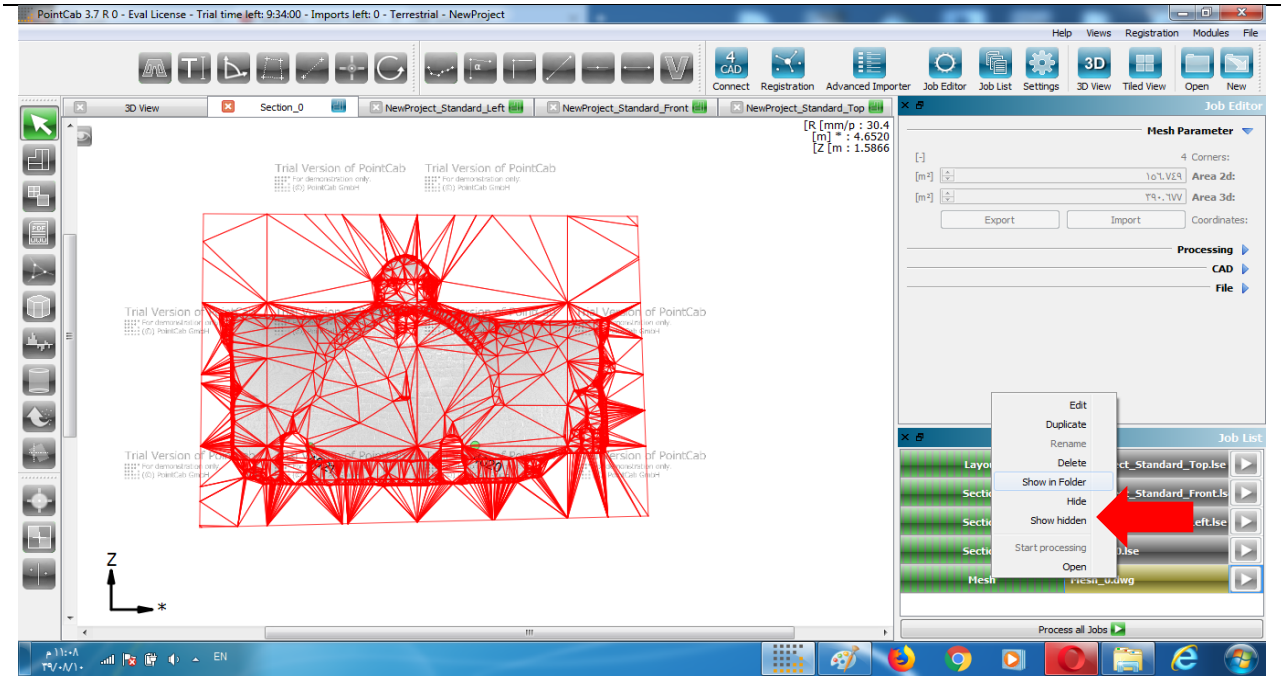

Figure (4-33): Show in Folder

Now select a CAD file :

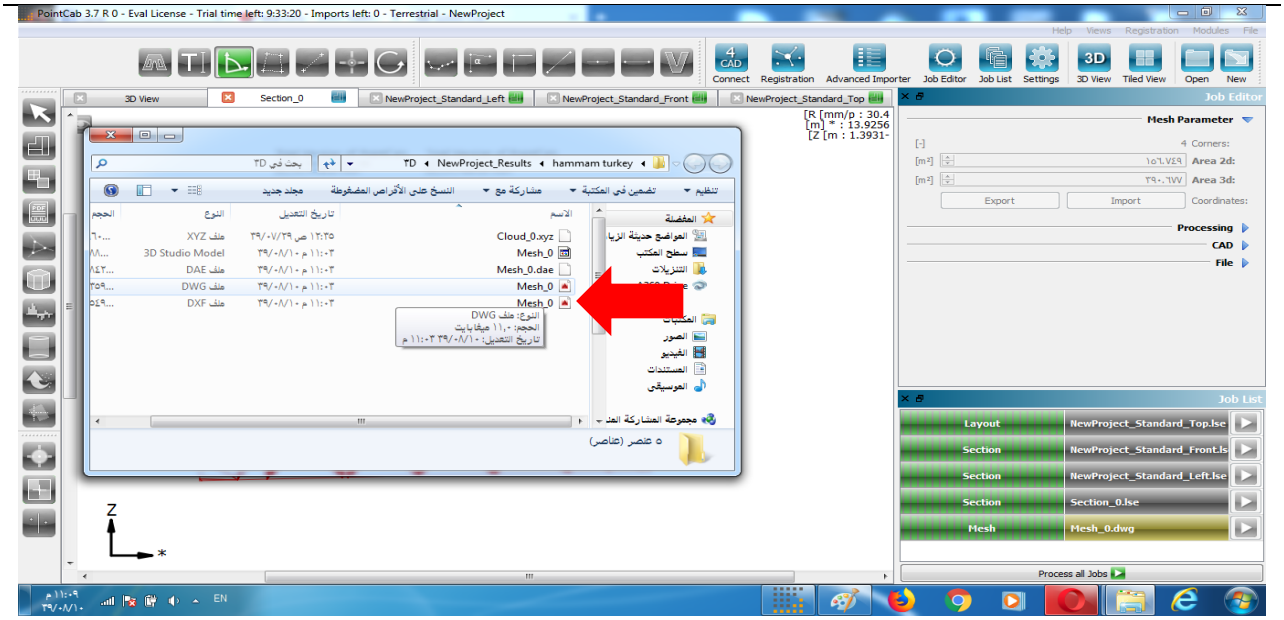

Figure (4-34): 3D area model as DWG

A facade model as DWG in TrueView :

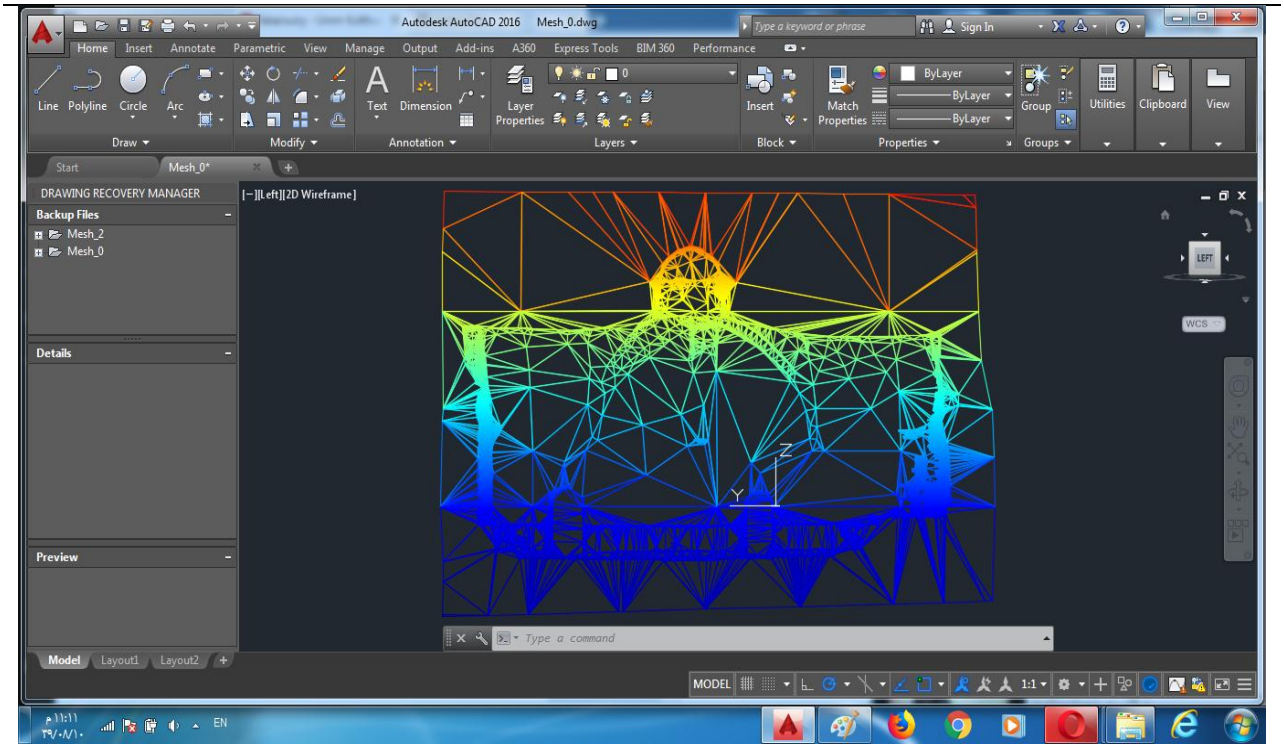

Figure (4-35): Facade model as DWG in True View

4-3-6-3 Create Layout:

Activate Layout tool:

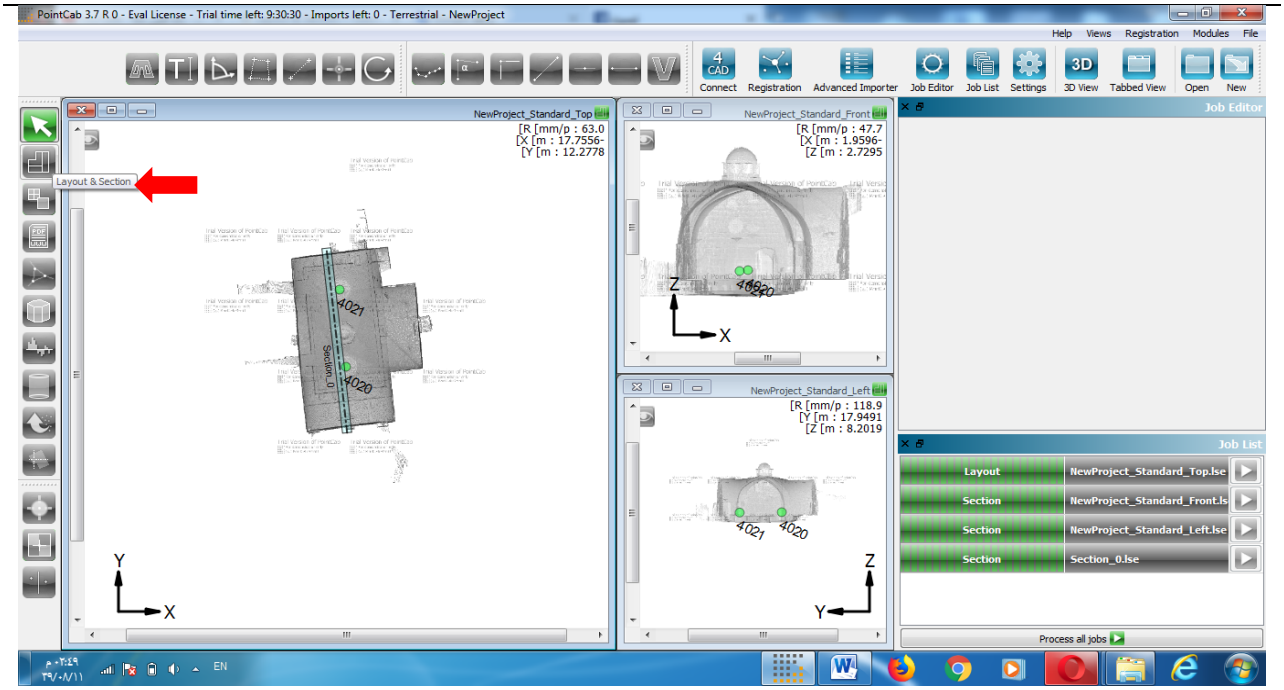

Figure (4-36): Activate Layout tool

For more precision switch to tabbed view by pressing F3 (or View–>Tabbed view)

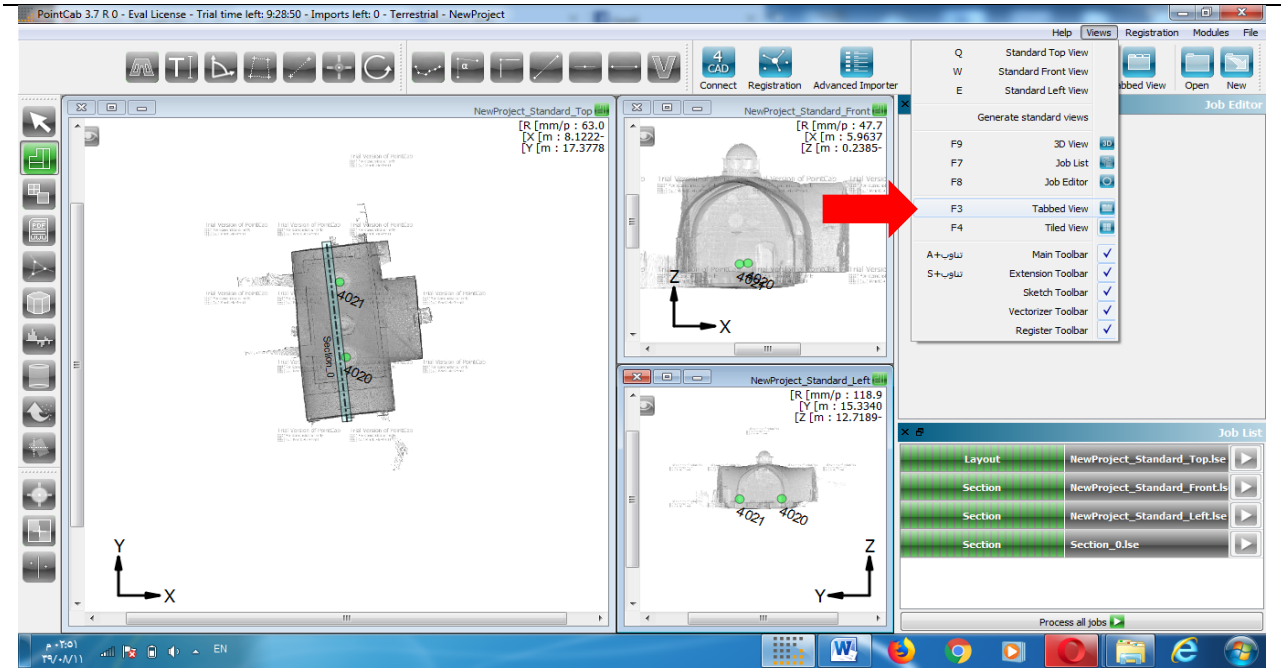

Figure (4-37): switch to tabbed view

Activate the front view:

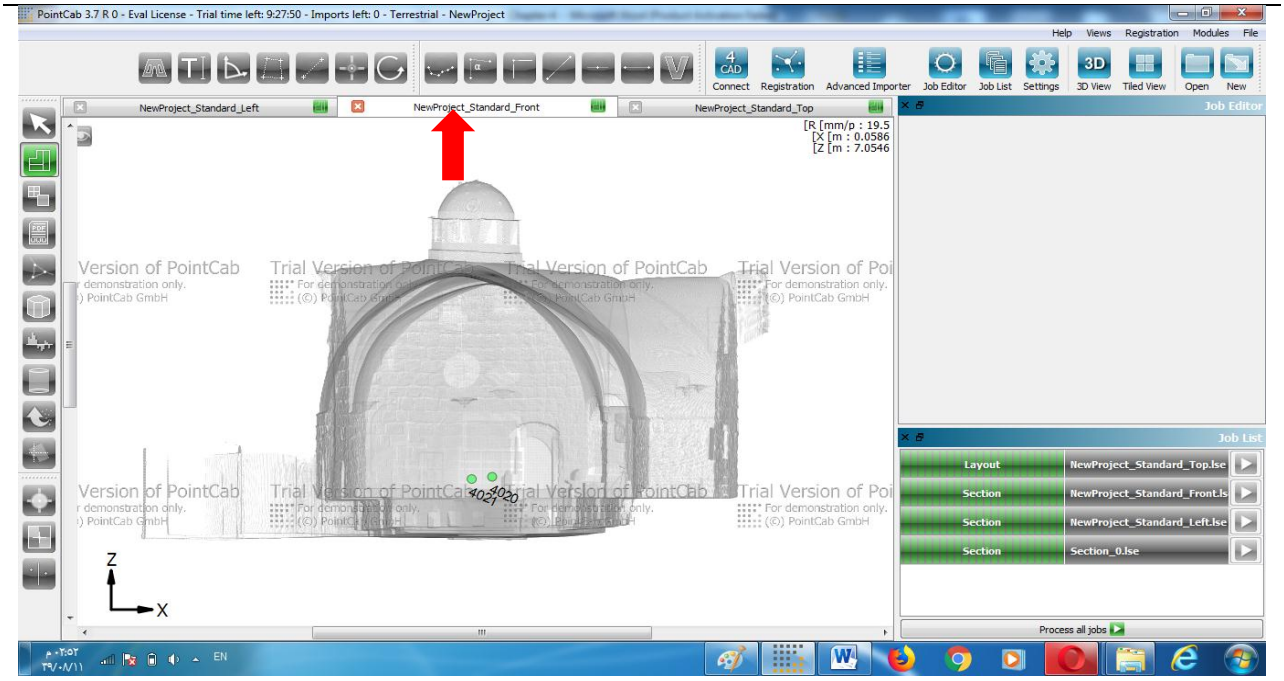

Figure (4-38): Activate the front view

Turn off scan positions by clicking the small icon or by pressing P key :

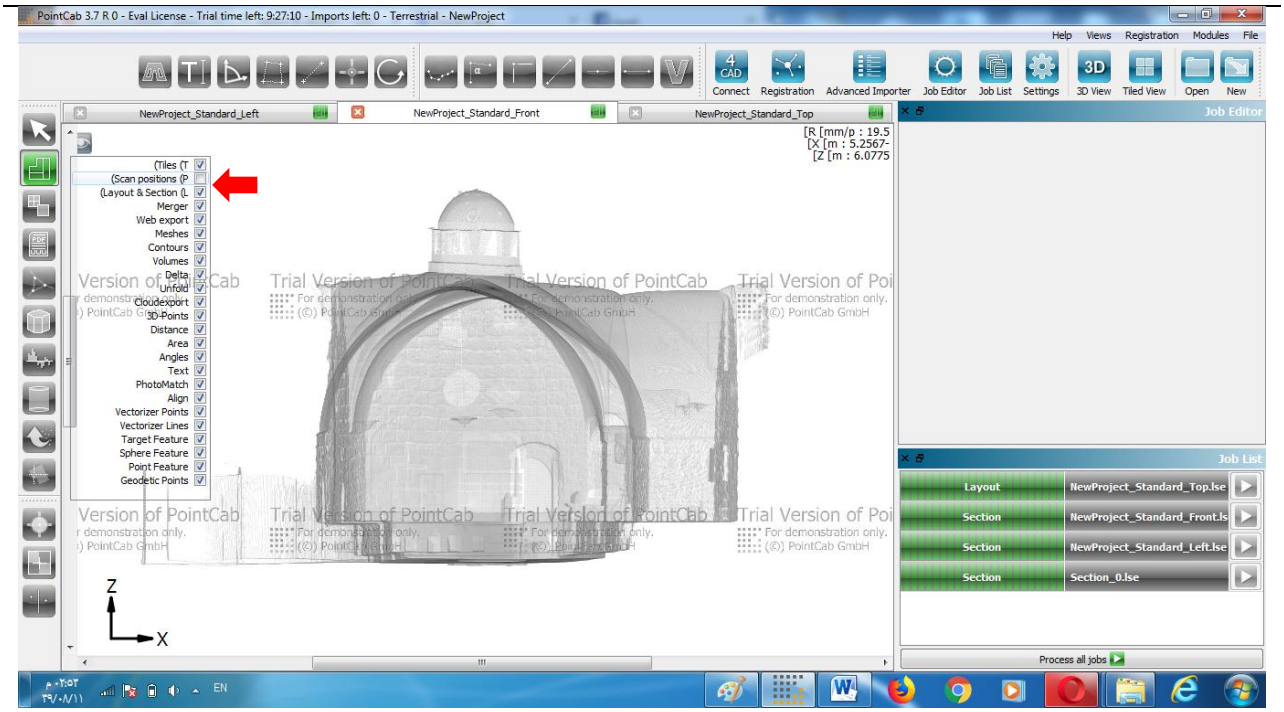

Figure (4-39): Turn off scan positions

Left-click start and end points of a section to define your layout:

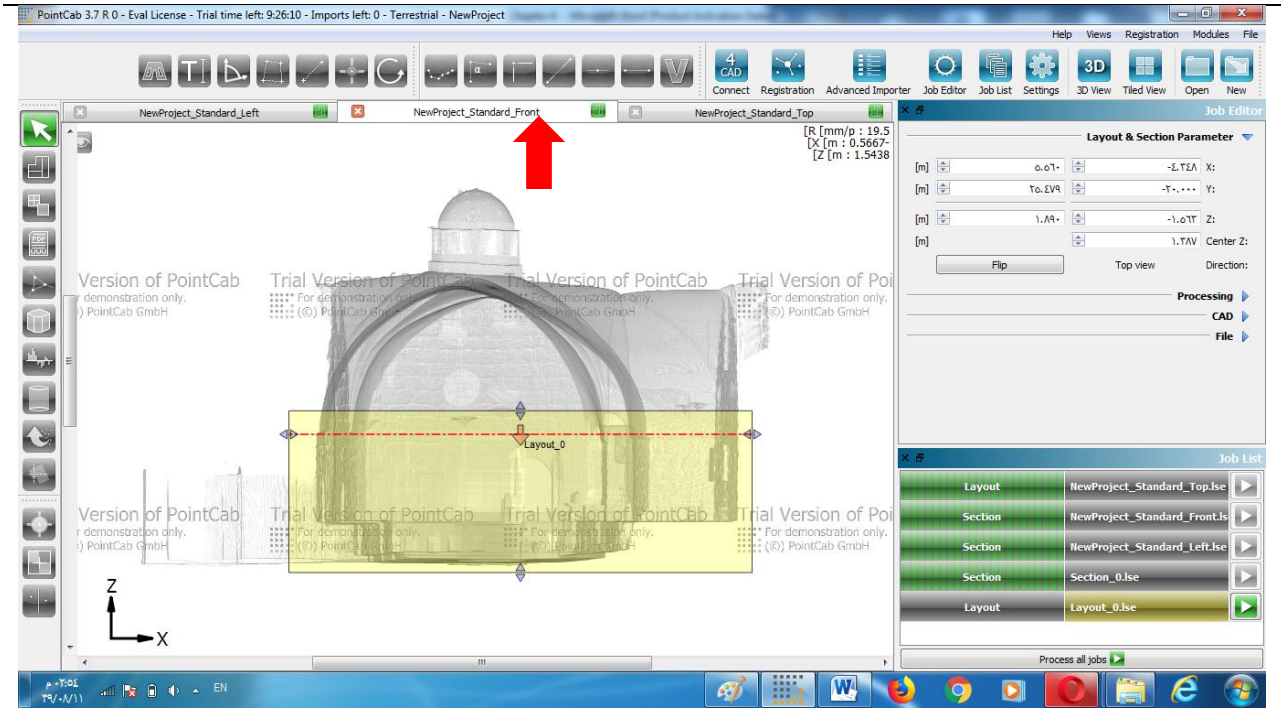

Figure (4-40): Activate the front view

Now activate the top view. Here you can sie the selected area:

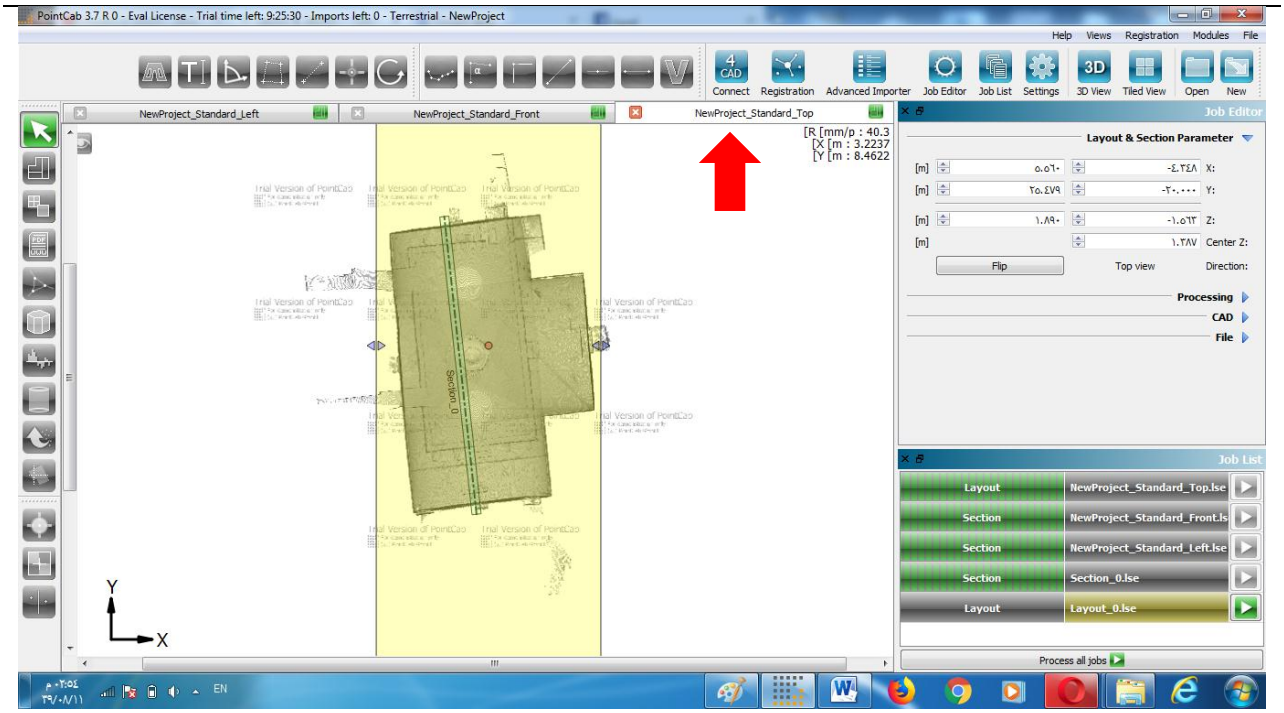

Figure (4-41): Activate the top view

Start calculation of your layout:

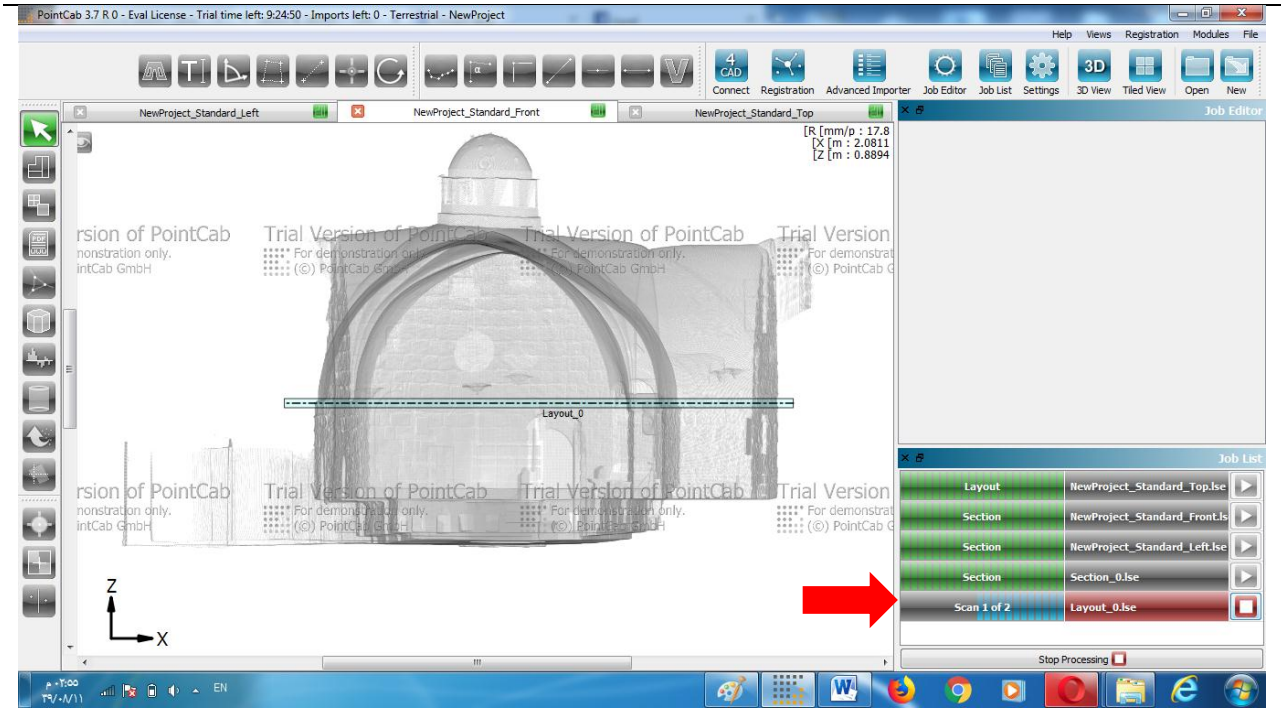

Figure (4-42): Start calculation of your layout

Right-click Job to open the layout as soon it turns green:

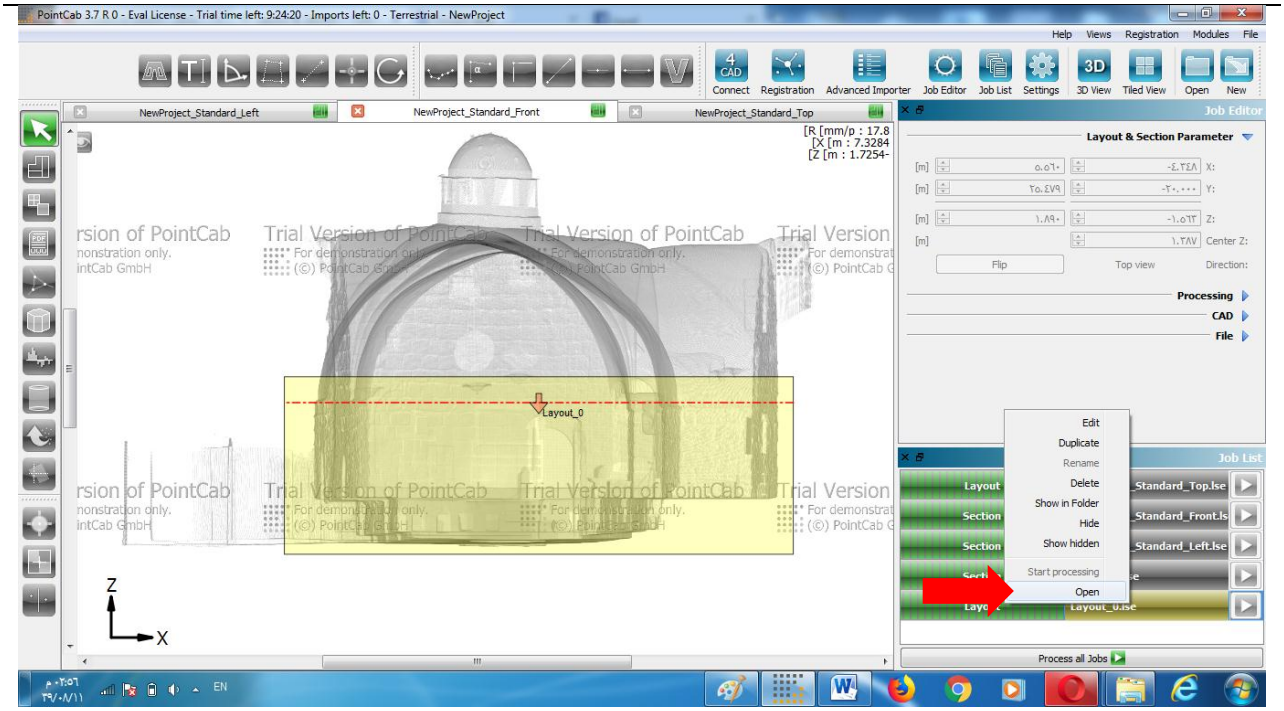

Figure (4-43): open the layout

Processed layout in PointCab :

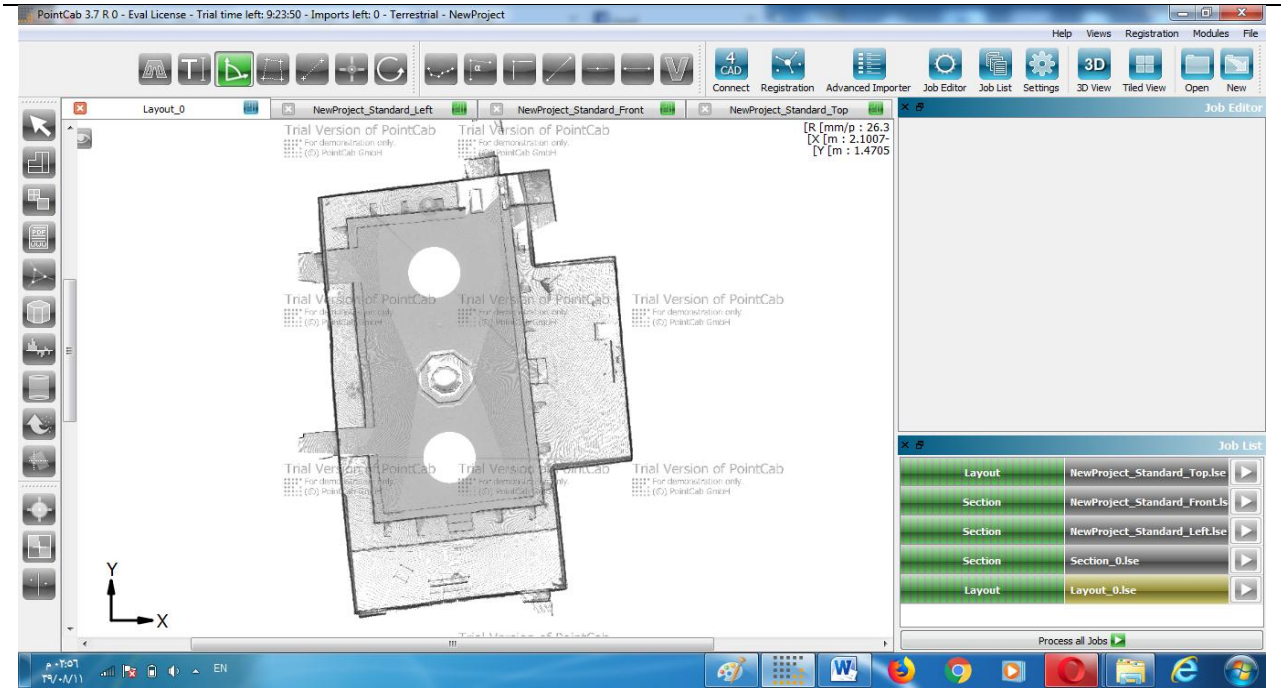

Figure (4-44): layout in PointCab

Alternatively you can open a folder containing your layout in DWG, DXF, DAE formats by right -click selected Job and click Show in folder :

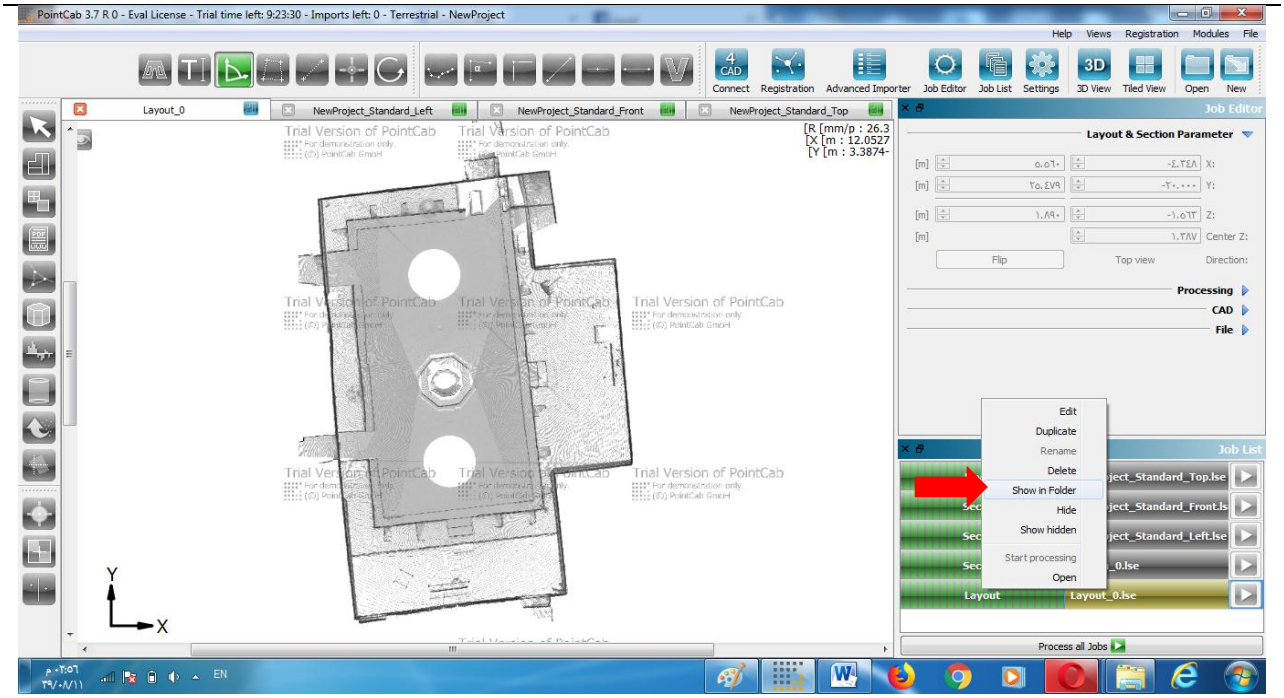

Figure (4-45): Show in folder

PointCab results in Windows Explorer:

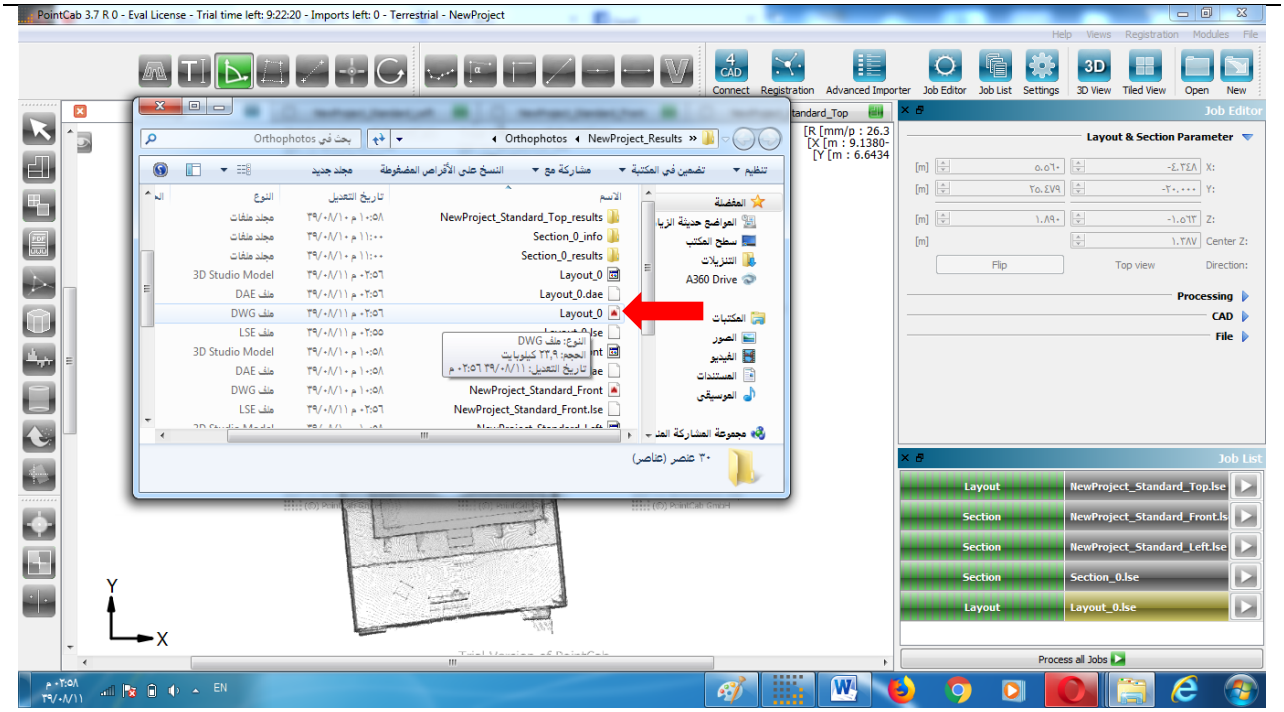

Figure (4-46): layout in PointCab

Double-click DWG file opens the layout in free program Autodesk DWG-True View:

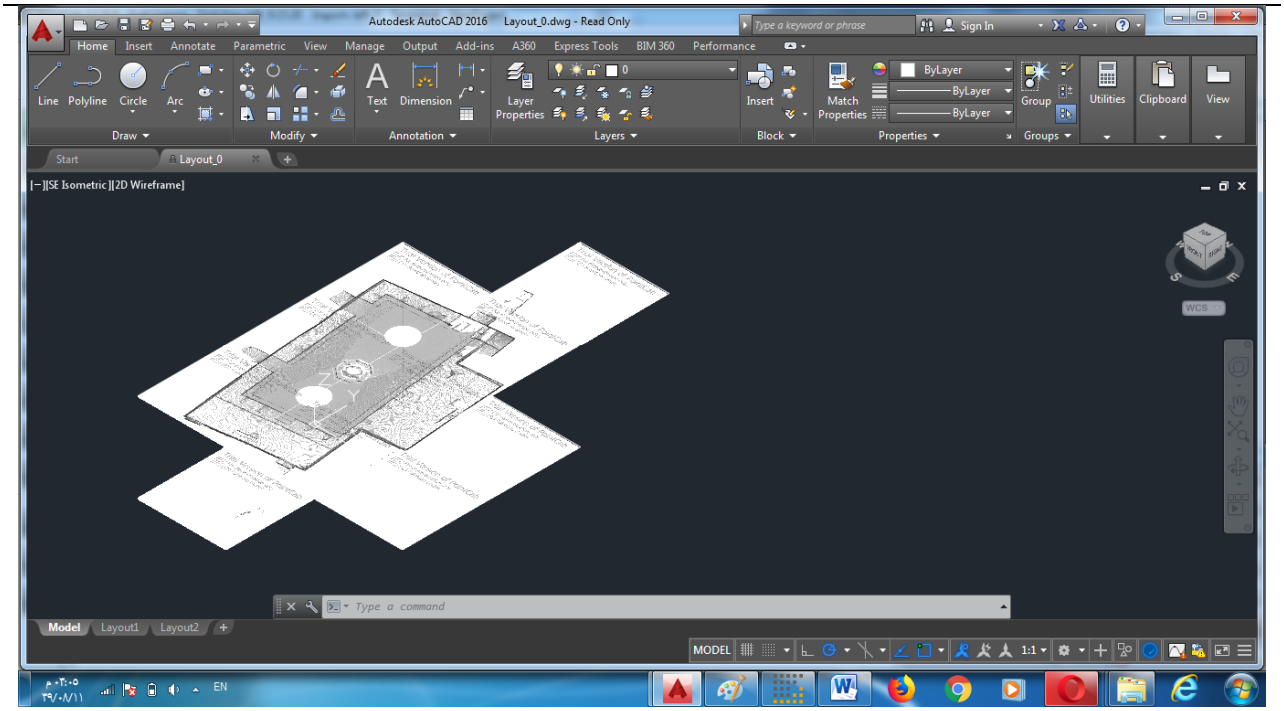

Figure (4-47): layout in Autocad

4-3-6-4 Export 3D-points

Export points to another system using export tool

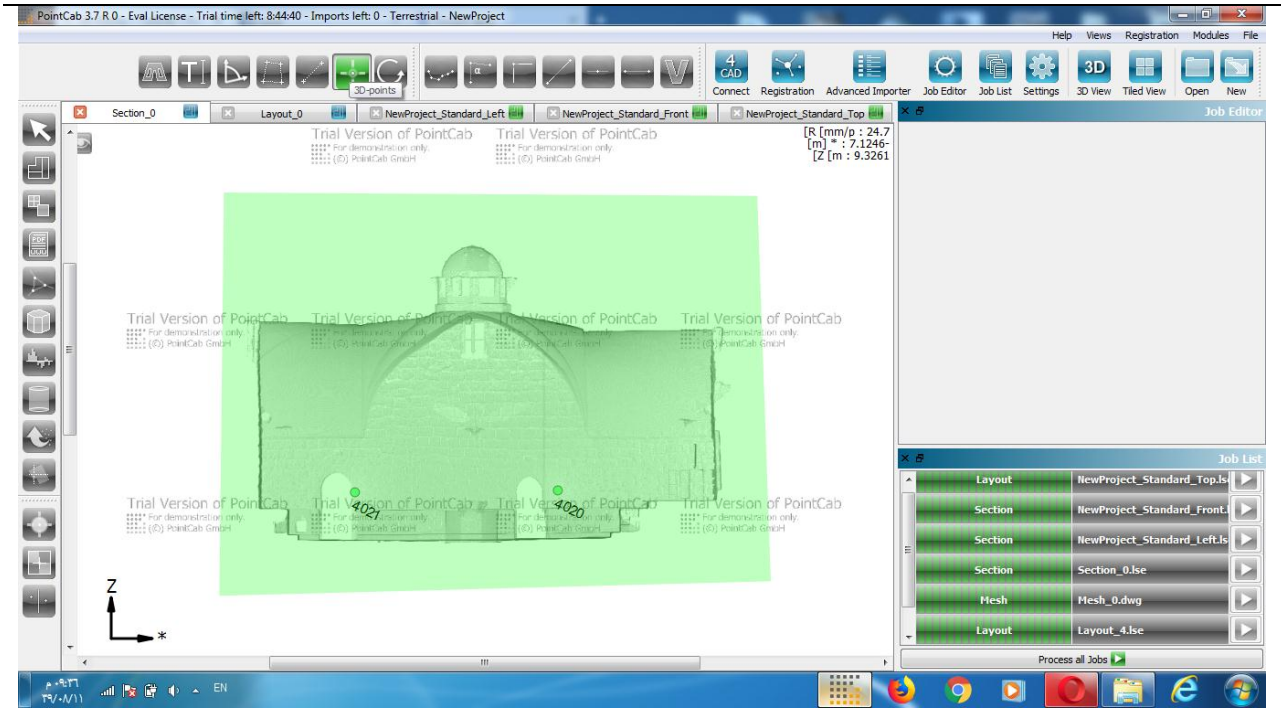

Figure (4-48): Activate the 3D Points tool

Click the required points on plan :

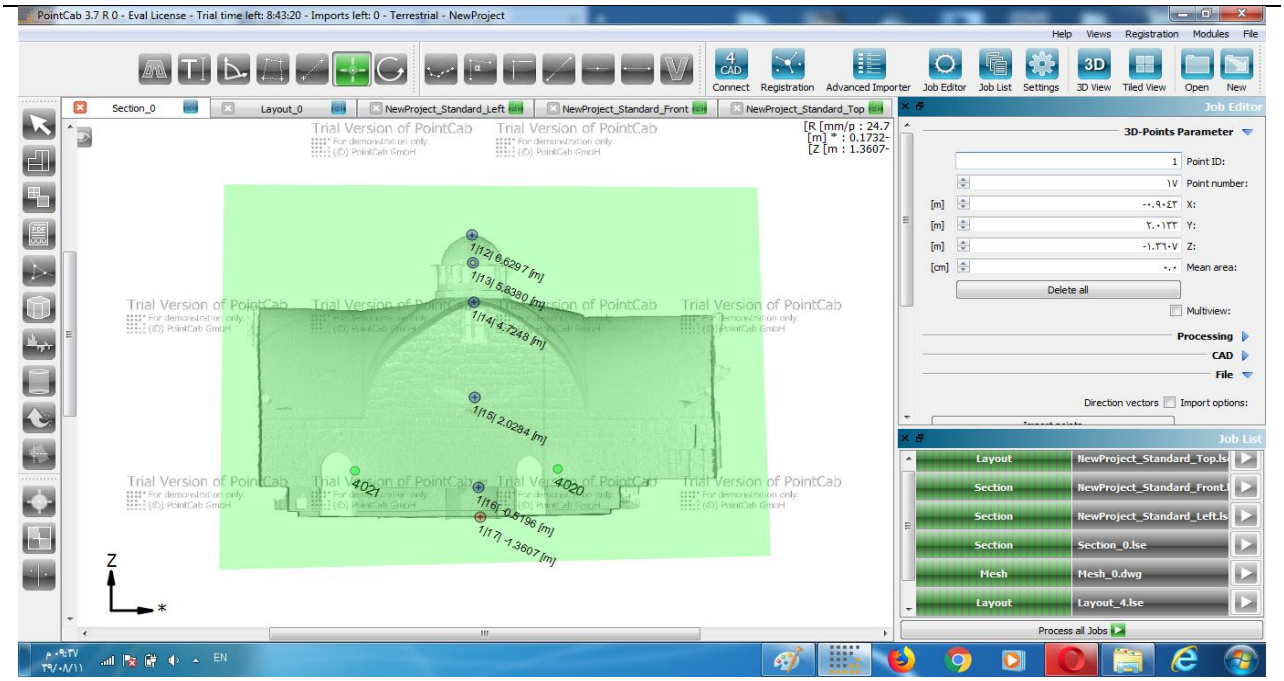

Figure (4-49): Mark Points

In Job Editor you can now export points :

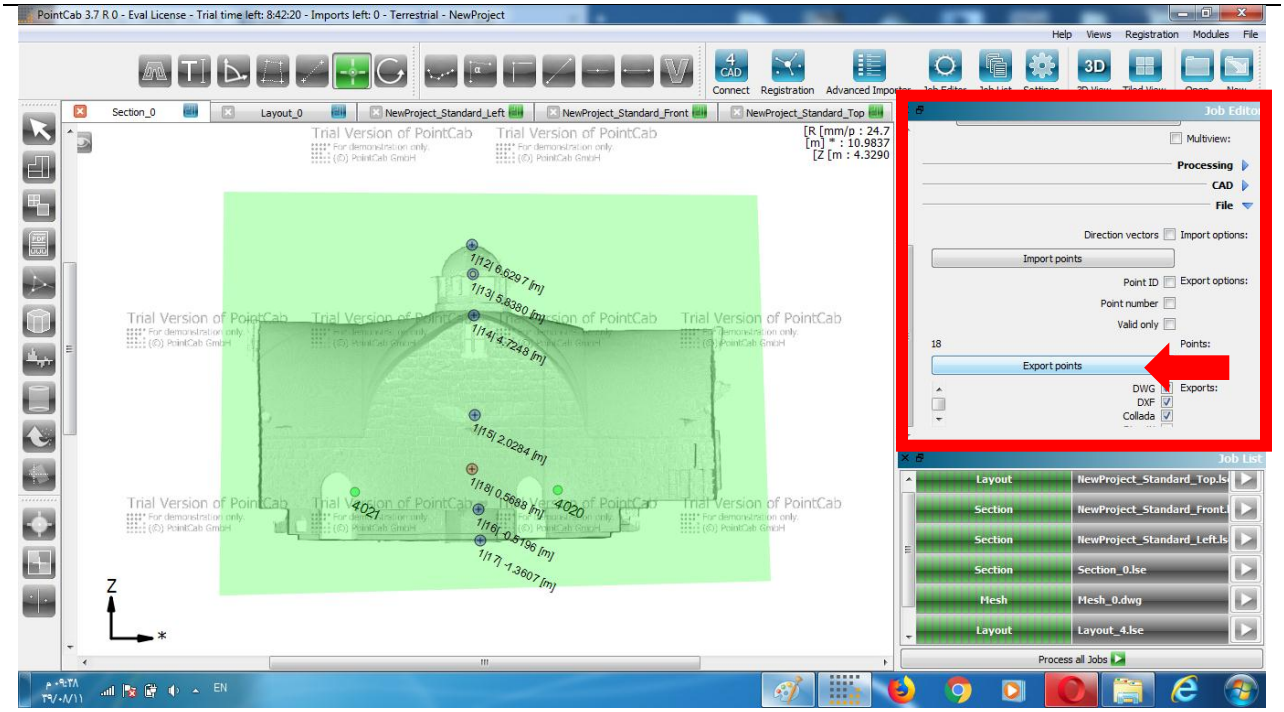

Figure (4-50): Export Points

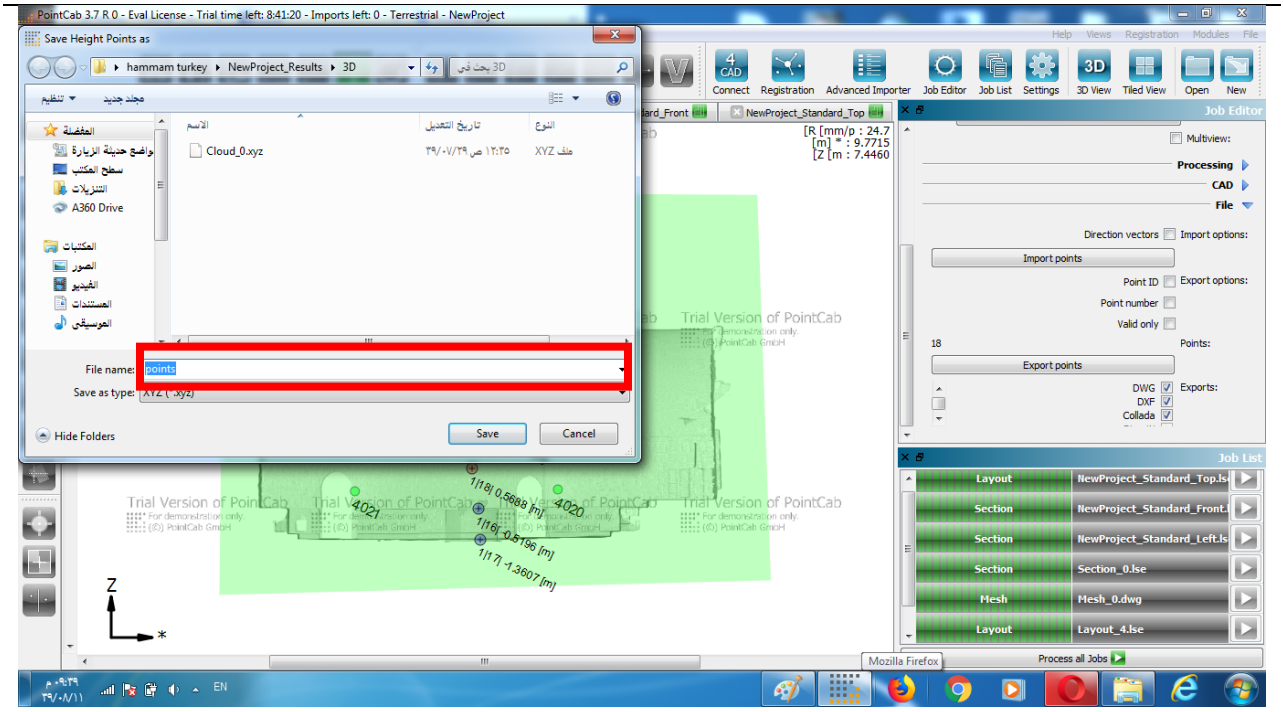

Figure (4-51): Name of file

The XYZ List will be saved under 3D in the folder Project_Results :

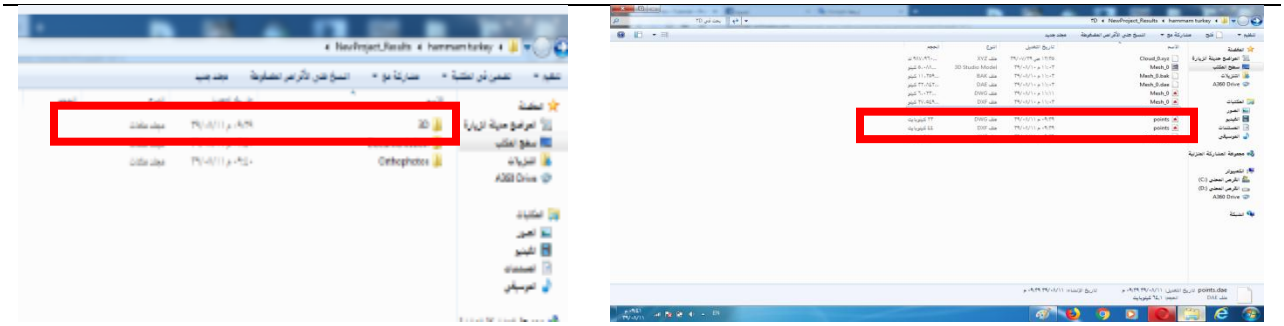

Figure (4-52): 3D Points will be saved in 3D Folder

The List of coordinates is in ASCII format and can be open as a text file in Editor:

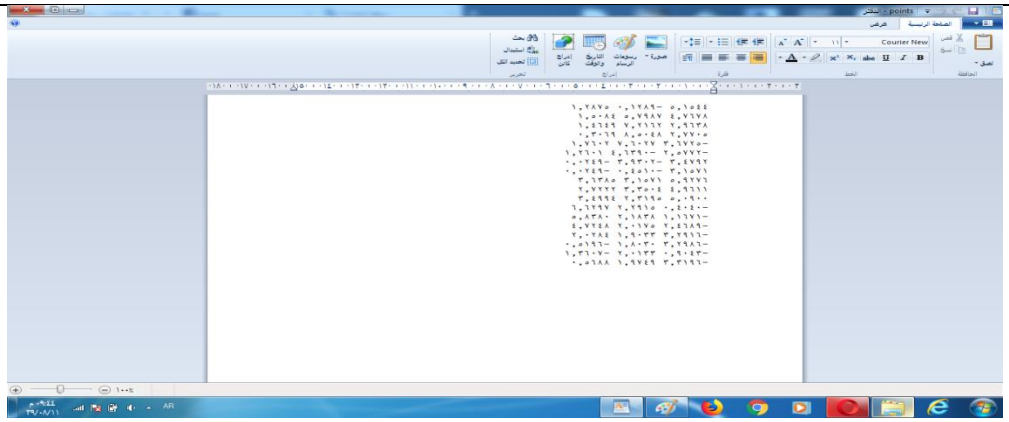

Figure (4-53): XYZ List of Points

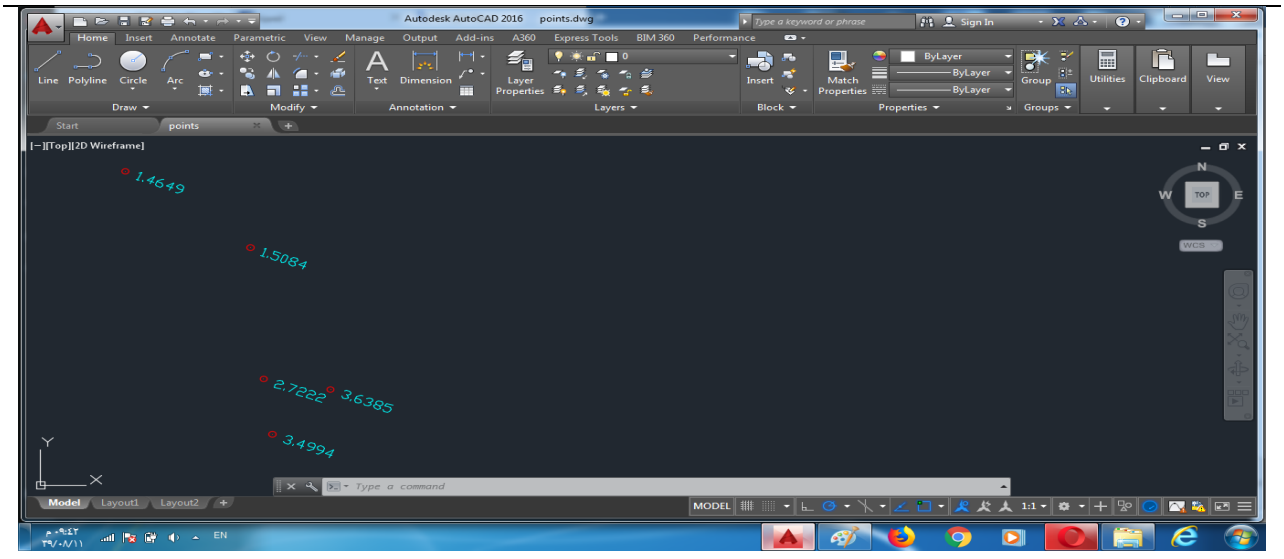

Figure (4-54): points in Autocad

4-3-7 Analyze facade deformations

To analyze the deformation of a facade due to our Delta tool

Activate our Delta tool

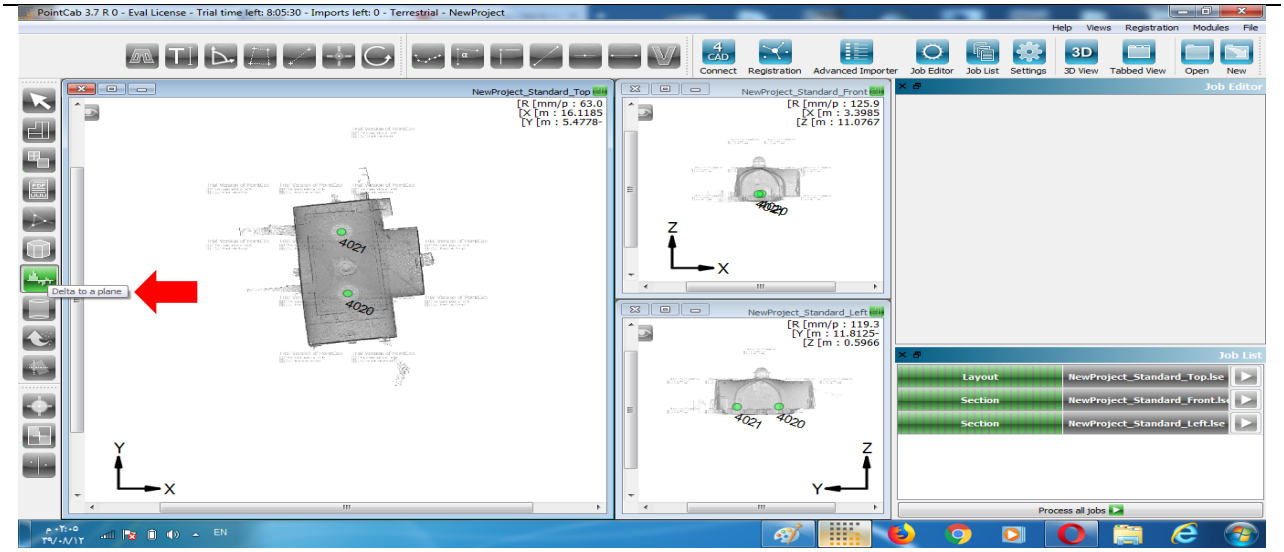

Figure (4-55): Activate our Delta tool

The area, which is highlighted in yellow, indicates the point clouds that are analyzed. You can adjust this area visually or by means of coordinates in the Job Editor:

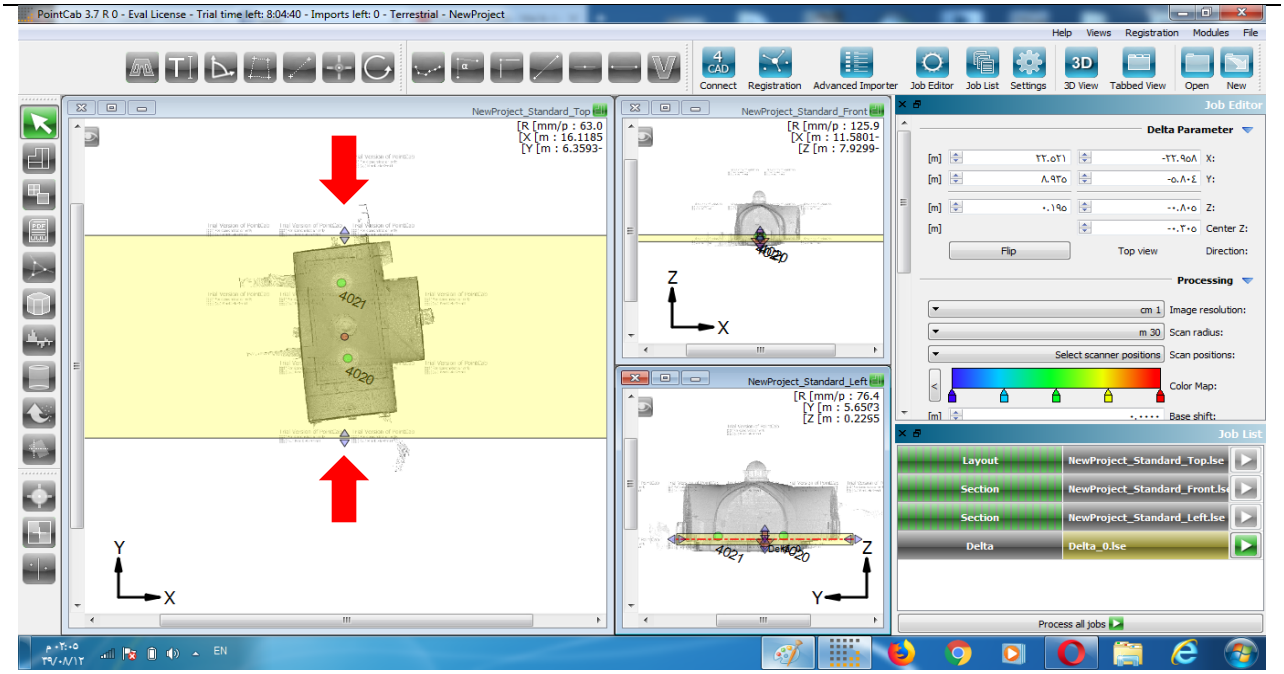

Figure (4-56): Limit the area to be analyzed

start processing

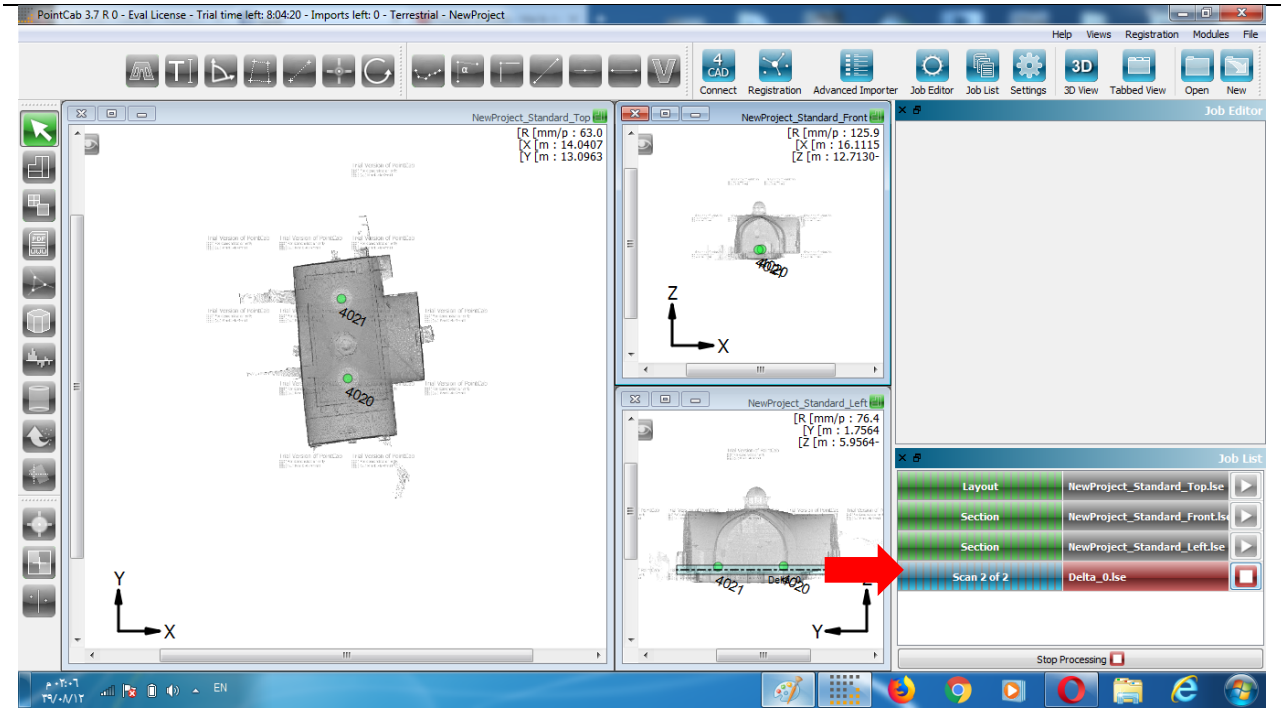

Figure (4-57): start processing

Double-click on the processed job to open the result of the Delta analysis in PointCab. You obtain the same result with the context menu and then with the option Open. You can open the context menu by right-clicking on the processed job.

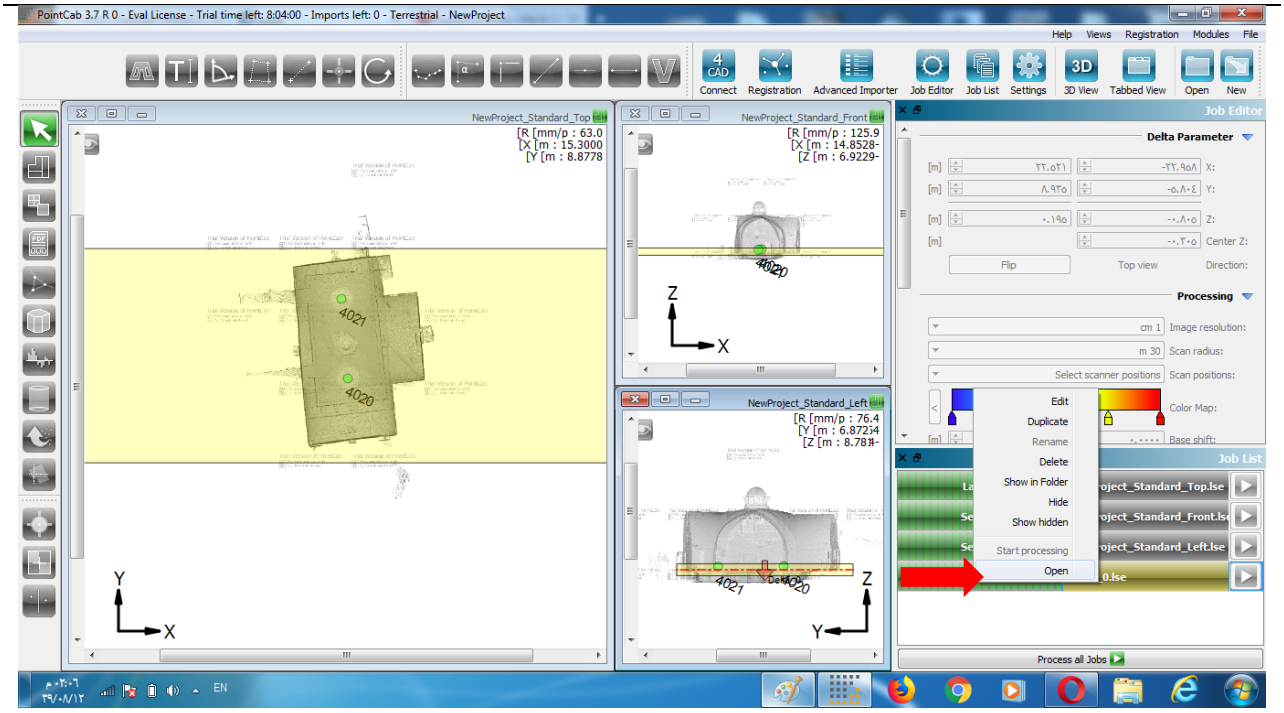

Figure (4-58): open the delta

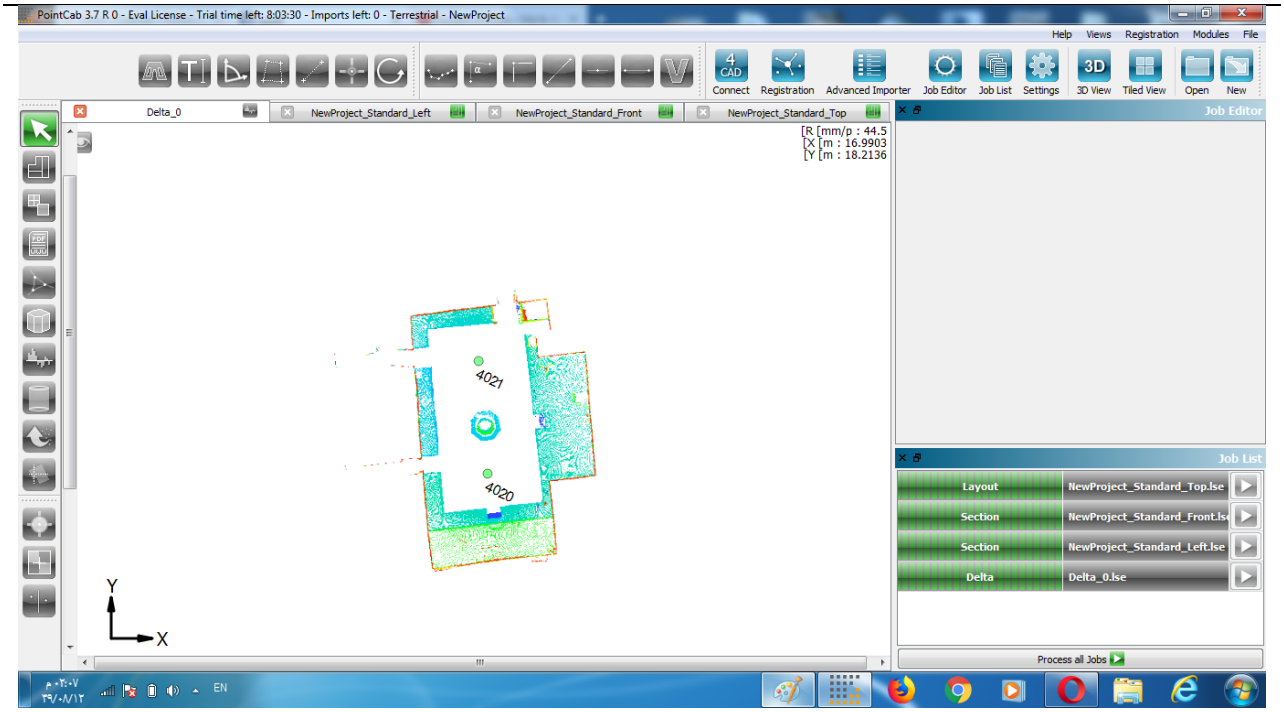

Figure (4-59): Delta analysis in PointCab

By using the context menu, you can display the results by clicking on Show in Folder:

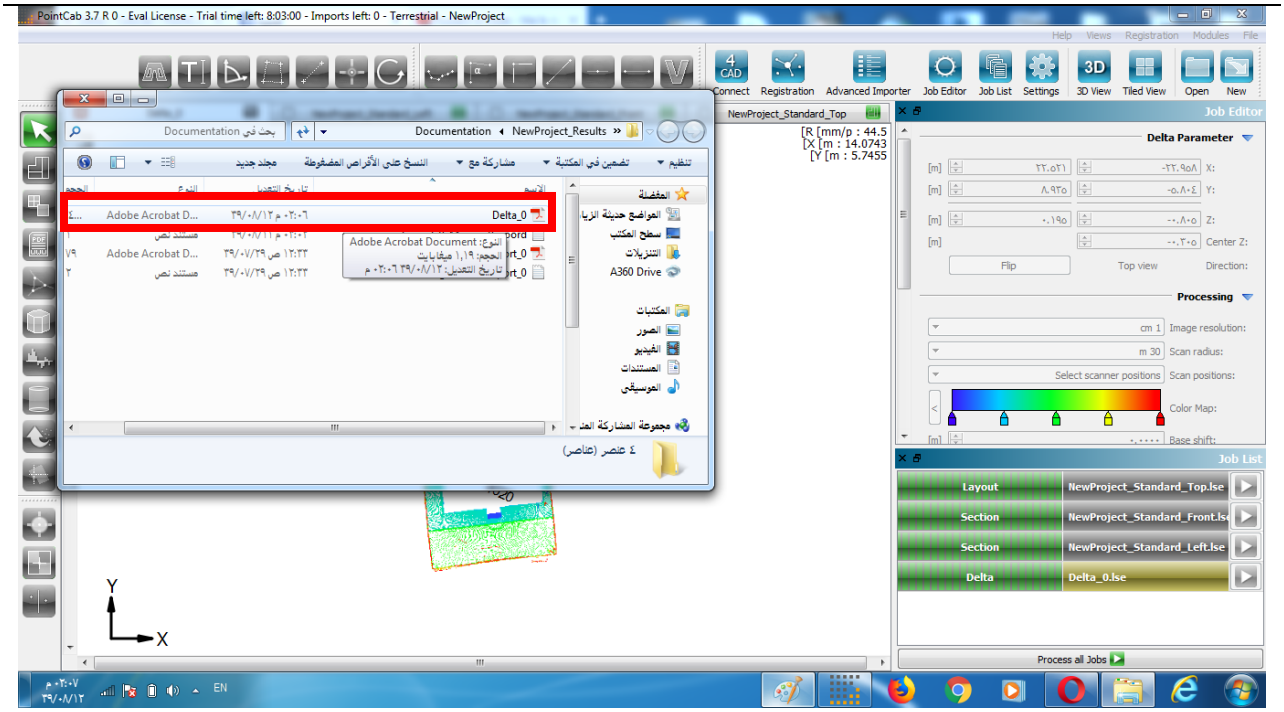

Figure (4-60): Show in Folder

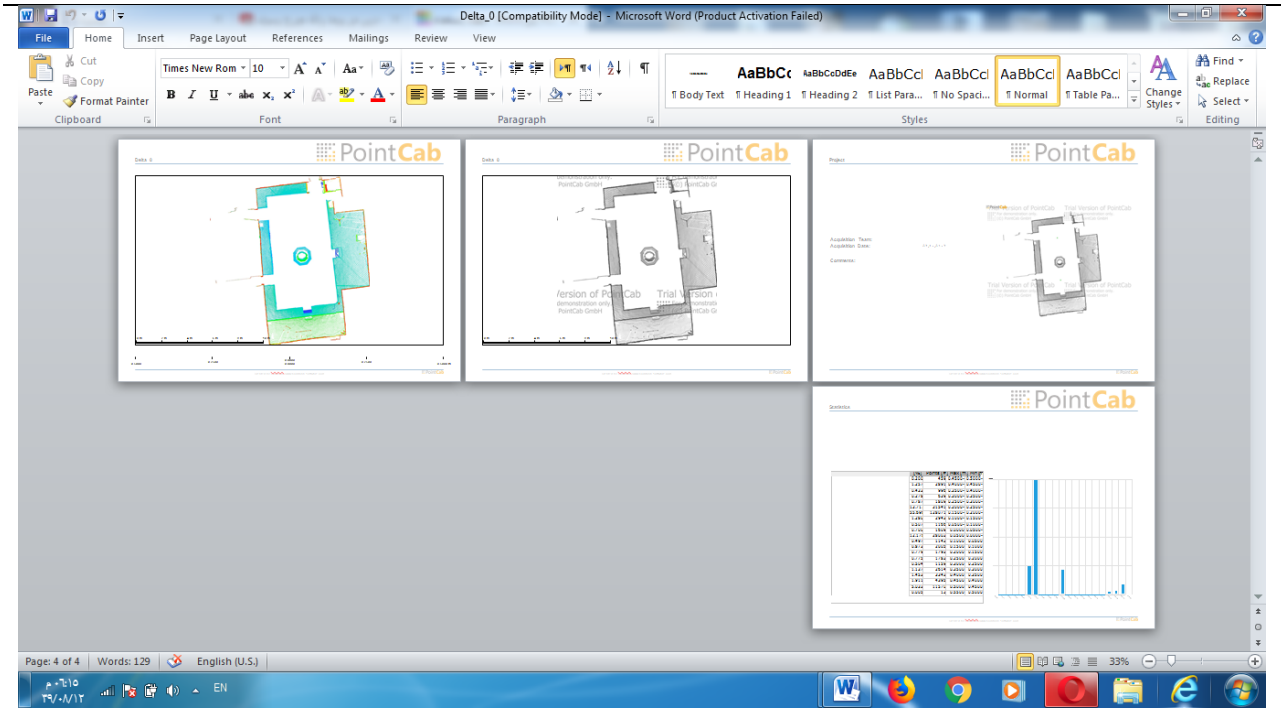

Figure (4-61): PDF protocol as documentation for the Delta analysis

You can open the DWG file in AutoCAD, for instance, and position it under your project. Here, the DWG is opened in Autodesk TrueView:

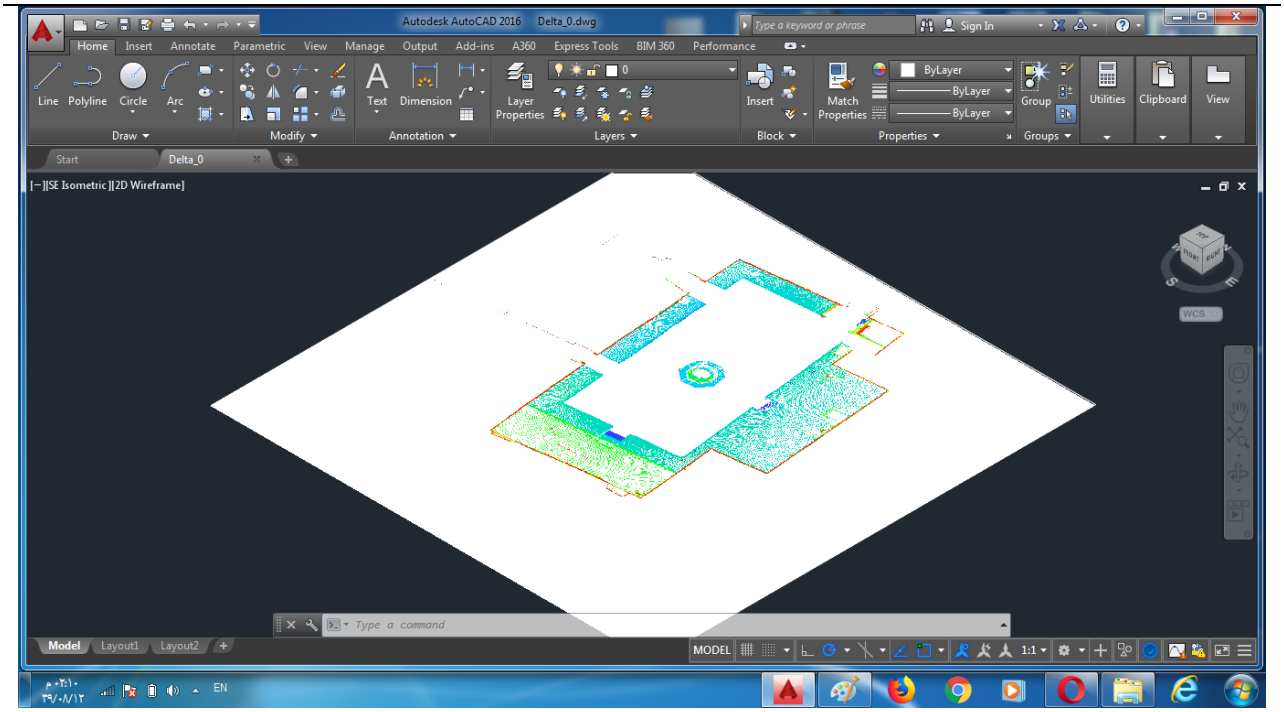

Figure (4-62): DWG of the Delta analysis in Autodesk True View

4-3-8 Volume of a foundation pit

The volume of a foundation pit can be calculated immediately using our Volume tool. Activate the Volume tool :

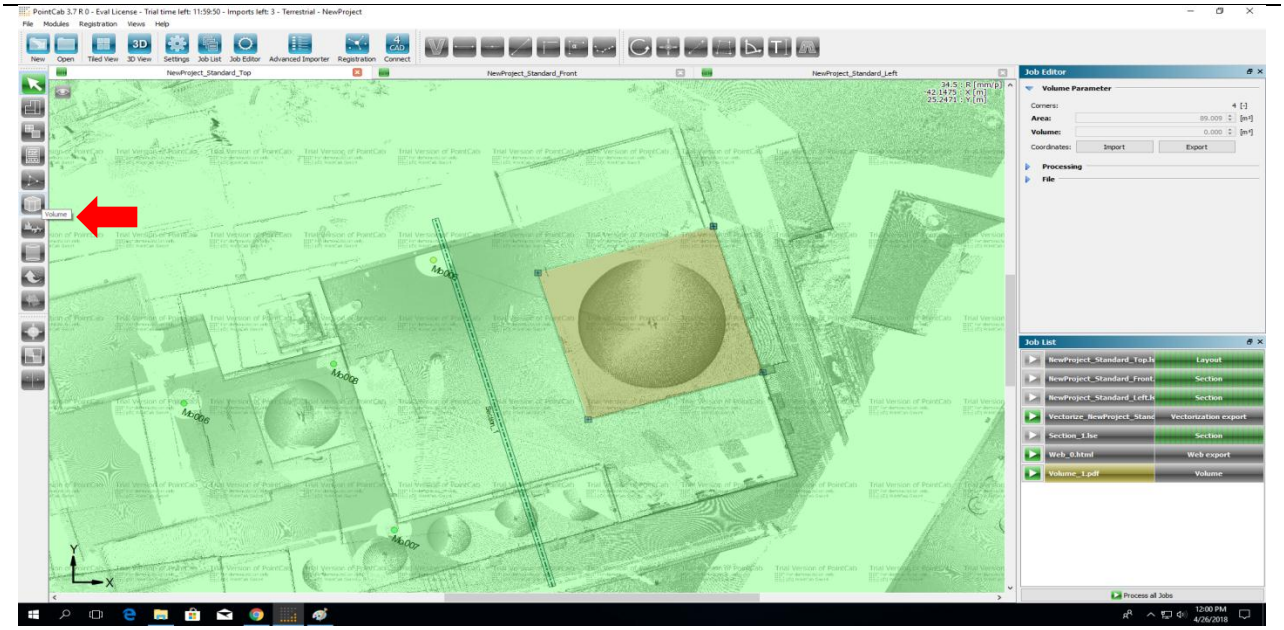

Figure (4-63): Activate the Volume tool

Select the foundation pit respectively the area to calculate the volume & Start processing:

Figure (4-64): Select area& Start processing

The result will be showed directly:

Figure (4-65): Volume calculation results

The result will be showed directly:

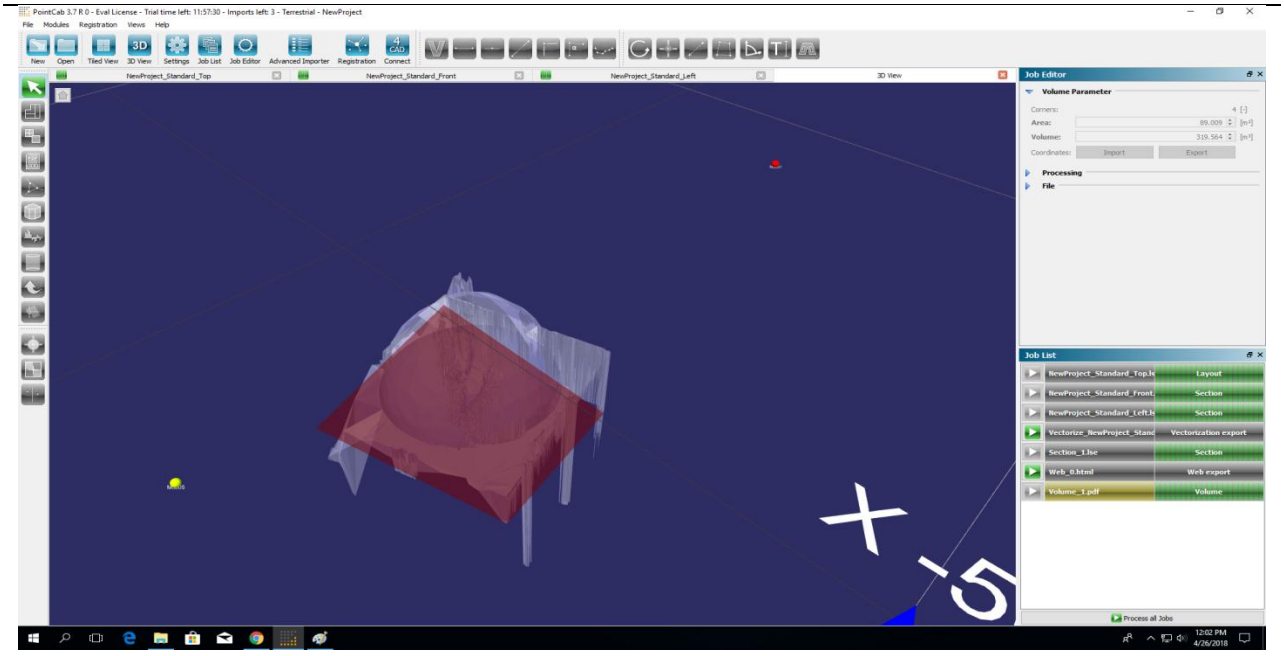

Figure (4-66): Volume in our 3D View

4-3-9 Correct resolution for your laser scanner:

In order to choose the correct resolution of the scanner, it is important not to lose sight of the task. Ultimately, laser scanning must always be economical. However, this is only guaranteed if the correct parameters are selected. One should ask the following questions:

-Is it outside or inside?

-What are the distances between the scanner and the object?

-How many scans will I do to avoid shading?

-Do I need a colored point cloud or is even a gray point cloud meaningful?

-How do I continue to process the scan data and, above all, with which software?

The farther the distances to the object the higher the resolution has to be chosen. For a simply clinkered house facade without ornamentation, e.g. a resolution of 1/4 and twice the quality is sufficient. Much more important than the resolution is to avoid shading by many laser scanner locations on a facade.

Measurements For mosque:

No.	Laser scanner RecapAutodesk	Reference	Accuracy	Relative Error
1	8.491	8.5	.009	1%
2	5.811	5.8	.011	1%
3	9.585	9.6	.015	1%
4	10.577	10.65	.073	1%
5	9.897	9.8	.097	1%
Average	8.8722	8.87	.041	.01
Max	10.577	10.65	0.097	.01
Min	5.811	5.8	0.009	.01
Standard devision	1.869552	1.879362	0.04111	0

Table (4.1): Compression Measurement for Palestine Polytechnic University Mosque

1

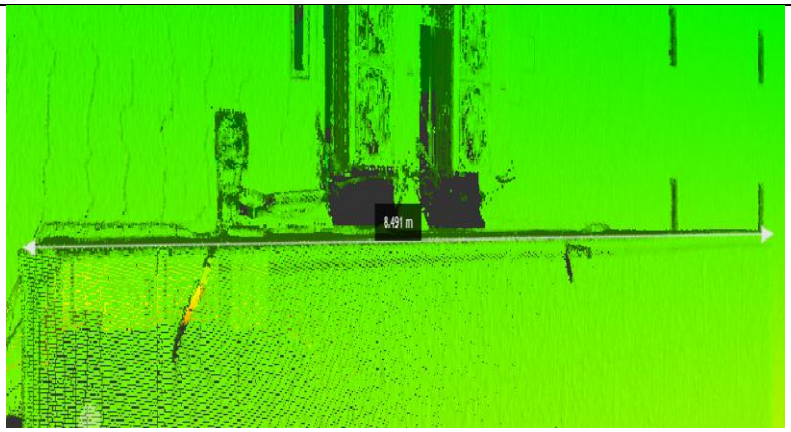

2

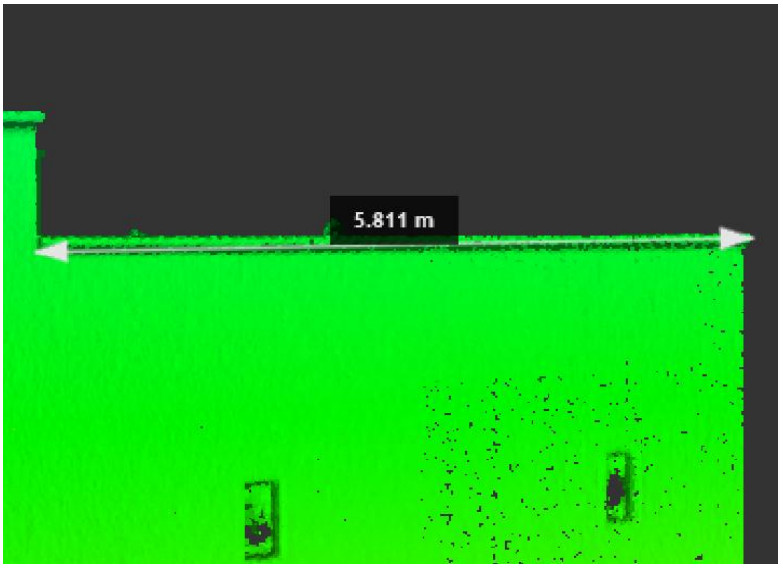

3

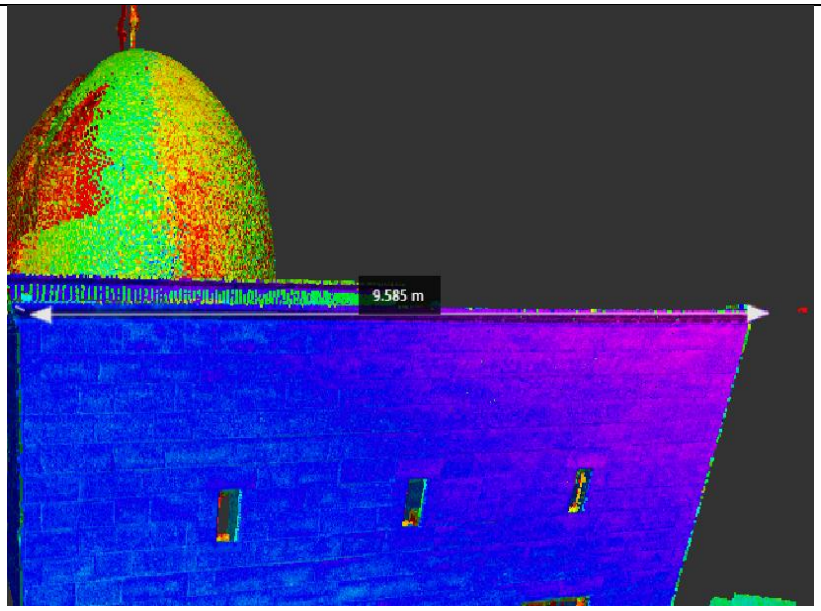

4

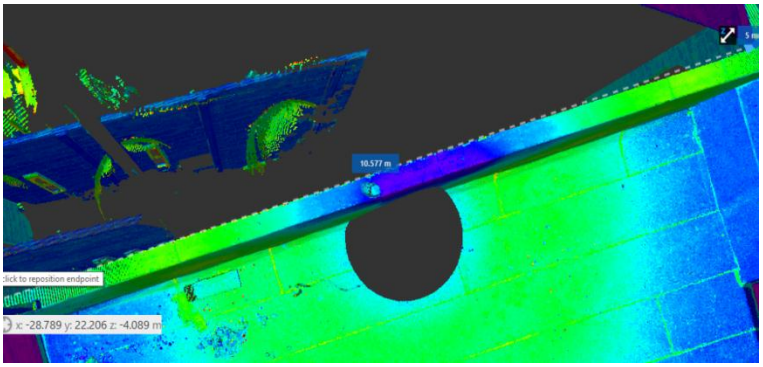

5

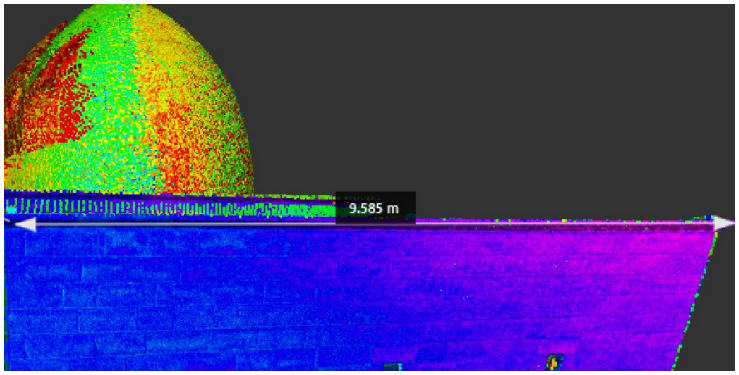

Figure (4-67): Trial Measurement for Palestine Polytechnic University Mosque

Figure (4-68): Test model for Al-Hammam AL-Turkey

Measurement for AL-Hammam AL- Turkey:

No.	Laser scanner Recap Autodesk	Reference	Accuracy	Relative Error
1	.619	.600	0.019	0.03167
2	3.725	4.00	0.275	0.06875
3	.898	1.00	0.102	0.102
Average	3.604333	3.666667	0.189	0.067473
Max	6.19	6	0.275	0.102
Min	0.898	1	0.102	0.03167
Standard	2.648063	2.516611478	0.086504	0.035182

Table (4-2): Compression Measurement for AL-Hammam AL- Turkey

1

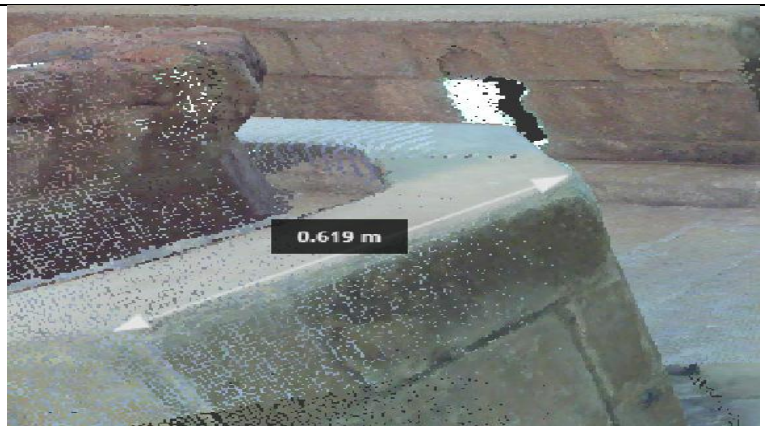

2

3	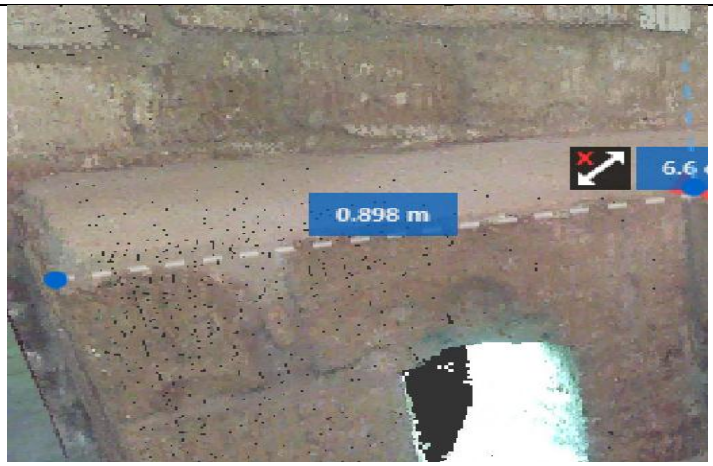

Figure (4-69): Trial Measurement AL-Hammam AL- Turkey

Chapter Five

Conclusions and recommendations

Chapter Five

Conclusions and recommendations

5-1 Conclusions

1. TX5 could be easily used for interior and exterior 3D cloud Modeling of objects .See section (4-3-5).
2. The results of the 3D Model can be easily exported to other formats and software like Autocad,3D studio Max and Autodesk Recap, where 3D Model can forther processed The 3D Model could be used to creat real world section and plans of Buildings and features .See section (4-3-5).
3. Using TX5 ,its easy to make models of large object like Building using multistation principle and GNSS/GPS.See section (4-3-3).
4. In 3D Laser scanning Millions of points are scanned in true color .This requires huge memory usage and processing time .for example the model had (5-8) GB storage and processing and Modeling required half hour of process using workstation. See section (4-3-4).

5-2 Recommendations

After finishing the project the following is recommended:

1. Use indoors better than use abroad.
2. The outside can be represented using Drone. See section (4-2-2)
3. The two devices can be combined See section (4-3-5)
4. It is used in the documentation of archaeological buildings and monuments because they have a high morgue.
5. They are easily used to make longitudinal and transverse sections used in architecture for their saving potential

5-3 Reference

[1] L. Truong-Hong and D. F. Laefer, Application of Terrestrial Laser Scanner in Bridge Inspection, Madrid, Spain: International Association for Bridge and Structural Engineering, 5-9-2014.

[2] M. A.-B. Ebrahim, October 2014. [Online]. Available: https://www.researchgate.net/publication/267037683_3D_LASER_SCANNERS_HISTORY_APPLICATIONS_AND_FUTURE. [Accessed 7 11 2017].

[3] Bienert et al, Application of terrestrial Photogrammetry, Remote Sensing and Spatial Information Sciences, 2006.

[4] F. Blais, "Review of 20 years of range sensor development," 2004.

[5] M. B. Light, "Terrestrial Laser scanning for Building," 2014. [Online]. Available: https://eprints.usq.edu.au/27323/1/Light_2014.pdf. [Accessed 7 11 2017].

[6] Maas et al, Automatic forest inventory parameter determination from terrestrial laserscanner data., International Journal of Remote Sensing, 2008.

[7] Norbert Pfeifer and Christian Briese, "SPRS Commission VII Mid-Term Symposium '100 Years ISPRS - Advancing Remote Sensing Science', ISPRS, Volume XXXVI, Espoo, Finland, p.311-319," 2007. [Online]. Available: http://foto.hut.fi/ls2007/final_papers/Pfeifer_2007_keynote.pdf. [Accessed 2007].

[8] Y. M. a. M. Selim, "Ability of Terrestrial Laser Scanner Trimble TX5 in," *World Applied Sciences Journal 34 ,* 2016.

[9] K. D. Services. [Online]. Available: http://floridalaserscanning.com/3d-laser-scanning/history-of-laser-scanning/. [Accessed 7 11 2017].

[10 J. S. a. C. K. Toth, Topograohical Laser Ranging And Scanning, France, 2009.

[11 Trimble, TRimble TX5 3D laser scanner USER GUIDE, USA: Trimble Navigation Limited, Oct 2012.

[12 L. Truong-Hong and D. F. Laefer, Application of Terrestrial Laser Scanner in Bridge Inspection:, Madrid, Spain: International Association for Bridge and Structural Engineering, 5-9-2014.

[13 L. S. University, "Terrestrial Laser Scanning-Based," Midwest Transportation Center, U.S, 2016.

[14 G. Vosselman, Airborne and Terrestrial, USA: Whittles Publishing,, 2010.

[15 W. Böhler and A.Marbs, 3D scanning instruments, Proceedings of the CIPA WG 6 International Workshop on Scanning for Cultural Heritage Recording, PP: Ziti, Thessaloniki, 2002.

[16 S. L. T. Yelda Turkan, Terrestrial Laser Scanning-Based Bridge Structural, U.S: Midwest Transportation Center, 2016.

[17 D. Younis, Digital PhOTOGRAMMETRY, Hebron: Palestine Polytechnic University, 2016.
]